



<https://theses.gla.ac.uk/>

Theses Digitisation:

<https://www.gla.ac.uk/myglasgow/research/enlighten/theses/digitisation/>

This is a digitised version of the original print thesis.

Copyright and moral rights for this work are retained by the author

A copy can be downloaded for personal non-commercial research or study,
without prior permission or charge

This work cannot be reproduced or quoted extensively from without first
obtaining permission in writing from the author

The content must not be changed in any way or sold commercially in any
format or medium without the formal permission of the author

When referring to this work, full bibliographic details including the author,
title, awarding institution and date of the thesis must be given

Enlighten: Theses

<https://theses.gla.ac.uk/>
research-enlighten@glasgow.ac.uk

THE THERMODYNAMIC PROPERTIES OF SILICA
IN SLAG SYSTEMS.

by

D.A.R. KAY, B.Sc., A.R.C.S.T.

Thesis submitted to the University of Glasgow
for the degree of Doctor of Philosophy.

November, 1959.

ProQuest Number: 10656275

All rights reserved

INFORMATION TO ALL USERS

The quality of this reproduction is dependent upon the quality of the copy submitted.

In the unlikely event that the author did not send a complete manuscript and there are missing pages, these will be noted. Also, if material had to be removed, a note will indicate the deletion.



ProQuest 10656275

Published by ProQuest LLC (2017). Copyright of the Dissertation is held by the Author.

All rights reserved.

This work is protected against unauthorized copying under Title 17, United States Code
Microform Edition © ProQuest LLC.

ProQuest LLC.
789 East Eisenhower Parkway
P.O. Box 1346
Ann Arbor, MI 48106 – 1346

CONTENTS.

	Page
CHAPTER I. Introduction	1
CHAPTER II. Apparatus and Eperimental Procedure	4
CHAPTER III. Discussion of Experimental Procedure	19
CHAPTER IV. Results	26
CHAPTER V. Discussion of results	44
CHAPTER VI. Comparative Review	55
General conclusions	75
References	
Appendix of Thermodynamic Data.	

CHAPTER I.

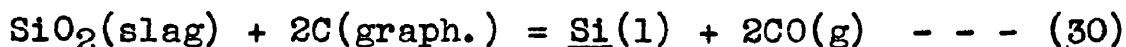
INTRODUCTION.

INTRODUCTION.

In the production of iron, the chemical properties of the slag largely determine the quality of the metal and in particular, which control the sulphur and silicon contents. The control of the silicon content is important in the manufacture of steel by the basic processes where the silicon content of the iron must be kept within fairly low limits. In the acid Bessemer process however, a high silicon content is required as that largely determines the heat produced during the process.

A start can be made in the control of the silicon content of iron by determining whether equilibrium conditions are being attained in the blast furnace or whether reaction kinetics are the controlling factors.

The equation

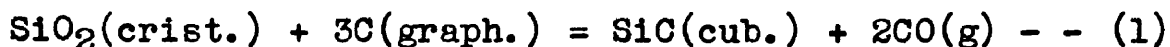


represents the reaction between slag, carbon monoxide and the silicon of graphite saturated metal. The equilibrium constant for this reaction is $K_{30} = a_{\text{Si}}/a_{\text{SiO}_2}$ when the pressure of carbon monoxide is one atmosphere and for the equilibrium relationship to be completely defined a knowledge is required of the free energy

change of the reaction, the activity coefficients of silicon and silica, the content of either the silicon in the metal or the silica in the slag and the effect of temperature on all these quantities. Silica, lime, alumina and magnesia account for about 95% of the constituents of blast furnace slags and the determination of the silica activities in laboratory slags containing these constituents provides some of the information required in the determination of the equilibrium conditions.

It is unfortunate that in the determination of silica activities, the results of different investigators are not in agreement. The reasons for these discrepancies are discussed in chapter VI.

In the present work, silica activities were determined by studying the slag-gas equilibrium



This reaction must be considered as the summation of two other equilibria



In the study of the standard reaction (1), the equilibrium pressure ($p_{\text{CO}} + p_{\text{SiO}}$) above compacts containing solid silicon carbide, solid graphite and solid quartz,

was measured at 1450, 1500 and 1550°C. Under these conditions the equilibrium constant for reaction (1) reduces to $K_1 = p^2\text{CO}(\text{standard})$, the partial pressure of carbon monoxide being obtained from the measured reaction pressure and the equilibrium constant for reaction (2). Substitution of a compact containing the given slag yields values of $p\text{CO}(\text{slag})$, this being obtained from the measured reaction pressure and the equilibrium constant of reaction (3). The silica activity of the slag, referred to the standard state of cristobalite, is thus $p^2\text{CO}(\text{slag}) / p^2\text{CO}(\text{standard})$.

The method and apparatus used are substantially those employed by Baird and Taylor¹⁵ who successfully initiated the equilibrium study. The repetition of some of the experiments of Baird and Taylor, undertaken in the present work, provides general confirmation of their experimental results, which is important in view of the disagreement with the results of other investigators.

CHAPTER II.

APPARATUS AND EXPERIMENTAL PROCEDURE.

APPARATUS AND EXPERIMENTAL PROCEDURE.General apparatus.

The apparatus used is shown in fig. 1, and with a few minor modifications is essentially that used by Baird and Taylor¹⁵. The apparatus is simple and the diagram is considered to be self-explanatory. The modifications which were made are given below.

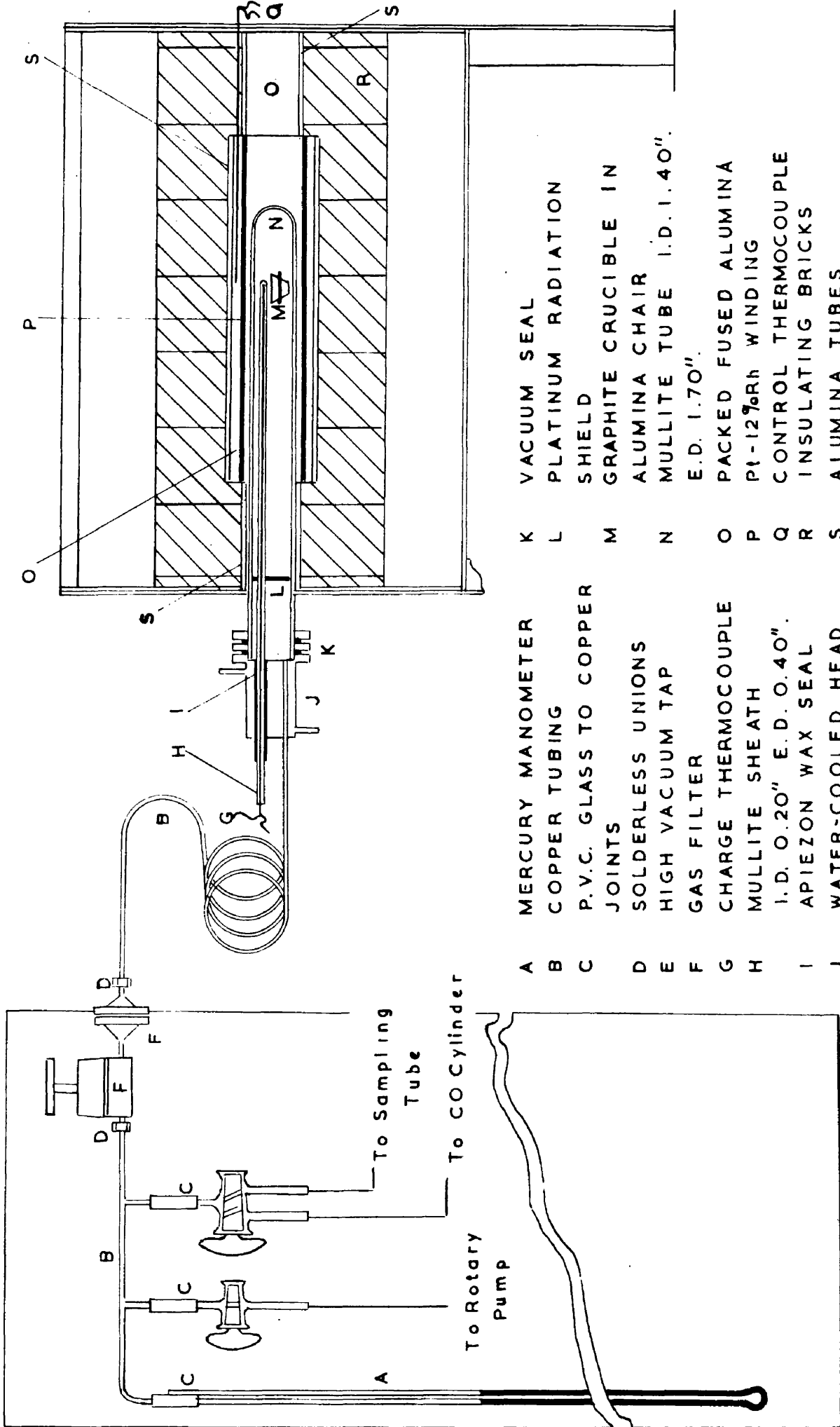
- 1). The substitution of a good high vacuum tap at 'E'.
- 2). The removal of mullite radiation shields and their replacement by a piece of platinum foil.
- 3). The use of three types of crucible.

Crucibles.

The three types of crucible used in the present investigation are illustrated in fig. 2.

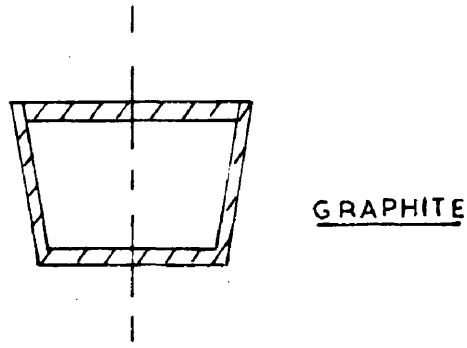
Type 'A' was a graphite crucible identical to that used by Baird and Taylor and weighed about 35 gms. This crucible, which was used in the preliminary runs 1 - 12, was laid on a thin alumina plaque inside the mullite furnace tube.

The crucibles of type 'B' consisted of an outer recrystallised alumina crucible which contained a smaller

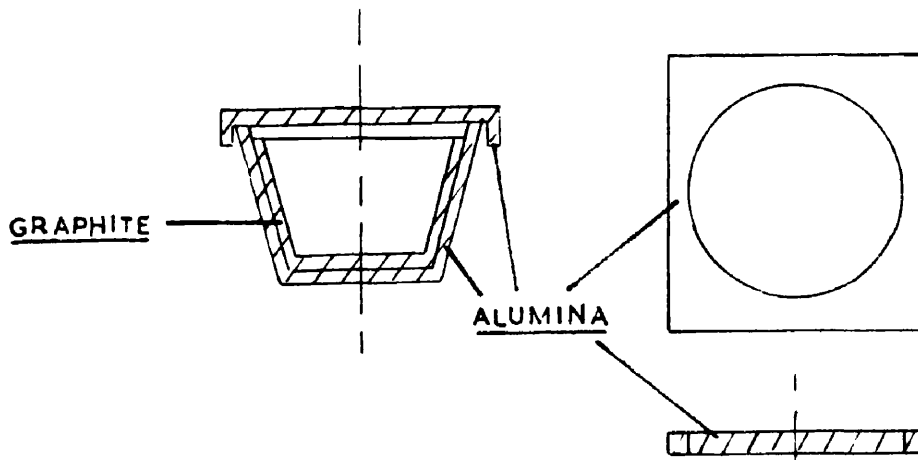


- A MERCURY MANOMETER
- B COPPER TUBING
- C P.V.C. GLASS TO COPPER JOINTS
- D SOLDERLESS UNIONS
- E HIGH VACUUM TAP
- F GAS FILTER
- G CHARGE THERMOCOUPLE
- H MULLITE SHEATH I.D. 0.20" E.D. 0.40"
- I APIEZON WAX SEAL
- J WATER-COOLED HEAD
- K VACUUM SEAL
- L PLATINUM RADIATION SHIELD
- M GRAPHITE CRUCIBLE IN ALUMINA CHAIR
- N MULLITE TUBE I.D. 1.40" E.D. 1.70"
- O PACKED FUSED ALUMINA
- P Pt-12%Rh WINDING
- Q CONTROL THERMOCOUPLE
- R INSULATING BRICKS
- S ALUMINA TUBES

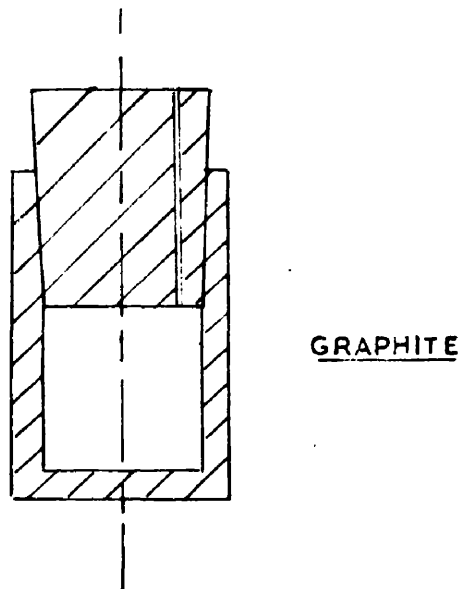
Fig. 1 - Diagram of Apparatus.



Crucible 'C'.



Crucible 'B' and support.



Crucible 'A'

FIG. 2 - CRUCIBLES.

graphite crucible which weighed about 1 - 2 gms. This crucible was fitted with a recrystallised alumina cap and was used in runs 13 - 24, 26 - 30 and in run 34.

Type 'C' was a thin graphite crucible which weighed about 6 - 8 gms. and was used in runs 25, 31 - 33, 35 - 71 and in run 34R.

Also shown in fig. 2 is the alumina support which served to locate crucibles 'B' and 'C' in the mullite furnace tube. This support prevented direct contact between the crucibles and the furnace tube, as did the alumina plaque which was used with crucibles of type 'A'.

The cap or stopper provided with each crucible prevented the free 'evaporation' of silicon monoxide from the crucible contents.

Master slags.

Master slags were made up from the following materials.

- 1). Ground, acid-washed quartz sand, which contained on analysis 99.0% SiO_2 , 0.8% Al_2O_3 and 0.2% FeO .
- 2). 'Analar' calcium carbonate.
- 3). 'Analar' alumina after ignition for 1 hr. at 1000°C .
- 4). 'Analar' magnesia after ignition for 3 hrs. at 1000°C .

The ground, acid-washed quartz sand was also used for the standard silica runs.

In making up the master slags these materials were first weighed out to the desired slag composition and then melted, after thorough mixing, in a graphite crucible heated by a high frequency induction coil. The molten slag was cast as a small 'button' which was crushed in a percussion mortar and then ground to -100 mesh in a mechanical agate mortar. The previous decomposition of the calcium carbonate to the oxide by heating to 1000°C was found to be unnecessary as decomposition readily took place as the slag was being heated in the graphite crucible.

The above procedure was modified for master slags W, X and Y. In these cases the molten slag was poured into water thus giving a granulated mass which, after drying for over 3 hrs. at 110°C, was more easily ground.

The analyses of these master slags is given in table 1. Standard methods were employed for the analyses of silica and alumina but particular mention may be made of the analyses for lime and magnesia in slags L - Y, which were done with great success by titration with the sodium salt of ethylene diamine tetracetic acid¹⁶. In all the CaO-Al₂O₃-SiO₂ slags lime was analysed by the standard

Table 1. - Analyses of master slags.

Slag	Composition wt.%				Duplicate difference wt.%			
	CaO	Al ₂ O ₃	MgO	SiO ₂	C	A	M	S
A	38.1	0.6	-	61.3	0.0	0.2	-	0.3
B	55.8	0.6	-	43.6	0.0	0.3	-	0.3
C	20.7	11.0	-	68.3	0.1	0.3	-	0.4
D	35.5	11.0	-	53.5	0.5	0.1	-	0.1
E	49.9	10.9	-	39.2	0.6	0.2	-	0.4
F	10.8	20.8	-	68.4	0.1	0.6	-	0.6
G	46.1	21.1	-	32.8	0.0	0.3	-	0.2
H	14.0	31.0	-	55.0	0.0	0.5	-	0.4
I	36.8	30.4	-	32.8	0.5	0.2	-	0.2
J	26.8	41.2	-	32.0	0.1	0.7	-	0.1
K	32.7	40.5	-	26.8	0.1	0.2	-	0.1
L	23.0	0.6	9.7	66.7	0.0	0.2	0.0	0.0
M	49.3	0.6	9.9	40.2	0.0	0.3	0.2	0.3
N	13.8	0.6	19.8	65.8	0.0	0.1	0.1	0.4
O	44.6	0.6	20.0	34.8	0.0	0.3	0.0	0.3
P	5.2	0.7	28.4	65.7	0.1	0.2	0.0	0.3
Q	26.7	0.4	30.0	42.9	0.0	0.2	0.0	0.3
R	9.8	11.0	9.9	69.3	0.1	0.3	0.1	0.3
S	44.9	9.9	9.9	35.3	0.5	0.2	0.0	0.3
T	3.4	11.0	19.6	66.0	0.3	0.4	0.1	0.1
U	34.8	10.7	19.7	34.8	0.1	0.0	0.1	0.5
V	0.0	20.4	9.8	69.8	0.0	-	0.0	0.1
W	45.0	20.1	9.9	25.0	0.3	0.1	0.2	0.4
X	0.0	20.4	19.7	59.9	0.0	0.4	0.0	0.1
Y	19.8	20.6	19.8	39.8	0.1	0.3	0.2	0.1
				<u>Mean</u>	<u>0.14</u>	<u>0.28</u>	<u>0.07</u>	<u>0.26</u>
				<u>Standard Deviation.</u>	<u>0.19</u>	<u>0.16</u>	<u>0.08</u>	<u>0.15</u>

oxalate method.

The duplicate differences of these analyses are also given in table 1 and these have been analysed statistically to give the shown means and standard deviations. An error in any slag analysis of $\pm 0.5\%$ has been obtained from these figures.

Compacts.

Compacts for the various runs were made from quartz or slag (-100 mesh), previously degassed Acheson graphite powder (-200 mesh) and commercial silicon carbide powder (-700 mesh).

4 gms. of quartz or slag, 1 gm. of graphite powder and 1 gm. of silicon carbide powder were first thoroughly mixed dry, and then with a little water. The damp mixture was then compressed at 25 tons/sq.inch to give a cylindrical compact. Although most of the water was removed by the compression, the compacts were oven dried for 2 - 3 days at 110°C. The addition of water was found to give the compacts an excellent 'green' strength.

This procedure was adopted for the majority of the compacts but in runs 1 - 17 inclusive, the compacts were compacted dry with difficulty.

Temperature measurement and control.

The temperature of the crucible assembly was measured by a Pt/Pt-13%Rh thermocouple and a Cambridge potentiometer. The combination of thermocouple and potentiometer was standardised at frequent intervals against the melting point of palladium. This standardisation was considered to be satisfactory in the experimental temperature range when it was combined with the British Standards "Reference Tables for Pt/Pt-13%Rh Thermocouples"¹⁷. The error in standardisation is estimated at $\pm 2^{\circ}\text{C}$.

The temperature was automatically controlled by a Kelvin-Hughes electronic controller used in conjunction with a Pt/Pt-13%Rh control thermocouple placed next to the furnace winding. When a new valve was fitted in the controller a swing of $\pm 2^{\circ}\text{C}$ about the mean temperature of the crucible assembly was obtained. As the valve deteriorated, however, the swing rose to as much as $\pm 5^{\circ}\text{C}$ about the mean.

In the earlier runs (1 - 12) control to an exact temperature was found to be unsatisfactory. The controller, in subsequent runs, was set as near the desired temperature as possible and during a specific determination of the equilibrium pressure the temperature apper-

taining to that particular instant was taken. The silica activity obtained from data corresponding to that temperature was then taken as the silica activity at the desired temperature i.e. 1450, 1500 or 1550°C.

On consideration of the errors involved in the standardisation of the thermocouple and potentiometer, in the cold junction corrections and in the actual measurement of the mean temperature, an error of $\pm 4^{\circ}\text{C}$ is placed on the measurement of the absolute temperature.

Pressure measurement, gas sampling and analysis.

The equilibrium reaction pressure was measured by a simple mercury manometer and any pressure reading was considered to be accurate to within ± 0.5 mm.Hg.

Carbon monoxide was introduced into the system direct from a cylinder and on analysis the cylinder gas contained 99.2% CO and 0.8% N₂.

A gas sample from the system was taken into a completely evacuated gas sampling tube containing a little mercury. Mercury was then admitted into the sampling tube until the sample was approximately at atmospheric pressure. This method nearly eliminated the leakage of air into the sample.

Gas analyses were carried out using a Bone and

Wheeler apparatus. Gas samples from the initial runs contained fractional percentages of carbon dioxide and subsequent analyses were for oxygen and carbon monoxide only, the residual gases being assumed to be nitrogen.

The presence of any oxygen in a gas sample was considered to be caused by the leakage of air during sampling and an appropriate correction was made to the analysis in order to obtain the composition of the gas in the system.

In runs 40 - 71 gas analyses were discontinued as gas compositions of 98 - 100% CO were being obtained invariably. The gas analyses were never of great accuracy and the error involved in the assumption that the furnace atmosphere contained 99% CO is considered to be small.

Adsorption, desorption and furnace deposits.

In the first 12 runs the experimental technique of Baird was adopted. This involved the separate degassing of the crucible and reaction chamber by continuous evacuation for 3 hrs. at 1550°C. The terms 'reaction chamber' refer to the walls of the mullite furnace tube, thermocouple sheath and radiation shields. Baird had found that high percentages of nitrogen in the furnace

atmosphere during a run were partly caused by the desorption of gases from the crucible and reaction chamber and partly by the desorption of gases from the furnace deposits which had been formed during the previous run. These deposits were apparently caused by the gradual 'evaporation' of silicon monoxide from the crucible contents and its resultant condensation on the cooler parts of the reaction chamber. These deposits consisted of a finely divided mixture of graphite, silica and silicon carbide indicating that the silicon monoxide had been reoxidised, at some stage, by the carbon monoxide.

During the rough equilibrium determinations of the first twelve runs the nitrogen content of the furnace atmosphere varied from 3 - 17%, and in order to try and correct this, a number of blank runs were undertaken.

In the first blank run, carbon monoxide was admitted into a new, empty reaction chamber which had been previously degassed for 3 hrs. at 1550°C. At a constant temperature of about 1500°C the pressure of carbon monoxide in the system did not vary by more than ± 2 mm. Hg over a period of about two hours. Any pressure change caused by the admittance or withdrawal of carbon monoxide was immediate and well defined and a 50°C change in temperature caused a pressure change of only 5 mm. Hg.

This change was also well defined. The behaviour of the empty reaction chamber was thus very satisfactory, no evidence of adsorption or desorption of gases being observed.

In the second blank run a previously degassed, empty graphite crucible of type 'A' was placed in the reaction chamber and the above procedure repeated. In this case the pressure of carbon monoxide in the system gradually increased at constant temperature and adsorption or desorption opposed any pressure change. A 50°C change in temperature at 1500°C caused a pressure change of 10 cms. Hg or more. 'Thorough' degassing of the crucible at 2000°C and a pressure of 10^{-5} cms. Hg proved to be fruitless.

The use of graphite as the sole crucible material was thus rejected, and a crucible assembly of type 'B' designed. The mass of crucible graphite was thus cut from about 35 gms. to about 2 gms.

At this stage the mullite radiation shields were replaced by a piece of thin platinum foil, which greatly eased handling and subsequent replacement.

The crucible of type 'B' was degassed for 3 hrs. at 1550°C and it was found to have the same characteristics as the degassed empty reaction chamber. Crucibles of this

type were used in runs 13 - 24, 26 - 30 and run 34. Furnace atmospheres containing 98 - 100% CO were obtained quite readily. During these runs any replaced components of the system were degassed before the equilibrium determination, as was the whole system if it had been exposed to the atmosphere for any length of time. The volume of the furnace deposit formed during these runs was very greatly reduced and in many cases was apparently completely eliminated. Any deposit which did accumulate, however, was removed before the start of the next run. The platinum radiation shield functioned very satisfactorily, although it became very brittle over a period of about 20 runs.

When crucibles of type 'B' contained the more basic slags, there was a tendency for the alumina lid and crucible to fuse together. Graphite crucibles of type 'C' were then made and used for the remainder of the runs. Satisfactory results were also obtained with these crucibles and carbon monoxide contents of 98 - 100% were obtained readily. The volume of deposit formed was slightly more than that formed when using crucibles of type 'B'. This was caused by the limited reaction between the top of the graphite crucible and the mullite thermocouple sheath, which took place when the sheath softened

at the high experimental temperatures and actually touched the top of the graphite crucible. The silicon monoxide formed from this reaction was free to diffuse throughout the system but the resultant increase in deposit apparently had no effect on the adsorption and desorption.

Leaks.

It was found that leaks in the mullite furnace tube and thermocouple sheath could be eliminated if there was no area of contact between mullite and graphite.

The furnace tube was well protected from the graphite crucibles by the alumina support which served to locate the crucible in the furnace, and there was no evidence of reaction between the mullite furnace tube and the crucible. Indeed, one of the furnace tubes lasted for over 30 runs.

Occasional leaks in the thermocouple sheath could not be avoided however, as the mullite softened at high temperatures and the sheath eventually bent and touched the top of the crucible. If the crucible was of type 'A' or 'C' the reaction between mullite and graphite quickly caused porosity in the sheath. This reaction caused the volume of furnace deposit to increase but when a leak

did occur the run was rejected.

Determination of the equilibrium reaction pressure.

The exact procedure adopted underwent minor modifications throughout the investigation but these had no effect on the consistency of the results. An account of the final procedure adopted in runs 25, 31 - 33 and 35 - 71, is first given.

The charged crucible and support were placed in the reaction chamber at 1000°C and the system closed and evacuated continuously by means of the rotary pump until the temperature had risen to about 1100°C - half an hour. At this temperature carbon monoxide was admitted to the approximate equilibrium pressure and the controller set at the desired temperature. The furnace was being controlled at approximately 1450°C in about two and a half hours from the time of charging and a final adjustment was then made on the controller in order to get the temperature as near 1450°C as possible. The system was also flushed out with carbon monoxide and that gas again admitted to the approximate equilibrium reaction pressure.

The rate of change of the reaction pressure with time was carefully watched at this stage and if the rate was too great, carbon monoxide was accordingly admitted to

or withdrawn from the system. When the rate became sufficiently small the system was allowed to come to equilibrium at the controlled temperature. When the pressure had remained steady for half an hour, the system was evacuated momentarily and fresh carbon monoxide admitted to the same pressure. If no further pressure change took place during the next half hour, equilibrium was considered to have been attained, and the furnace atmosphere assumed to contain 98 - 100% CO. If a further pressure change occurred - this took place very rarely - the reaction pressure was again allowed to become steady and then fresh carbon monoxide admitted to the new pressure. In every case no further pressure change was observed.

The mean temperature corresponding to a particular equilibrium determination was also taken.

The equilibrium pressure was usually determined from 'above' and 'below' by this procedure and the mean taken. This mean was considered to be within $\pm 0.5\%$ of the true equilibrium pressure.

The procedures were repeated at temperatures of approximately 1500 and 1550°C.

Although it is stated above, that the equilibrium was considered to have been attained after the pressure

had remained steady for half an hour, this time applied to the more basic slags. In the more acid slags and in particular the standard silica runs, where the reaction rate was comparatively slow, this time was increased to two hours or more.

The minor changes in procedure for runs 1 - 34 are now given below.

In run 34R the compact was placed in a new graphite crucible of type 'C' and charged into a new reaction chamber at 1000°C. The system was then closed and momentarily evacuated to allow the admittance of carbon monoxide to the approximate equilibrium pressure. When a temperature of about 1450°C was reached the procedure was the same as in runs 35 - 71. The main change in procedure was that no continuous evacuation was employed.

In runs 26 - 30 and in run 34 the furnace was charged at 600°C and continuously evacuated until a temperature of about 1100°C was reached. The procedure from this temperature on was as described above. Gas samples were taken in conjunction with each of these determinations, however, and gas analyses of between 98 and 100% carbon monoxide were obtained readily.

In runs 13 - 24 the furnace was charged at room temperature and then continuously evacuated until a

temperature of 1100°C was reached. At this temperature carbon monoxide was admitted to the approximate equilibrium pressure and the temperature raised to 1450°C. Fresh carbon monoxide was then admitted and the equilibrium pressure determined in the manner described above, but in this case the furnace atmosphere was not renewed and that pressure was taken as one approach to equilibrium. Gas samples were taken with each determination and it is significant that even in these cases, samples of gas which had been in the furnace for as long as five or six hours, contained 98 - 100% carbon monoxide.

Runs 1 - 12 were purely preliminary but they were the foundation upon which the final experimental techniques were built.

The elimination of degassing.

In the course of the last twenty runs or so it was discovered that degassing of the crucibles and reaction chamber could be dispensed with altogether. As a result it is now thought that the large mass of the graphite crucible 'A', caused the major contribution to the impurities of the furnace atmosphere.

CHAPTER III.

DISCUSSION OF EXPERIMENTAL PROCEDURE.

DISCUSSION OF EXPERIMENTAL PROCEDURE.

This chapter also includes the discussion of several factors which might have been thought to influence the experimental results.

Furnace deposits.

In the experimental runs in which crucibles of type 'B' were used, it was noted that the volume of furnace deposit was greatly reduced and in many cases apparently eliminated. It is now thought that the vast majority of the furnace deposit formed in runs 1 - 12 was caused by the reaction between the mullite thermocouple sheath and the top of the graphite crucible. Crucibles of type 'A' were, in the circumstances, slightly too large for the reaction chamber. As a result the gap between the thermocouple sheath and the top of the crucible was very small indeed and any softening of the sheath caused actual contact between the two. Slow reaction then took place between the mullite and graphite producing carbon monoxide and silicon monoxide. This silicon monoxide was free to diffuse away from the zone of reaction and furnace deposits caused by the condensation and oxidation of this silicon monoxide were also free to form.

The crucibles of type 'C' occupied less space in the reaction chamber and the gap between mullite and graphite could therefore be greatly increased. The volume of furnace deposit formed in these cases thus showed only a slight increase on the volume formed when using crucibles of type 'B'.

Confirmation of the above reason is obtained from the observation that the volume of furnace deposit increased whenever reaction between the mullite thermocouple sheath and the top of a graphite crucible occurred.

The practical elimination of furnace deposit when using the alumina crucible 'B' also confirms that the crucible caps or stoppers effectively prevented the 'free diffusion' of silicon monoxide away from the crucible contents.

Adsorption and desorption.

It is seen from the results of the blank runs with crucibles of types 'A' and 'B' that the presence of a large amount of graphite in the system was the cause of much of the adsorption and desorption of gases. The mass of graphite in the system was greatly decreased when crucibles of types 'B' and 'C' were used, and since the rate of formation of furnace deposits had also been

greatly decreased, the eventual discovery that degassing could be dispensed with, was not altogether surprising.

Adsorption and desorption caused by the actual walls of the reaction chamber was apparently comparatively small.

The graphite - 'mullite' reaction.

The reaction between graphite and mullite has been examined experimentally and gives an equilibrium reaction pressure of 0.3 - 0.4 atm. carbon monoxide.

The criticism could be made that this 'external' reaction can have an effect on the value of the equilibrium pressure of the system, the effect being to increase the silica activities of slags having a 'true' equilibrium pressure of less than 0.3 - 0.4 atm. carbon monoxide. This criticism is unfounded, however, as in the runs where a crucible of type 'B' was used, reaction between mullite and graphite was impossible. The results of these runs were completely consistent with the results obtained when a graphite crucible of type 'C' was used. Not only is the general consistency of results to be noted, but in nearly every case where the determination involved a silica saturated slag, the reaction pressure

of the standard silica run was repeated. It has also been mentioned in a previous section that the 'external' graphite-mullite reaction had been all but eliminated.

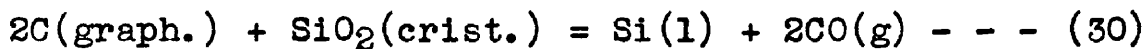
The general agreement of the present results with those of Baird and Taylor¹⁵ indicate that even when graphite crucibles of type 'A' were used, the mullite-graphite reaction had no effect on the equilibrium study.

Reaction between alumina and silicon carbide.

The reaction between alumina and silicon carbide in the presence of carbon monoxide, enables graphite and 'mullite' to be formed. This would tend to lower the equilibrium pressure of slags whose 'true' equilibrium pressure was greater than 0.3 - 0.4 atm. carbon monoxide. The results of determinations where the presence of alumina and silicon carbide together was impossible are in complete agreement with the rest of the results. The possibility of such a reaction influencing the experimental results can thus be dismissed.

The effect of evacuation on the system.

In a recent paper, Chipman¹⁸ has suggested that the continuous evacuation of the system while the temperature was being raised to 1100°C caused the reaction



to proceed from left to right. A significant amount of silicon would then be formed and on the admittance of carbon monoxide the above reaction would be reversed and a dynamic equilibrium set up between reaction (30) and reaction (1).



This suggestion would then satisfactorily account for the much lower reaction pressures recorded in the present investigation compared with those predicted by thermochemical data.

At the time of publication of this suggestion the time of continuous evacuation had already been cut to one half hour and the explanation appeared to be invalid as the results were consistent with those of previous runs.

As a check, however, the experimental procedure for run 34R was changed, as has been described. Each part of the reaction chamber was new and not even degassed. The only evacuations employed were connected with the admittance of carbon monoxide and these were purely momentary. The results of 34R are given in table 3 and they are seen to be in complete agreement with the rest of

the results.

Change in silica content of the slag.

The loss or gain in silica of the charge, caused by the reaction between silica, graphite, silicon carbide and carbon monoxide, could become significant if the net change in reaction pressure was too large.

On determination of the volume of the system it was found that a change in the reaction pressure of 1 cm. Hg corresponded theoretically to $0.36 \cdot 10^{-2}$ gms. of silica. The compact usually contained 4 gms. of slag and a net pressure change of 10 cms. Hg corresponded to a change of approximately 0.5% in the silica content of a slag originally containing 50 wt.% silica. The net pressure change was seldom more than 10 cms. Hg and an error of $\pm 0.5\%$ silica is placed on the slag composition.

Experimental accuracy.

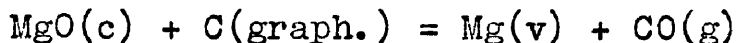
In the determination of the free energy change of reaction (1), errors in the measurement of the equilibrium pressure and the temperature must be taken into account. The estimated errors in these measurements have been given under the appropriate sections and on their combination by the 'method of squares' it can be calculated

that the error in the experimental work amounts to less than ± 500 cal.

It is not proposed to place any figure on the accuracy of the silica activities as the value would be of doubtful significance. A general indication however, can be obtained from the experimental results given in the next chapter. These results are consistent and give good agreement with other independent data.

The effect of oxide additions on the standard reaction.

It has been calculated from thermodynamic data that the equilibrium pressures of carbon monoxide obtained in the present work are too high to allow the formation of aluminium or calcium carbide. Available thermodynamic data indicate that magnesium carbide is thermodynamically unstable but the possible effect of the reaction



must be considered. The vapour pressure of magnesium over pure magnesia has been estimated as 1.2 mm. Hg at 1800°K. The uncertainty of this value is very high and no correction has been made for the effect of this reaction. It is possible, however, that there is an appreciable error in the silica activities of slags near magnesia saturation but at lower magnesia activities any such error must be well within the limits of experimental accuracy.

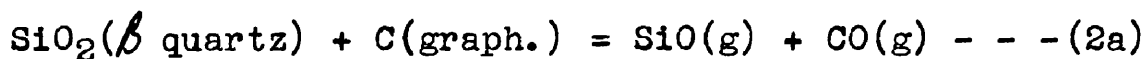
CHAPTER IV.

RESULTS.

RESULTS.STANDARD SILICA RUNS.

The equilibrium partial pressures of carbon monoxide over compacts containing pure silica are shown in table 2.

These have been obtained from the measured equilibrium reaction pressures ($p_{CO} + p_{SiO}$) using the free energy change for reaction (2a), given by equation (D) in the appendix.



$$\Delta_{2a} G_T^0 = + 154,400 - 78.99T \text{ cal./mol.}, (1600-1883^\circ K) \quad \text{--- (D)}$$

In the presence of solid quartz and solid graphite the equilibrium constant reduces to $K_{2a} = p_{CO} \cdot p_{SiO} \text{ atm.}^2$.

Values of this constant obtained from equation (D) are $4.79 \cdot 10^{-3}$, $1.70 \cdot 10^{-2}$ and $5.62 \cdot 10^{-2}$ at 1450, 1500 and 1550°C respectively. Values of p_{SiO} and hence p_{CO} are obtained by approximating ($p_{CO} + p_{SiO}$) to p_{CO} in the above constants.

The values of $\log_{10} p_{CO}$ are plotted against $1/T^\circ K$ in fig. 3 and the relationship may be represented by the linear equation

$$\log_{10} p_{CO} = - 15,950/T + 8.874, (1705 - 1828^\circ K) \quad \text{--- (5a)}$$

Also plotted in fig. 3 is the relationship obtained by Baird and Taylor¹⁵, $\log_{10} p_{CO} = -16,150/T + 8.950$.

Table 2. - Equilibrium partial pressures of carbon monoxide for $\text{SiO}_2(\text{quartz}) + \text{C}(\text{graph.}) + \text{SiC}(\beta)$ compacts.

Run No.	%CO	$p_{\text{CO}}+p_{\text{SiO}}$ atm.	p_{CO} atm.	$T^{\circ}\text{K.}$	$1/T^{\circ}\text{K}$	$\log_{10}p_{\text{CO}}$
16	97.0	0.449	0.437	1727	0.5790	-0.360
	99.0	0.436	0.424	1727	0.5790	-0.373
	98.9	0.440	0.427	1728	0.5787	-0.369
17	98.1	0.812	0.789	1777	0.5627	-0.103
	98.9	0.776	0.754	1773	0.5640	-0.123
	98.6	0.801	0.779	1775	0.5634	-0.108
	98.6	0.344	0.335	1705	0.5865	-0.475
	97.3	0.327	0.318	1703	0.5872	-0.497
18	96.0	0.427	0.416	1722	0.5807	-0.381
	98.3	0.413	0.402	1722	0.5807	-0.396
	99.3	1.444	1.400	1828	0.5470	+0.146
	98.3	1.418	1.374	1827	0.5473	+0.138
	98.8	1.430	1.388	1826	0.5476	+0.143
	98.9	0.462	0.450	1729	0.5784	-0.347

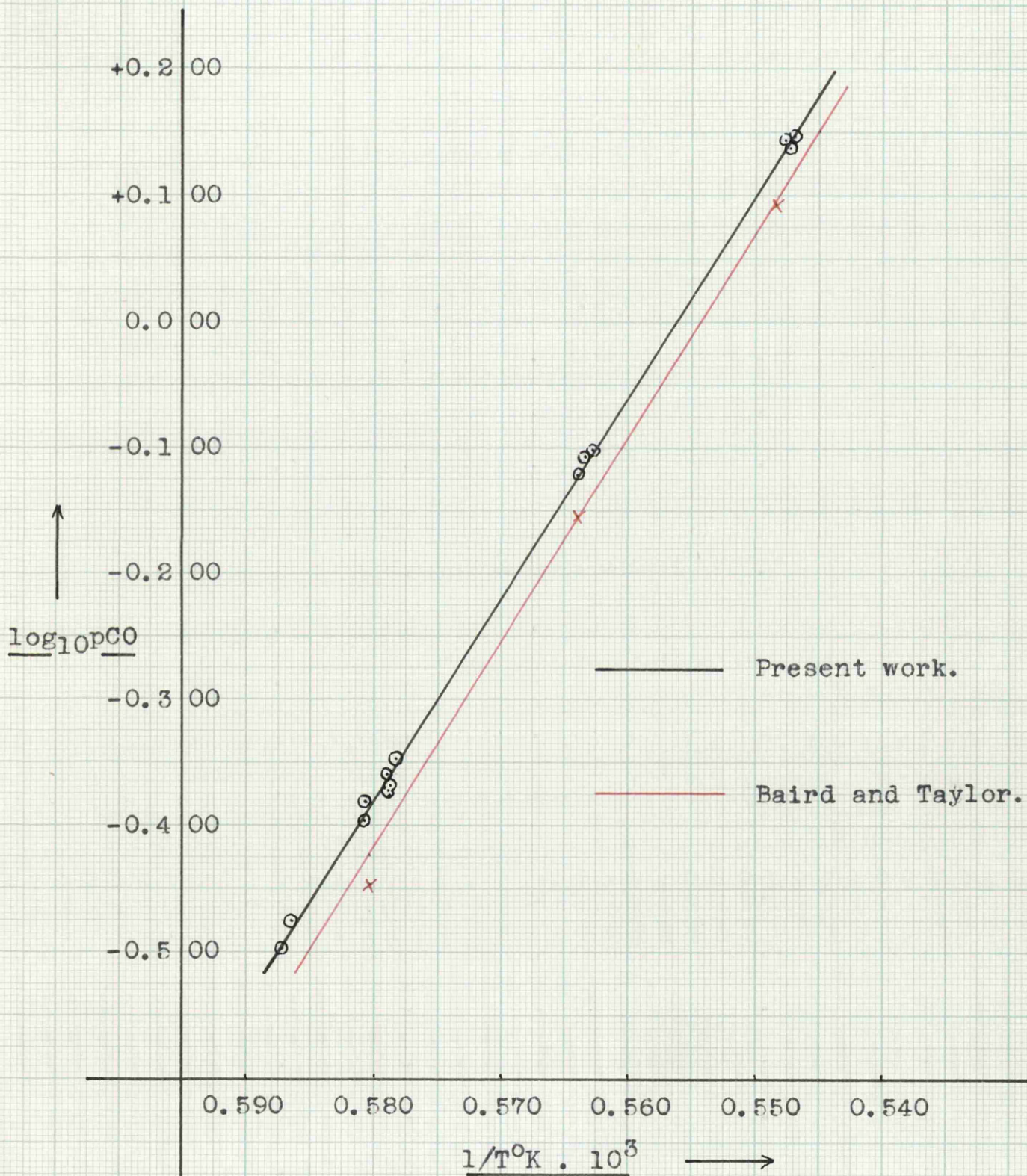
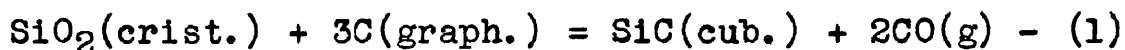


Fig. 3 . Graph of $\log_{10} p_{CO}$ against $1/T^{\circ}K$ for the reaction : $SiO_2 + 3C = SiC + 2CO$

The free energy change for reaction (1) can be obtained from equation (5a)



$$\Delta_1 G_T^0 = + 146,010 - 81.22T \text{ cal./mol.}, (1705-1828^\circ\text{K}) - (6a)$$

The free energy of formation of cubic silicon carbide can be obtained by combining equation (6a) with the free energies of formation of carbon monoxide and quartz given by equations (C) and (A) respectively, in the appendix.



$$\Delta_7 G_T^0 = -17,170 + 6.92T \text{ cal./mol.}, (1705-1828^\circ\text{K}) - - - (8a)$$

Using the entropy of formation at 1800°K given by table H in the appendix, equation (8a) can be adjusted to give

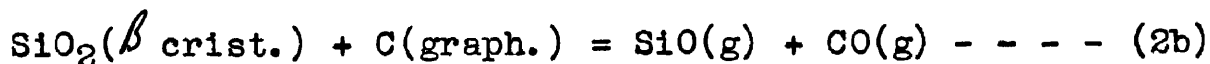
$$\Delta_7 G_T^0 = - 20,450 + 8.74T \text{ cal./mol.}, (1705-1828^\circ\text{K}) - - - (8b)$$

The heat of formation of cubic silicon carbide is thus - 20,450 cal./mol. at 1800°K and with the aid of the enthalpy increments used in the compilation of table H the heat of formation of cubic silicon carbide at 298°K is calculated as $\Delta H_{298}^0 = - 8,700 \text{ cal./mol.}$

The heat of formation determined thermochemically by Humphrey et al⁷ is $\Delta H_{298}^0 = -13.0 \pm 1 \text{ k.cal./mol.}$ On the assumption that the present experimental results are accurate, the difference between these two values must be made up of the errors in the thermodynamic and

thermochemical data employed in their calculation. This question will be discussed more fully at a later stage.

The equilibrium partial pressures of carbon monoxide may also be resolved from the measured reaction pressures ($p_{\text{SiO}} + p_{\text{CO}}$) by using equation (E) in the appendix.



$$\Delta_{2b} G_T^{\circ} = + 154,100 - 79.16 \text{ cal./mol.}, (1600-1900^{\circ}\text{K}) - (E)$$

This anomaly arises from the fact that the free energies of formation of quartz and cristobalite should be almost identical in the experimental temperature range. Unfortunately the thermochemical data is inaccurate, the free energies of formation differing by about 600 cal., and it is not known which value approaches the true free energy change.

The use of equation (E) yields the following results,

$$\log_{10} p_{\text{CO}} = - 15,930/T + 8.860, (1705-1828^{\circ}\text{K}) - (5b)$$

$$\Delta_1 G_T^{\circ} = + 145,810 - 81.10T \text{ cal./mol.}, (1705-1828^{\circ}\text{K}) - - (6b)$$

$$\Delta_7 G_T^{\circ} = - 19,900 + 8.74T \text{ cal./mol.}, (1705-1828^{\circ}\text{K}) - - (8c)$$

The heat of formation of cubic silicon carbide derived from equation (8c) is $\Delta H_{298}^{\circ} = - 8,150 \text{ cal./mol.}$

On inspection of equation (6a) and (6b) it can be seen that they yield the same free energy values in the experimental temperature range. This establishes the

important fact that these equations are practically independent of any moderate error in the data employed in their derivation.

CALCULATION OF SILICA ACTIVITIES.

In the presence of solid graphite, silicon carbide and silica, the equilibrium constant for reaction (1) reduces to $K_1 = p^2\text{CO}(\text{standard})$. The values of K_1 obtained from equation (5a), at 1450, 1500 and 1550°C are 0.170, 0.567 and 1.767 respectively.

For a given slag in the presence of solid graphite and silicon carbide the partial pressure of carbon monoxide is obtained from the measured equilibrium reaction pressure ($p_{\text{CO}} + p_{\text{SiO}}$) and the free energy change for reaction (3). This is obtained from equation (6a) and equation (D) given in the appendix.



$$\Delta_3 G_T^0 = - 8,430 - 2.23T \text{ cal/mol.}, (1705 - 1828^\circ\text{K}) \quad \text{--- (10)}$$

Values of $K_3 = p_{\text{CO}}/p_{\text{SiO}}$ obtained from equation (10), at 1450, 1500 and 1550°C are $2.77 \cdot 10^{-2}$, $2.97 \cdot 10^{-2}$ and $3.17 \cdot 10^{-2}$ respectively.

In the presence of solid graphite and silicon carbide the silica activity of any slag is given by the equation

$$a_{\text{SiO}_2} = p^2\text{CO}(\text{slag})/p^2\text{CO}(\text{standard}) \quad \text{--- (9)}$$

THE CaO-SiO₂ and CaO-Al₂O₃-SiO₂ SYSTEMS.

The silica activities of liquid slags in the CaO-SiO₂ system are given in table 3 and fig. 5. The slags investigated contained 0.6% Al₂O₃ but in the present work they are considered as simple binary slags. The slag compositions given in table 3 refer to the liquid slag and in the case of slags in equilibrium with a solid phase at the experimental temperature, the liquid compositions have been obtained from the phase diagram.

The CaO-Al₂O₃-SiO₂ phase diagram is shown in fig. 4,¹⁹ and the silica activities of liquid slags in this system are given in table 3 and figs. 5, 6, 7, 8, 9, 10 and 11. The actual temperatures at which the determinations were made are given in table 3 and the silica activities calculated from data corresponding to these temperatures were then taken uncorrected as applying to one of the three 'rounded' temperatures i.e. 1450, 1500 or 1550°C. Figs. 5, 6, 7 and 8 also show silica activities at 1600 and 1700°C which have been obtained by extrapolation of the present results. These are considered in a later section.

Table 4 gives the activities of calcium orthosilicate in binary CaO-SiO₂ slags at 1500 and 1550°C, calculated from the binary silica activities by the Gibbs-Duhem

Table 3. - Silica activities of CaO-Al₂O₃-SiO₂ slags.

1450°C.

Run No.	Liquid slag comp.			t°C	pSiO+pCO atm.	pCO atm.	aSiO ₂
	CaO	wt.% Al ₂ O ₃	SiO ₂				
34	1-38.1	0.6	61.3	1451	0.423	0.411	0.967
34R	1-38.1	0.6	61.3	1451	0.428	0.416	0.989
35	1-37.8	1.0	61.2	1448	0.405	0.394	0.958
36	1-38.5	5.2	56.3	1450	0.390	0.379	0.863
37	1-54.0	1.0	45.0	1449	0.146	0.142	0.122
38	2-54.0	3.0	43.0	1450	0.137	0.133	0.104
13	36.5	11.0	53.5	1451	0.330	0.321	0.589
13R	36.5	11.0	53.5	1447	0.326	0.317	0.635
14	21.7	11.0	68.3	1455	0.470	0.456	1.081
14R	21.7	11.0	68.3	1452	0.434	0.422	0.993
15	31.6	11.0	58.4	1455	0.402	0.391	0.793
24	35.2	11.0	53.8	1452	0.356	0.436	0.667
25	49.8	11.0	39.2	1448	0.120	0.117	0.084
26	28.0	11.0	61.0	1449	0.401	0.390	0.915
27	42.5	11.0	46.5	1450	0.213	0.207	0.255
19	28.4	21.0	50.6	1449	0.316	0.307	0.568
20	19.5	21.0	59.5	1451	0.393	0.382	0.834
21	37.0	21.0	42.0	1448	0.195	0.189	0.223
23	10.8	20.8	68.4	1447	0.390	0.379	0.907
28	13.0	29.0	58.0	1451	0.362	0.352	0.708
29	23.0	24.0	53.0	1454	0.351	0.341	0.619
30	29.4	30.4	40.2	1453	0.225	0.219	0.261
31	36.5	30.0	33.5	1448	0.121	0.117	0.085
32	26.8	41.2	32.0	1449	0.166	0.161	0.165
*	47.0	16.8	36.2	1450	0.082	0.080	0.046
*	47.0	16.8	36.2	1450	0.090	0.087	0.055
*	43.4	19.4	38.5	1450	0.117	0.114	0.093
*	38.8	19.5	42.0	1450	0.173	0.168	0.204
*	35.7	19.6	45.0	1450	0.218	0.212	0.324
*	27.2	19.7	54.0	1450	0.299	0.290	0.606
*	11.0	19.9	69.5	1450	0.363	0.352	0.893

* - Results of Baird and Taylor.

1 - CS sat^d.

2 - C₂S sat^d.

Table 3. - Silica activities of CaO-Al₂O₃-SiO₂ slags.1500°C.

Run No.	Liquid slag comp.			t°C.	pSiO+pCO atm.	pCO atm.	aSiO ₂
	CaO	wt.% Al ₂ O ₃	SiO ₂				
34	38.1	0.6	61.3	1499	0.744	0.722	0.941
34R	38.1	0.6	61.3	1499	0.728	0.706	0.901
35	1-41.9	0.6	57.5	1496	0.619	0.600	0.698
36	1-43.0	2.8	54.2	1497	0.575	0.558	0.589
37	1-51.8	0.7	47.5	1499	0.313	0.304	0.166
38	2-55.5	0.6	43.9	1499	0.259	0.251	0.114
13	36.5	11.0	53.5	1505	0.604	0.586	0.539
13R	36.5	11.0	53.5	1499	0.608	0.590	0.629
14	21.7	11.0	68.3	1501	0.782	0.759	0.969
14R	21.7	11.0	68.3	1498	0.742	0.720	0.945
15	31.6	11.0	48.4	1503	0.696	0.675	0.749
24	35.2	11.0	53.8	1498	0.597	0.579	0.605
25	49.8	11.0	39.2	1499	0.217	0.211	0.084
26	28.0	11.0	61.0	1497	0.688	0.664	0.835
27	42.5	11.0	46.5	1500	0.367	0.356	0.226
19	28.4	21.0	50.6	1506	0.539	0.523	0.420
20	19.5	21.0	59.5	1499	0.652	0.632	0.722
21	37.0	21.0	42.0	1499	0.318	0.309	0.172
22	47.2	18.0	34.8	1503	0.189	0.183	0.053
23	10.8	20.8	68.4	1499	0.691	0.671	0.813
28	14.0	31.0	55.0	1498	0.620	0.602	0.669
29	22.4	27.4	50.2	1498	0.558	0.542	0.542
30	29.2	30.6	40.2	1497	0.413	0.406	0.311
31	36.8	30.4	32.8	1498	0.191	0.185	0.063
32	26.8	41.2	32.0	1497	0.308	0.300	0.169
*	45.0	19.0	35.0	1500	0.148	0.143	0.042
*	43.4	19.5	38.5	1500	0.206	0.199	0.081
*	38.8	19.4	42.0	1500	0.314	0.304	0.189
*	35.7	19.6	45.0	1500	0.380	0.368	0.276
*	27.2	19.7	54.0	1500	0.539	0.521	0.544
*	27.2	19.7	54.0	1500	0.532	0.515	0.542
*	11.0	19.9	69.5	1500	0.656	0.635	0.824

* - Results of Baird and Taylor.

1 - CS sat^d.2 - C₂S sat^d.

Table 3. - Silica activities of CaO-Al₂O₃-SiO₂ slags.1550°C.

Run No.	Liquid slag comp.			t°C.	pSiO+pCO atm.	pCO atm.	aSiO ₂
	CaO	wt.% Al ₂ O ₃	SiO ₂				
34	38.1	0.6	61.3	1548	1.172	1.135	0.762
34R	38.1	0.6	61.3	1548	1.175	1.138	0.766
35	42.5	0.6	56.9	1547	1.002	0.970	0.569
36	46.9	0.6	52.5	1548	0.694	0.672	0.267
37	51.4	0.6	48.0	1549	0.577	0.558	0.180
38	55.8	0.6	43.6	1549	0.420	0.407	0.096
13	36.5	11.0	53.5	1556	1.027	0.994	0.490
13R	36.5	11.0	53.5	1558	1.017	0.984	0.460
14	21.7	11.0	68.3	1555	1.398	1.354	0.929
14R	21.7	11.0	68.3	1548	1.260	1.220	0.890
15	31.6	11.0	58.4	1554	1.169	1.132	0.664
24	35.2	11.0	53.8	1550	0.983	0.952	0.513
25	49.8	11.0	39.2	1548	0.375	0.363	0.078
26	28.0	11.0	61.0	1547	1.062	1.028	0.640
27	42.5	11.0	46.5	1549	0.590	0.571	0.189
19	28.4	21.0	50.6	1554	0.785	0.760	0.299
20	19.5	21.0	59.5	1548	1.071	1.037	0.636
21	37.0	21.0	42.0	1547	0.499	0.483	0.140
23	10.8	20.8	68.4	1549	1.200	1.121	0.764
28	14.0	31.0	55.0	1549	1.067	1.033	0.617
29	21.3	30.8	47.9	1549	0.890	0.862	0.430
30	29.2	30.6	40.2	1549	0.593	0.574	0.191
31	36.8	30.4	32.8	1546	0.309	0.299	0.055
32	26.8	41.2	32.0	1548	0.517	0.501	0.148
*	55.5	0.8	43.4	1550	0.419	0.404	0.108
*	51.3	0.8	47.7	1550	0.584	0.563	0.210
*	46.2	0.8	53.1	1550	0.735	0.709	0.332
*	41.4	0.7	58.8	1550	0.903	0.871	0.502
*	34.3	0.8	66.0	1550	1.158	1.117	0.823
*	46.7	20.3	33.5	1550	0.257	0.248	0.041
*	43.4	19.5	38.5	1550	0.365	0.352	0.082
*	38.8	19.4	42.0	1550	0.538	0.519	0.178
*	35.7	19.6	45.0	1550	0.645	0.622	0.256
*	27.2	19.7	54.0	1550	0.940	0.907	0.544
*	11.0	19.9	69.5	1550	1.135	1.095	0.794

* - Results of Baird and Taylor.

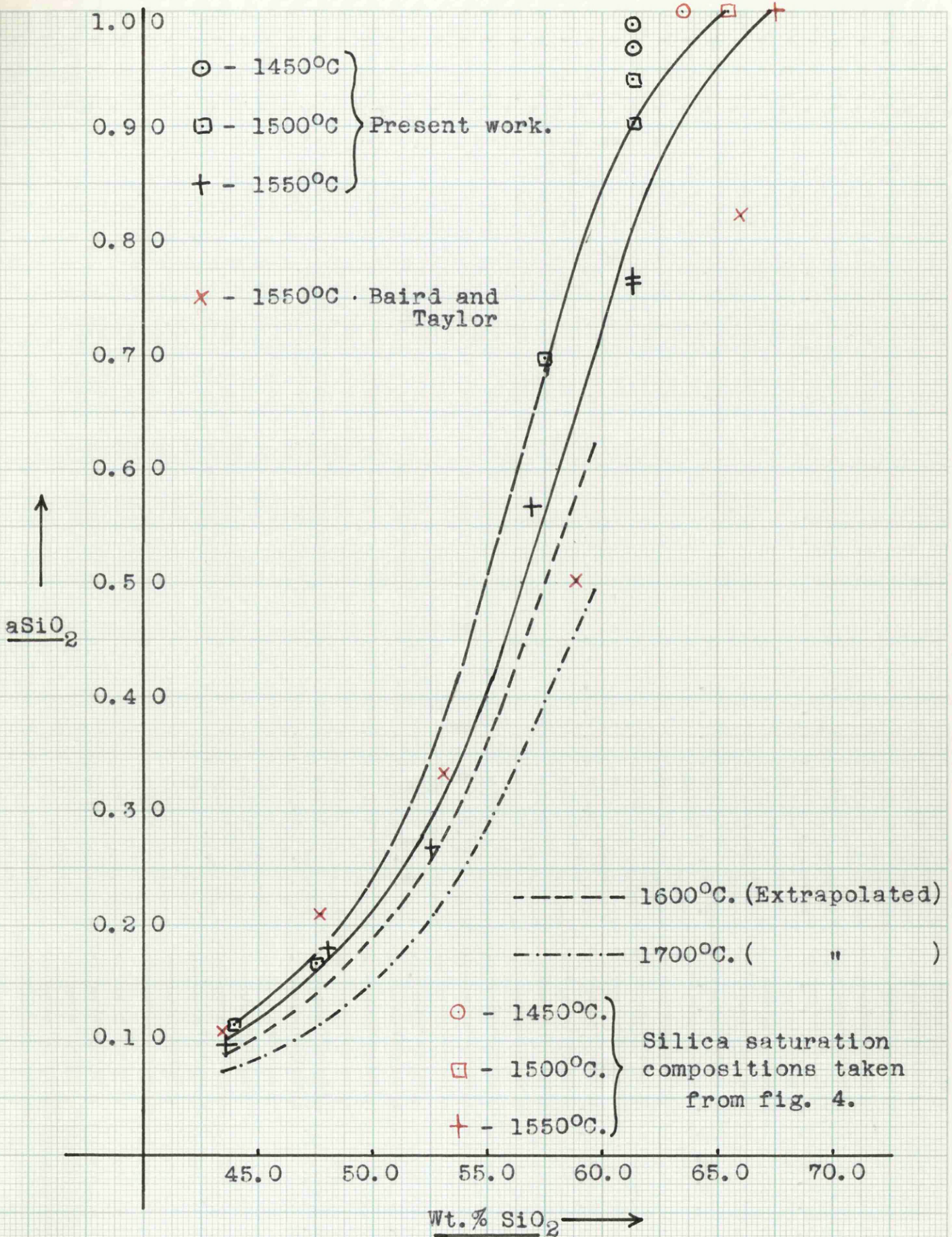


Fig. 5 - Silica activities of CaO-SiO₂ slags.

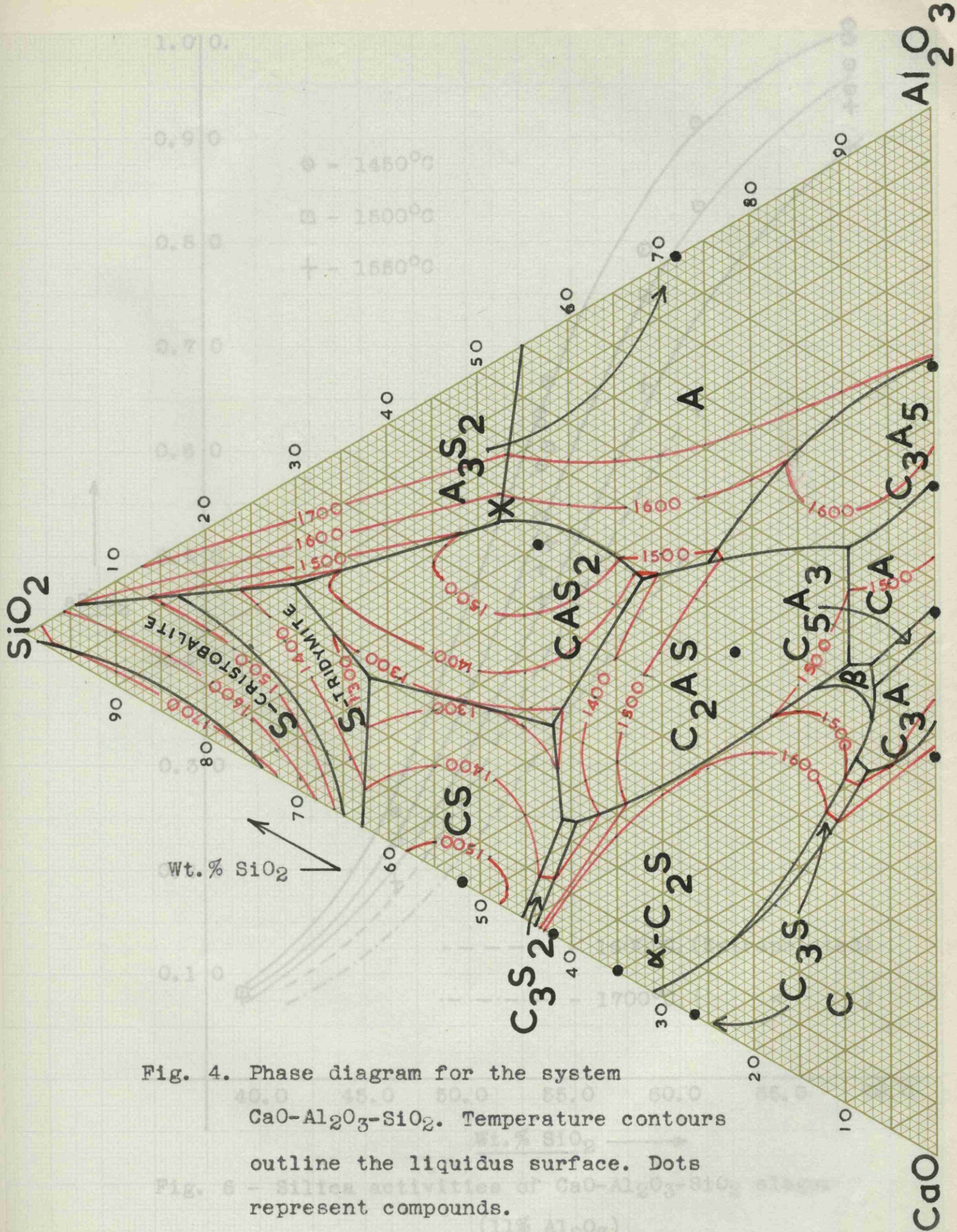


Fig. 4. Phase diagram for the system CaO-Al₂O₃-SiO₂. Temperature contours outline the liquidus surface. Dots represent compounds.

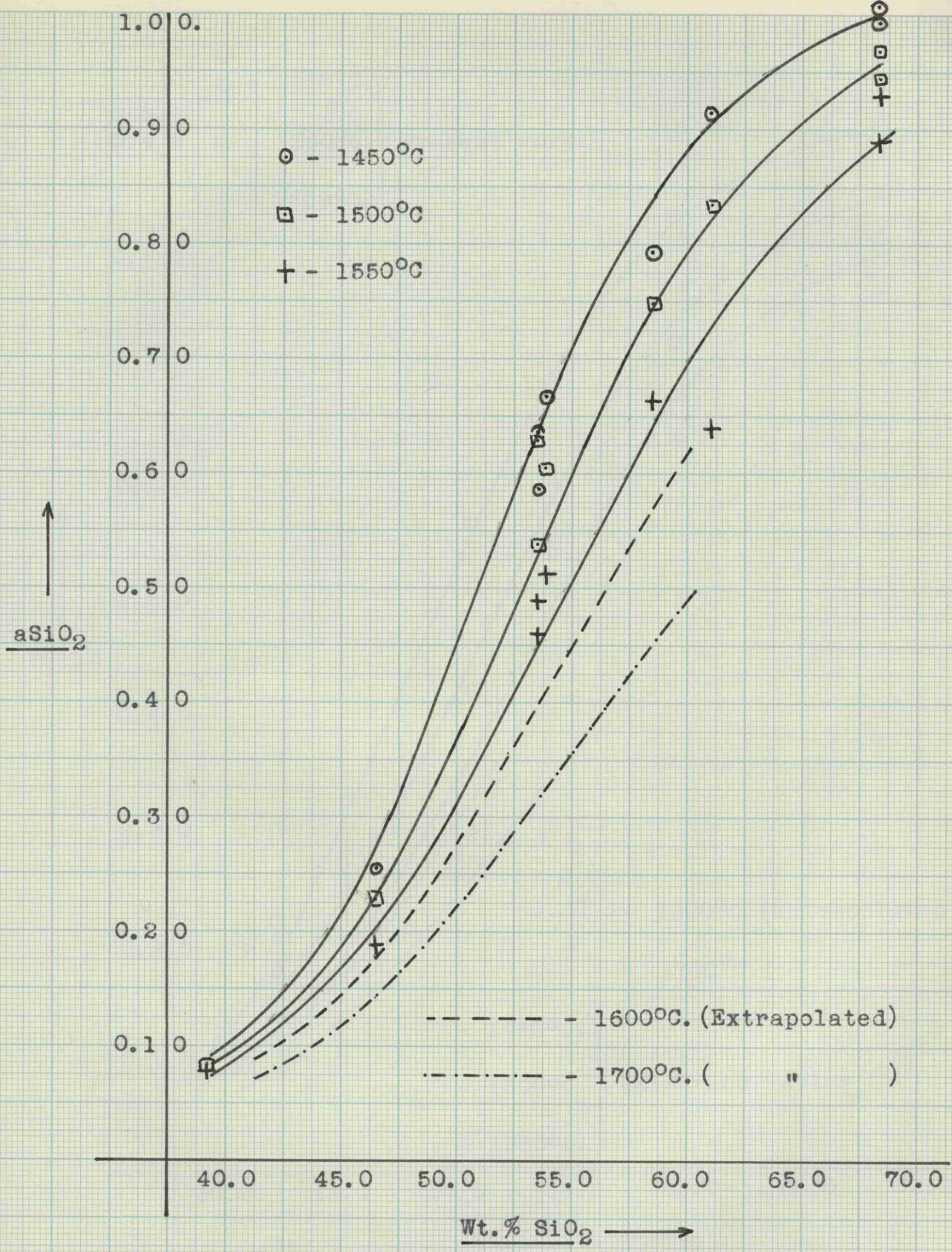


Fig. 6 - Silica activities of $CaO-Al_2O_3-SiO_2$ slags.
 (11% Al_2O_3)

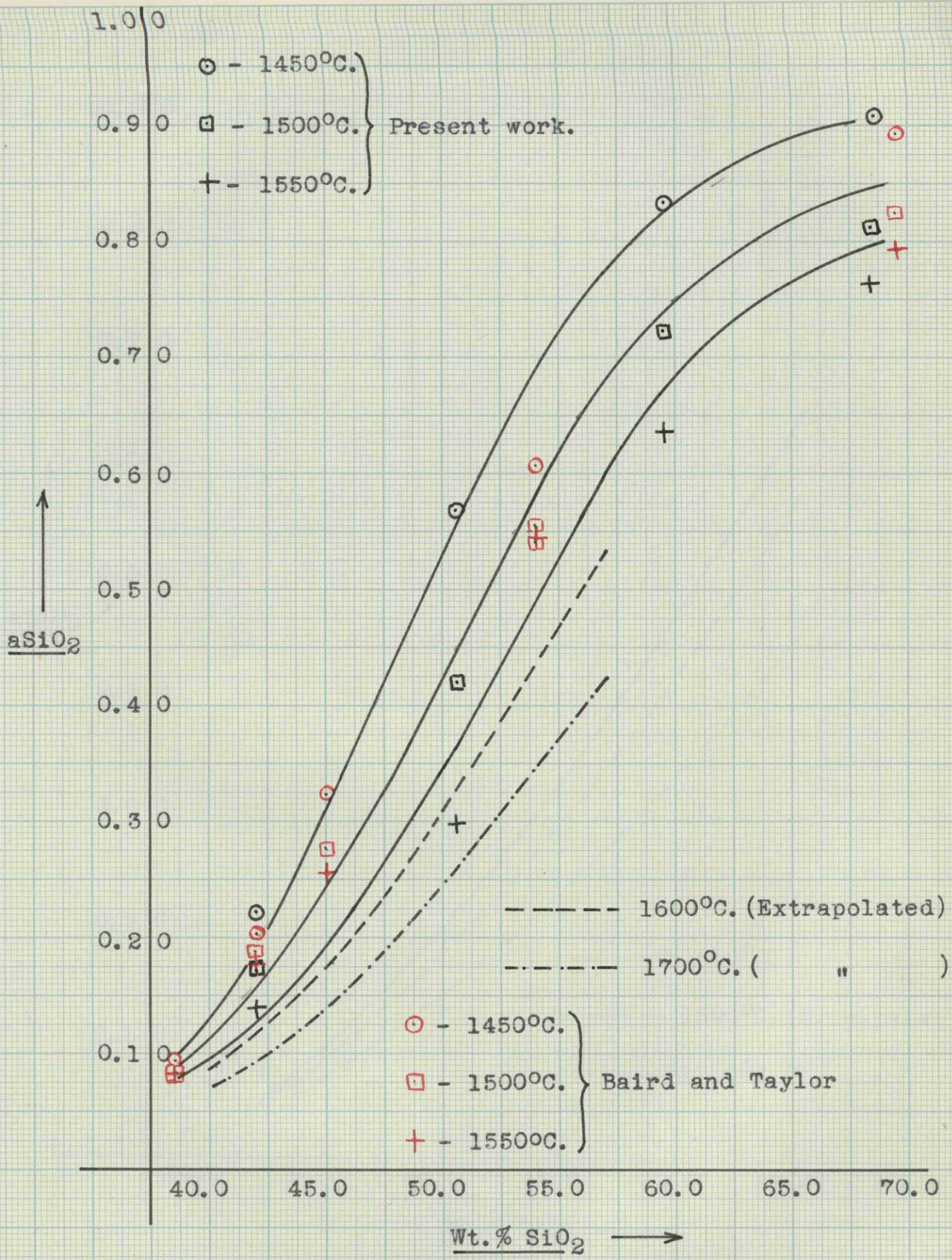


Fig.7 - Silica activities of CaO-Al₂O₃-SiO₂ slags.
(21% Al₂O₃)

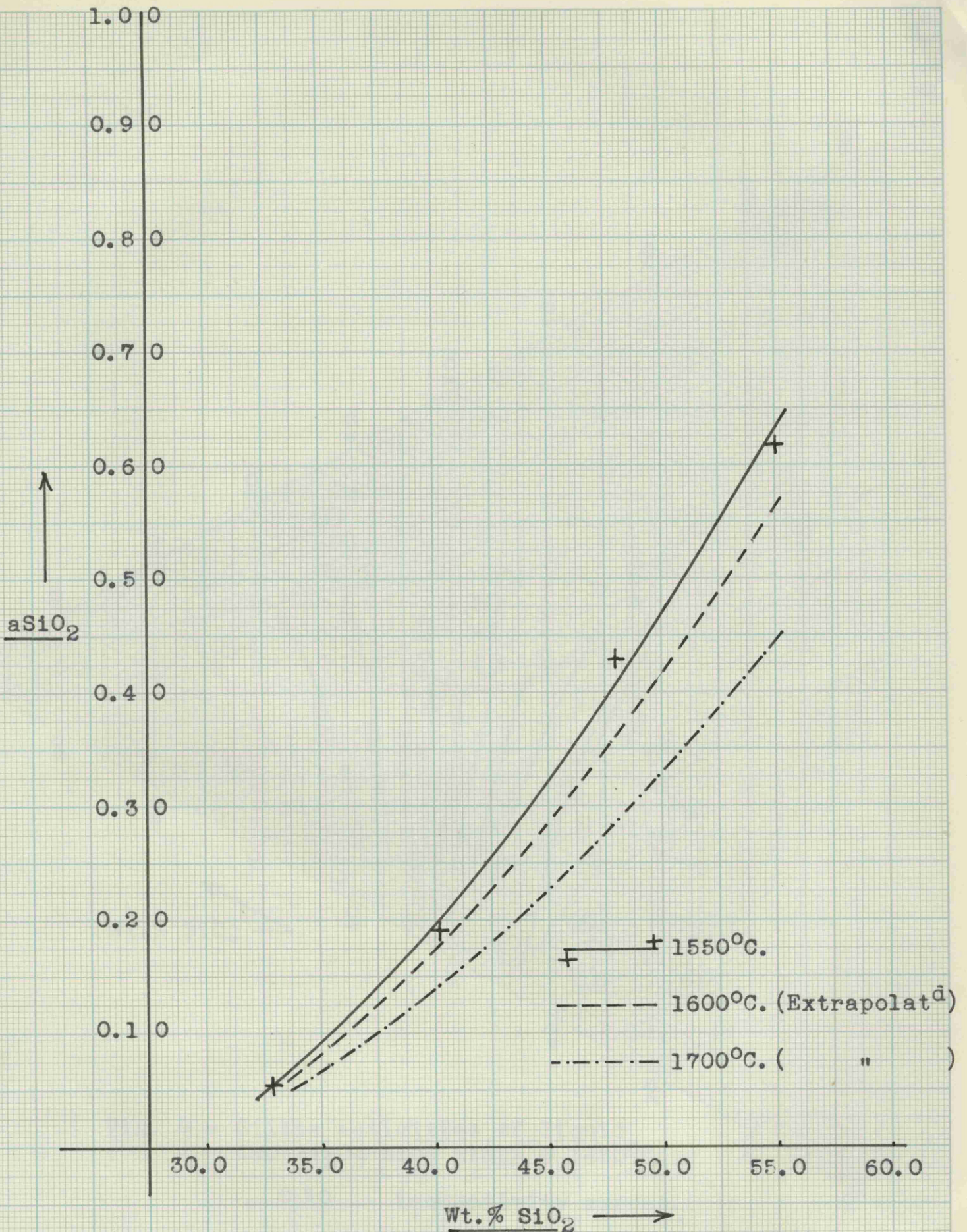


Fig. 8 - Silica activities in CaO- Al_2O_3 - SiO_2 slags.
(31% Al_2O_3)

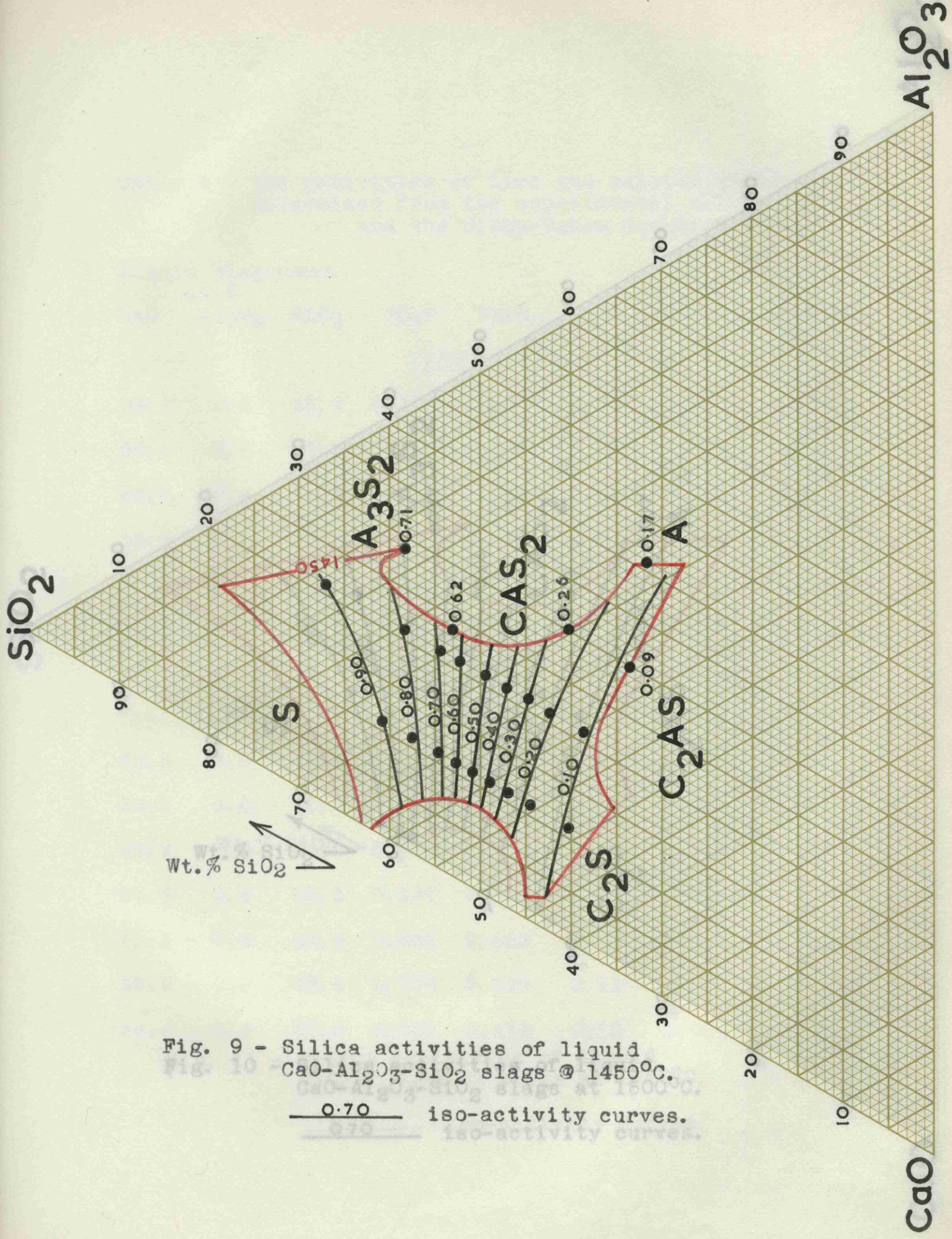


Fig. 9 - Silica activities of liquid CaO-Al₂O₃-SiO₂ slags @ 1450°C.

0.70 iso-activity curves.
 0.70 iso-activity curves.

Table 4 - The activities of lime and calcium orthosilicate determined from the experimental silica activities and the Gibbs-Duhem equation.

Liquid slag comp.

CaO	wt. % Al ₂ O ₃	SiO ₂	NCaO	NSiO ₂	aSiO ₂	aC ₂ S	aCaO
<u>1500°C.</u>							
33.7	0.6	65.7	0.356	0.644	1.00	0.060	0.002
38.1	0.6	61.3	0.398	0.598	0.90	0.078	0.003
42.5	0.6	56.9	0.442	0.553	0.65	0.160	0.004
46.9	0.6	52.5	0.487	0.509	0.34	0.370	0.009
51.4	0.6	48.0	0.532	0.463	0.19	0.680	0.016
55.8	0.6	43.6	0.576	0.420	0.12	1.000	0.025
<u>1550°C.</u>							
32.8	0.6	66.6	0.345	0.655	1.00	0.055	0.002
38.1	0.6	61.3	0.398	0.598	0.81	0.092	0.003
42.5	0.6	56.9	0.442	0.553	0.53	0.191	0.005
46.9	0.6	52.5	0.487	0.509	0.29	0.390	0.010
51.4	0.6	48.0	0.532	0.463	0.17	0.650	0.018
55.8	0.6	43.6	0.576	0.420	0.11	0.960	0.027
56.4	0.6	43.0	0.582	0.414	0.10	1.000	0.028

equation. Silica saturation and calcium orthosilicate saturation compositions were taken as the limits of integration. In fig. 12, silica and calcium orthosilicate activities are plotted against the silica mol. fraction. Also shown in fig. 12 are the results of Sakagami and Matsushita²⁰, and Chang and Derge²¹ which have been introduced at this stage in order to relieve the congestion in a later diagram.

Lime activities calculated from the calcium orthosilicate activities and the free energies of calcium ortho silicate given in the appendix are also tabulated in table 5 and plotted in fig. 13. It will be noticed in fig. 12 that the silica activity curve at 1500°C has been continued through the region of calcium metasilicate saturation. This enabled lime activities to be calculated at 1500°C and made possible direct comparison with the lime activities of Carter and Macfarlane²² which are also shown in fig. 13.

The free energy of formation of calcium metasilicate (X).

The slags of runs 37 and 38 may be considered to be in equilibrium with both the orthosilicate and the metasilicate. at 1450°C. This is only an approximation as the tricalcium silicate phase field intervenes between those

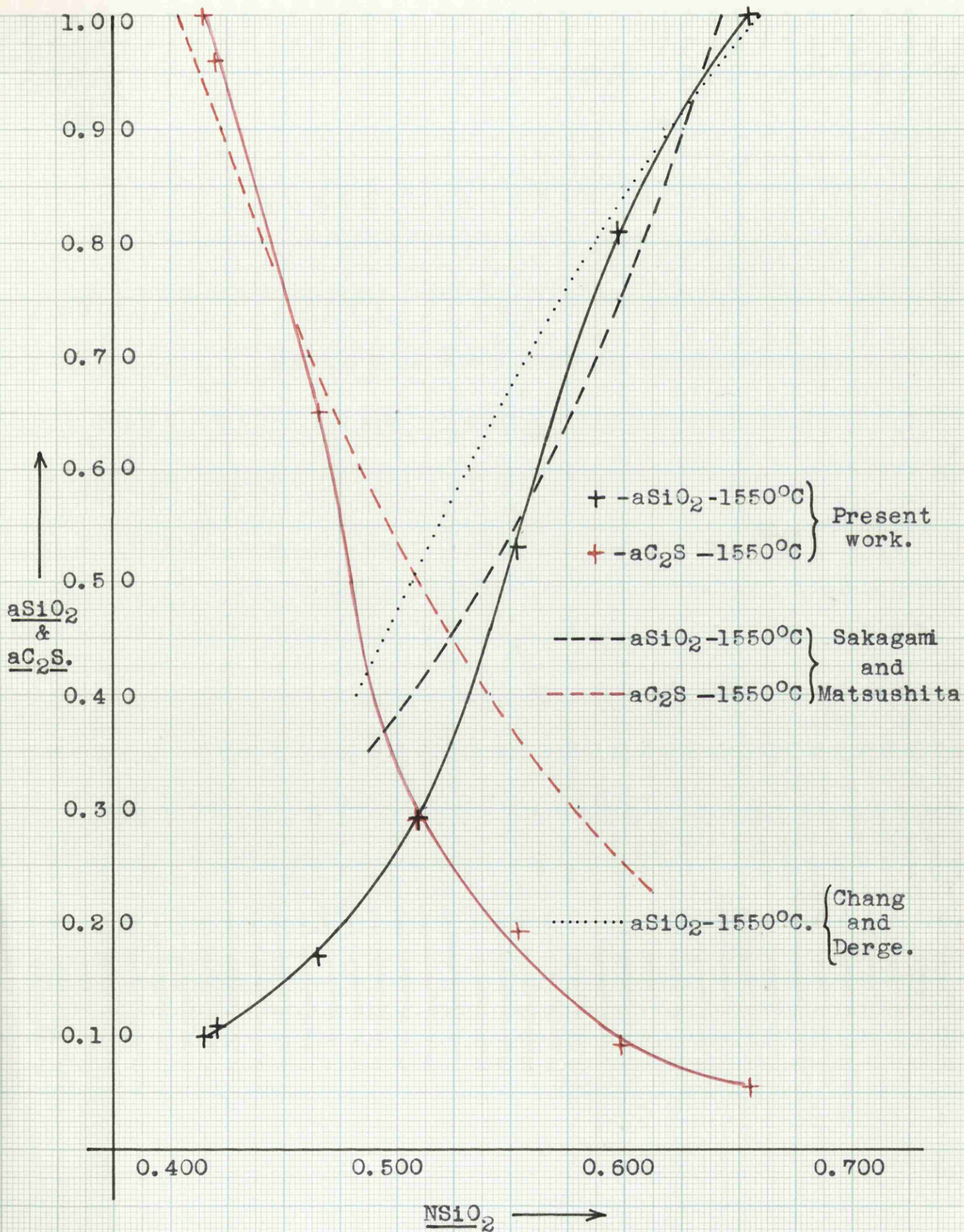


Fig. 12 - The activities of silica and calcium orthosilicate in liquid CaO-SiO₂ slags.

Table 5.- The lime activities of liquid slags in equilibrium with either calcium metasilicate or calcium orthosilicate.

Run No.	Liquid slag comp.						aCaO
	CaO	wt.% Al ₂ O ₃	SiO ₂	aSiO ₂	NSiO ₂	NCaO	
<u>1450°C.</u>							
34	1-38.1	0.6	61.3	0.97	0.598	0.398	0.003
35	1-37.8	1.8	61.2	0.96	0.597	0.395	0.003
36	1-38.5	5.2	56.3	0.86	0.560	0.410	0.003
37	1-54.0	1.0	45.0	0.12	0.434	0.558	0.021
38	2-54.0	3.0	43.0	0.10	0.423	0.577	0.023
<u>1500°C.</u>							
35	1-41.9	0.6	57.5	0.70	0.560	0.436	0.004
36	1-43.0	2.8	54.2	0.59	0.529	0.450	0.005
37	1-51.8	0.7	47.5	0.17	0.459	0.536	0.018
38	2-55.5	0.6	43.9	0.11	0.419	0.575	0.025

1 - CaO.SiO₂ saturated.

2 - 2CaO.SiO₂ saturated.

----- 1500°C - Carter and Macfarlane.

Present work.

- - 1500°C.)
 - + - 1550°C.)
 - - 1450°C.)
 - - 1500°C.)
 - - 1500°C. C₂S saturated slag.
 - △ - 1435°C CS and SiO₂ saturated slag.
- } Gibbs-Duhem.
- } CS saturated slags.

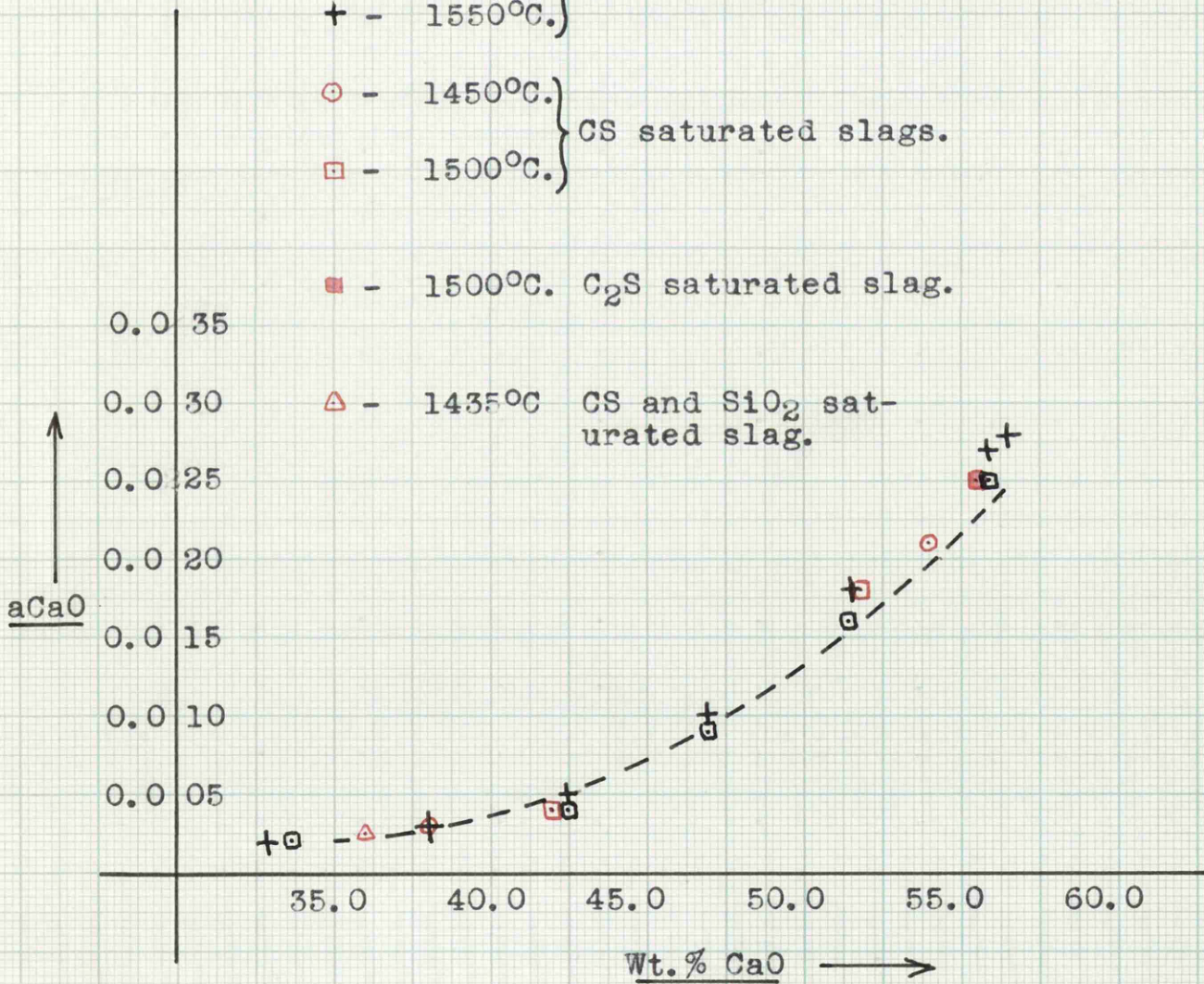
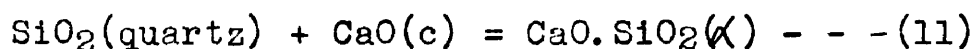


Fig. 13 - Lime activities of CaO-SiO₂ slags.

of the orthosilicate and metasilicate. Using the free energy of formation of calcium orthosilicate given in the appendix and the experimentally determined silica activities, lime activities of 0.021 and 0.023 are calculated. The mean free energy of formation of calcium metasilicate calculated from the lime and silica activities is - 20,500 cal./mol.



$$\Delta_{11} G_{T=1723}^{\circ} = - 20,500 \text{ cal./mol.} \quad \text{--- (12)}$$

The free energy of formation of calcium metasilicate can also be obtained at 1500°C using the experimentally determined silica activities and the lime activities derived by the Gibbs-Duhem equation. As can be seen from the CaO-SiO₂ join in fig. 4, the boundaries of the metasilicate field are 58.0% SiO₂, 42.0% CaO and 47.5% SiO₂, 52.5% CaO at 1500°C. The silica activities at these compositions are 0.71 and 0.18 respectively, and the corresponding lime activities are 0.004 and 0.017. These values lead to a mean free energy of formation of calcium metasilicate from the constituent oxides of -20,550 cal./mol. Comparison with equation(12) indicates that the temperature effect is small and a value of -20,500 cal./mol. is adopted in the experimental temperature range (1723 - 1823°K).

Slags in equilibrium with CaO.SiO₂ at 1450 and 1500°C.

In the presence of solid calcium metasilicate the equilibrium constant for equation (11) reduces to $K_{11} = 1/a_{CaO} \cdot a_{SiO_2}$ and values of this constant obtained from equation (12) are $3.98 \cdot 10^2$ and $3.36 \cdot 10^2$ at 1450 and 1500°C respectively. Using these values and the experimentally determined silica activities, the lime activities of slags in equilibrium with the metasilicate are calculated at 1450 and 1500°C. The activities obtained are tabulated in table 5 and plotted in fig. 13.

Slag in equilibrium with silica and CaO.SiO₂.

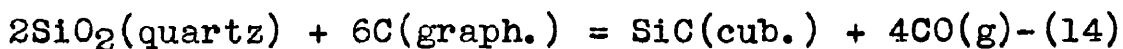
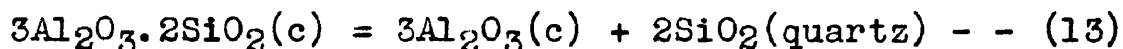
The binary CaO-SiO₂ phase diagram shows a eutectic between liquid slag, metasilicate and silica at a temperature of 1435°C and a composition of 36% CaO, 64% SiO₂. Under these conditions $K_{11} = 1/a_{CaO}$ and if the eutectic temperature is taken as 1450°C a lime activity of $2.5 \cdot 10^{-3}$ is obtained. This value, although approximate, is plotted also in fig. 13.

In all calculations involving slags which are in equilibrium with calcium orthosilicate and/or calcium metasilicate it is assumed that these compounds are stoichiometric.

The silica activity of 'mullite' ($3\text{Al}_2\text{O}_3 \cdot 2\text{SiO}_2$).

The general significance of the silica activity of 'mullite' is first considered in this section before the actual results are given.

In the determination of the silica activity of 'mullite' the following reactions may be considered,



A phase diagram of the Al_2O_3 - SiO_2 system, based on that of Aramaki and Roy²⁴, is given in figure 14. The only addition to the diagram of these workers, the eutectoid at 1240°C , is discussed in a later section. Slags in the 'mullite' + corundum (Al_2O_3) phase field have a constant silica activity and slags in the silica + 'mullite' phase field have a silica activity of unity. In the 'mullite' phase field the silica activity is not constant and drops in value as 'mullite' compositions move from the silica phase boundary to the alumina phase boundary. This provides a convenient method for the determination of the boundaries of the 'mullite' phase field in the Al_2O_3 - SiO_2 system. During the determination of the silica activity of a mullite in equilibrium with silica, reaction (14) can be allowed to proceed from left to right causing a loss of silica from the system. Thus, as

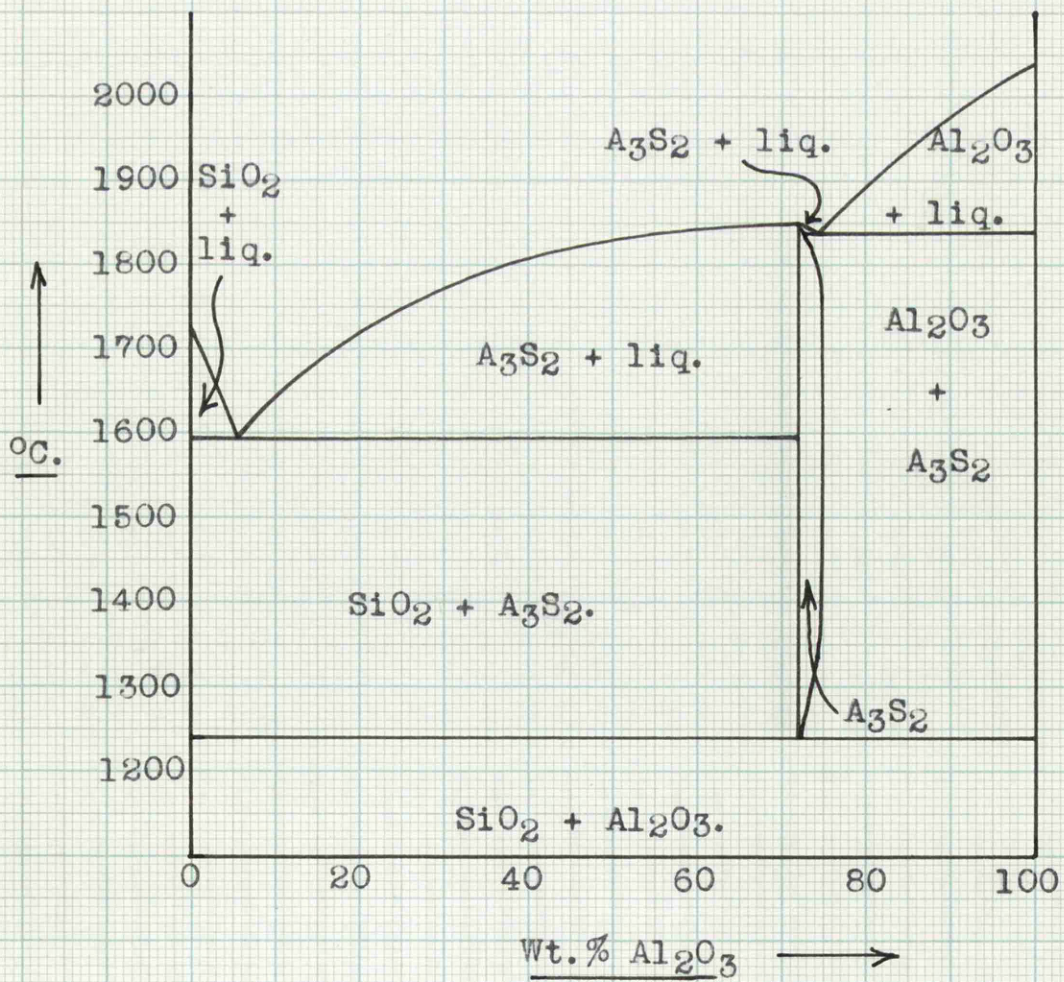


Fig. 14 - Phase diagram for the system Al_2O_3 - SiO_2 .

A = Al_2O_3 , S = SiO_2 and A_3S_2 = mullite.

the 'mullite' loses silica the equilibrium pressure of carbon monoxide should fall from one constant value to the other, thus defining the boundaries of the 'mullite' phase field if the loss of silica is known.

For a 'mullite' in equilibrium with alumina the silica activity which can be obtained at a given temperature is the same as that for a ternary $\text{CaO-Al}_2\text{O}_3\text{-SiO}_2$ liquid slag in equilibrium with 'mullite' and alumina at the same temperature. In the phase diagram of fig. 4¹⁹, the composition of such a slag at 1550°C is indicated by the point X, and fig. 11 gives the experimentally determined silica activity of this slag as 0.45. Toropow and Galakhow²³, however, consider that the phase boundary between liquid slag, 'mullite' and corundum in the $\text{CaO-Al}_2\text{O}_3\text{-SiO}_2$ system should be displaced towards the alumina end of the diagram. This would result in a silica activity of about 0.1 at 1550°C for a slag in equilibrium with 'mullite' and corundum. The determination of the silica activity of 'mullite' should indicate the correct position of the phase boundary.

When 'mullite' is in equilibrium with corundum, the equilibrium constant for reaction (13) reduces to $K_{13} = a^2\text{SiO}_2$ and the free energy of formation of such a 'mullite' can be calculated from the experimentally

determined silica activity.

The determination of the silica activity of 'mullite' can thus give the following information.

1) The extent, if any, of the 'mullite' phase field in the system $\text{Al}_2\text{O}_3\text{-SiO}_2$.

2). The correct position of the phase boundary between liquid slag, 'mullite' and corundum in the system $\text{CaO-Al}_2\text{O}_3\text{-SiO}_2$.

3). The free energy of formation of 'mullite' which is in equilibrium with alumina.

The results of the determinations are shown in table 6A. The 'mullite' used in the compacts with graphite and silicon carbide, was obtained from an external source and apparently gave an X-ray diffraction photograph identical to that of a sample of very pure 'mullite'. Unfortunately, analysis yielded the results given in table 6B - the compound $3\text{Al}_2\text{O}_3\text{-2SiO}_2$ corresponds approximately to 72% Al_2O_3 , 28 % SiO_2 . The results, however, are applicable for a 'mullite' containing 39.4% SiO_2 , 59.5% Al_2O_3 and 1.1%($\text{TiO}_2\text{+CaO+MgO}$) if it is assumed that the volatilisation of the soda and potash and the reduction of the iron oxide take place fairly rapidly during the determination. As a result of the presence of impurities the results cannot be considered as completely

Table 6A - Results of the 'mullite' runs.

Run No.	Loss of silica from the system. gms.	t°C	pCO	aSiO ₂	G _T ⁰ of form ⁿ . 'mullite' cal./mol.	
61	- - - Nil - - -	1448	0.369	0.840	-	
		1498	0.639	0.753	-	
		1549	1.008	0.590	-	
61R	- - - Unknown - - -	1398	0.168	0.622	-3,160	
		1450	0.308	0.556	-4,020	
		1500	0.532	0.498	-4,910	
		1550	0.886	0.444	-5,880	
		1598	1.427	0.391	-7,110	
61R ²	- - - Nil - - -	1448	0.371	0.847	-	
		1498	0.639	0.753	-	
	0.81	- - -	1499	0.531	0.510	-
	0.99	- - -	1550	0.884	0.439	-

Table 6B - 'Mullite' analysis - wt. %.

SiO ₂	Al ₂ O ₃	FeO	TiO ₂	CaO	MgO	K ₂ O	Na ₂ O
38.04	57.31	2.35	0.72	0.16	0.16	0.88	0.31

conclusive.

The results of run 61 refer to the 'mullite' containing 39.4% SiO_2 , 59.5% Al_2O_3 and 1.1% impurities. The highest silica activity obtained is 0.84 at 1450°C and in run 61R loss of silica from the system caused a drop in the silica activity indicating that the 'mullite' of run 61 lay in the 'mullite' phase field at the experimental temperatures. The solubility of silica in 'mullite' thus appears to be quite extensive but as stated above the evidence cannot be regarded as conclusive because of the impure mullite. The result is in agreement with the work of Tromel²⁵ but is not in agreement with the recent work of Aramaki and Roy²⁴.

In run 61R the evacuation of the system at 1450°C before the determination of the equilibrium pressures, caused an unknown amount of reaction to occur with a corresponding loss of an unknown amount of silica from the system. As can be seen from table 6A the results are significantly different from those of run 61. In run 61R² the results of run 61 were first confirmed at 1450 and 1500°C and then known amounts of reaction were caused at 1450 and 1500°C by periodically removing carbon monoxide from the system and measuring the increase in pressure as equilibrium was approached from 'below'. The loss in

silica from the system corresponding to an increase in the pressure of carbon monoxide has already been given as $0.36 \cdot 10^{-2}$ gms. - see p.24. By this method it was found that a constant equilibrium pressure was attained after a loss of 0.81 gms. of silica from the system and that a further loss of 0.18 gms. caused no change in this value at constant temperature. The compact originally contained 4gms. of 'mullite' and the loss of 0.81gms. of silica gives a 'mullite' of 24.0%SiO₂, 74.6% Al₂O₃ and 1.4% impurities. The alumina-'mullite' phase boundary thus corresponds to the approximate composition 75% Al₂O₃, 25% SiO₂ within the experimental temperature range. This result is in excellent agreement with Aramaki and Roy who indicate a composition of 74.4% Al₂O₃, 25.6% SiO₂.

The silica activity of 'mullite' in equilibrium with alumina at 1550°C given in table 6A is 0.44. This result confirms the position of the phase boundary between liquid slag, alumina and 'mullite' at 1550°C given in the CaO-Al₂O₃-SiO₂ diagram of fig. 4. It is emphasised, however, that the above results give no indication of the position of the boundary near the binary Al₂O₃-SiO₂ join. The recent work of Aramaki and Roy confirm the position of the boundary in the CaO-Al₂O₃-SiO₂ system given in fig. 4, in complete agreement with the present work.

The results of run 61R² indicate that the results of 61R also refer to 'mullite' in equilibrium with alumina and since the results in this run cover a wider temperature range, the free energies of formation of 'mullite' in equilibrium with alumina are calculated from those results. The free energies of this 'mullite' are also given in fig. 6A and may be represented by the linear equation

$$\Delta_{13}G_T^0 = + 29,600 - 19.52T \text{ cal./mol.}, (1673 - 1873^\circ\text{K}) - (15)$$

Extrapolation of equation (15) indicates that 'mullite' is thermodynamically unstable with respect to silica and corundum at temperatures below 1240°C. This result accounts for the 'eutectoid' addition to the Al₂O₃-SiO₂ phase diagram of fig. 14.

Although the presence of impurities in the 'mullite' used prevents rigid conclusions it is thought that the results for pure 'mullite' will be very similar to the present results.

The relationship between silica activity and temperature.

The silica activities of slags which were liquid at 1450°C and 1500°C have been treated statistically and slags in both the CaO-Al₂O₃-SiO₂ and CaO-Al₂O₃-MgO-SiO₂ systems were included.

The ratio, (a_{SiO_2} at $1500^\circ\text{C}/a_{\text{SiO}_2}$ at 1450°C), obtained from the analysis of 36 pairs of results is 0.89, with a standard deviation of 0.07.

A similar analysis of slags liquid at 1500 and 1550°C gives a ratio, (a_{SiO_2} at $1550^\circ\text{C}/a_{\text{SiO}_2}$ at 1500°C), of 0.88 with a standard deviation of 0.07, from 47 pairs of results.

The temperature relationship adopted is

$$a_{\text{SiO}_2} \text{ at } t^\circ\text{C}/a_{\text{SiO}_2} \text{ at } t-50^\circ\text{C} = 0.89 - - - - - (16)$$

The application of this equation must obviously be limited but extrapolation of the present results to 1600°C , particularly at low silica activities, is considered to be reliable. Extrapolations for slags in the CaO-SiO_2 and $\text{CaO-Al}_2\text{O}_3\text{-SiO}_2$ systems are shown in figs. 5, 6, 7 and 8. These extrapolations will be used in the comparison of the present work with the results of other investigators.

In the above analyses it is assumed that the temperature coefficient is not a function of slag composition.

The effect of lime and alumina on the activity of silica.

The decrease in the silica activities caused by the addition of 10% Al_2O_3 or 10% CaO to slags containing 0 and 20% Al_2O_3 are given in table 7. As can be seen

Table 7 - The relative effect of lime and alumina additions on the silica activities of CaO-Al₂O₃-SiO₂ liquid slags at 1550°C.

aSiO ₂	$\Delta_{AaSiO_2, C:S=k}$, after addition of 10% Al ₂ O ₃	$\Delta_{CaSiO_2, A:S=k}$, after addition of 10% CaO.	$\frac{\Delta_{CaSiO_2}}{\Delta_{AaSiO_2}}$
0.0% Al ₂ O ₃			
0.90	0.32	0.58	1.8
0.80	0.30	0.55	1.8
0.70	0.28	0.51	1.8
0.60	0.24	0.43	1.8
0.50	0.20	0.35	1.8
0.40	0.14	0.28	2.0
0.30	0.10	0.20	2.0
0.20	0.06	0.17	2.8
20.0% Al ₂ O ₃			
0.80	0.14	0.11	0.8
0.70	0.17	0.22	1.3
0.60	0.16	0.30	1.9
0.50	0.15	0.27	1.8
0.40	0.12	0.24	2.0
0.30	0.09	0.18	2.0
0.20	0.04	0.15	3.7

from this table, the effect of lime is nearly 3 times that of alumina, on a wt.% basis, near calcium orthosilicate saturation. On a mol. basis approximately 1.5 mols. alumina is equivalent to 1 mol. of lime.

It is not proposed to consider the effect of the results given in table 7 on the theories of slag constitution, as these theories involve a large amount of speculation.

THE CaO-MgO-SiO₂ SYSTEM.

The phase diagram for the system CaO-MgO-SiO₂²⁶, is shown in fig. 15 and the silica activities of liquid slags at 1450, 1500 and 1550°C are given in table 8 and shown in figs. 16, 17, 18, 19, 20 and 21. The slags investigated actually contained 0.6% Al₂O₃ but these are considered as simple ternary CaO-MgO-SiO₂ slags.

The free energy of formation of magnesium orthosilicate.

The phase diagram for the binary MgO-SiO₂ system indicates that a liquid slag containing 62% SiO₂ and 38% MgO is in equilibrium with magnesium orthosilicate and metasilicate at 1557°C. This point is also shown on the MgO-SiO₂ join of fig. 15 and in the interpretation given below the temperature of 1557°C is taken as 1550°C.

Table 8 - The silica activities of CaO-MgO-SiO₂ liquid slags.

1450°C.

Run No.	Liquid slag comp.				t°C.	pSiO+pCO atm.	pCO atm.	aSiO ₂
	CaO	wt.% Al ₂ O ₃	MgO	SiO ₂				
48	24.2	0.6	10.4	64.8	1450	0.426	0.414	1.010
49	29.6	0.6	9.7	60.1	1453	0.426	0.414	0.933
50	36.2	0.6	9.8	53.4	1449	0.274	0.266	0.427
51	40.6	0.6	9.8	49.0	1450	0.241	0.234	0.321
52	44.9	0.6	9.9	44.6	1448	0.153	0.149	0.137
53	14.2	0.6	20.4	64.8	1449	0.422	0.410	1.010
54	21.5	0.6	19.8	58.1	1449	0.381	0.371	0.826
55	29.3	0.6	19.8	50.3	1448	0.268	0.261	0.419
56	34.4	0.6	19.9	45.1	1449	0.195	0.190	0.217

Table 8 - The silica activities of CaO-MgO-SiO₂ liquid slags.

1500°C.

Run No.	Liquid slag comp.				t°C	pCO+pSiO	pCO	aSiO ₂
	CaO	Al ₂ O ₃	MgO	SiO ₂				
48	23.0	0.6	9.7	66.7	1500	0.771	0.748	0.985
49	29.6	0.6	9.7	60.1	1499	0.700	0.679	0.832
50	36.2	0.6	9.8	53.4	1499	0.489	0.475	0.407
51	40.6	0.6	9.8	49.0	1499	0.407	0.395	0.281
52	44.9	0.6	9.9	44.6	1498	0.273	0.265	0.129
53	14.8	0.6	19.8	64.8	1499	0.751	0.728	0.956
54	21.5	0.6	19.8	58.1	1498	0.639	0.620	0.710
55	29.3	0.6	19.8	50.3	1498	0.466	0.452	0.377
56	34.4	0.6	19.9	45.1	1499	0.342	0.332	0.200
57	38.4	0.6	20.0	41.0	1501	0.310	0.301	0.156
58	5.2	0.7	28.4	65.7	1498	0.749	0.727	0.977
59	12.3	0.6	29.0	58.1	1499	0.653	0.633	0.724
60	19.5	0.5	29.5	50.5	1497	0.465	0.451	0.385

Table 8 - The silica activities of CaO-MgO-SiO₂ liquid slags.

1550°C.

Run No.	Liquid slag comp.				t°C	pCO+pSiO atm.	pCO atm.	aSiO ₂
	CaO	wt.% Al ₂ O ₃	MgO	SiO ₂				
48	23.0	0.6	9.7	66.7	1547	1.233	1.194	0.864
49	29.6	0.6	9.7	60.1	1549	1.113	1.078	0.673
50	36.2	0.6	9.8	53.4	1549	0.805	0.780	0.352
51	40.6	0.6	9.8	49.0	1548	0.651	0.631	0.235
52	44.9	0.6	9.9	44.6	1548	0.455	0.441	0.115
53	14.8	0.6	19.8	64.8	1548	1.233	1.194	0.843
54	21.5	0.6	19.8	58.1	1548	1.039	1.006	0.600
55	29.3	0.6	19.8	50.3	1548	0.755	0.731	0.316
56	34.4	0.6	19.9	45.1	1550	0.573	0.554	0.174
57	38.4	0.6	20.0	41.0	1549	0.523	0.507	0.149
58	5.2	0.7	28.4	65.7	1548	1.274	1.234	0.901
59	12.3	0.6	29.0	58.1	1549	1.066	1.032	0.616
60	19.5	0.5	29.5	50.5	1547	0.716	0.694	0.298

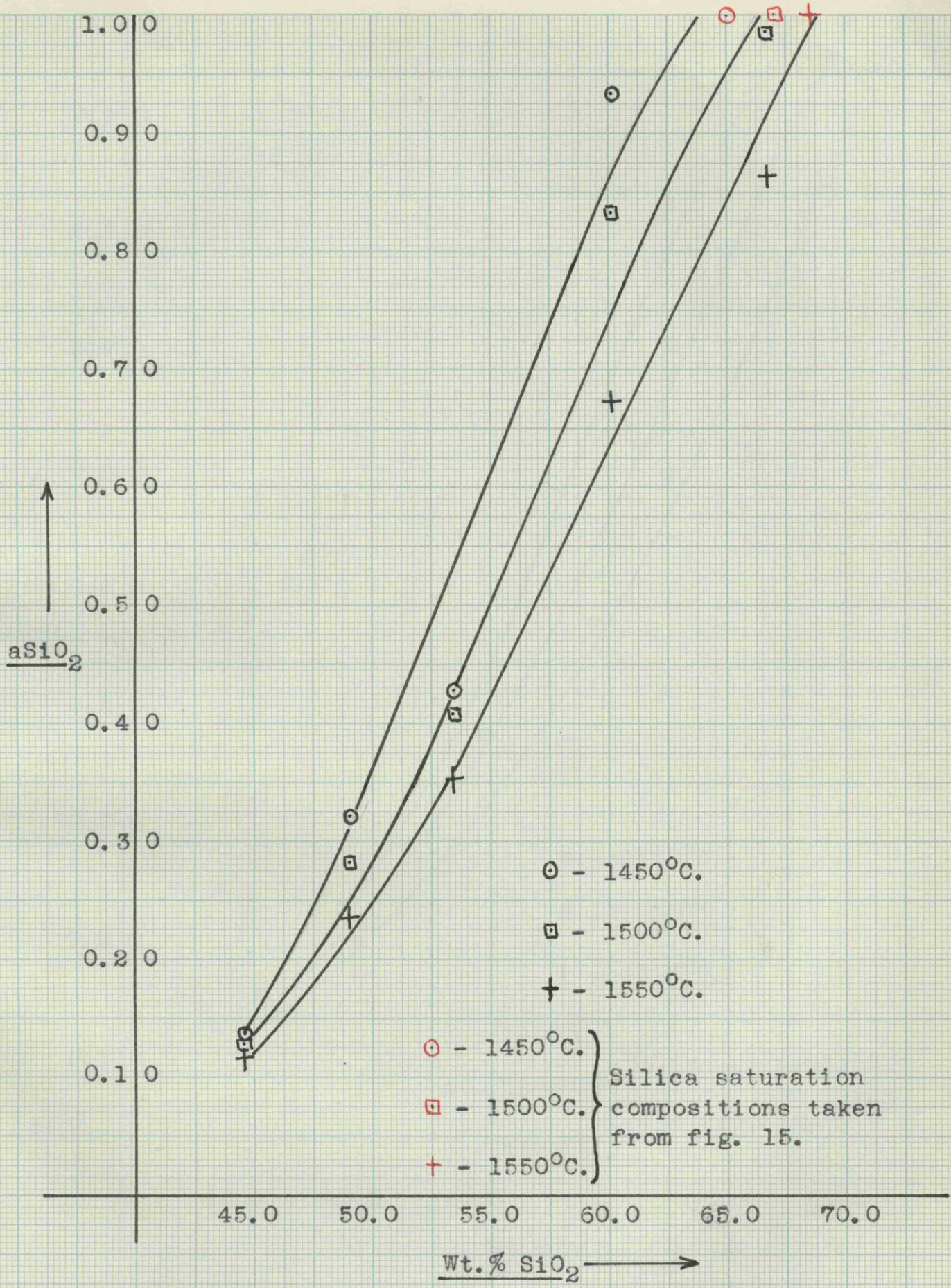


Fig. 16 - Silica activities of CaO-MgO-SiO₂ slags.
(10% MgO)

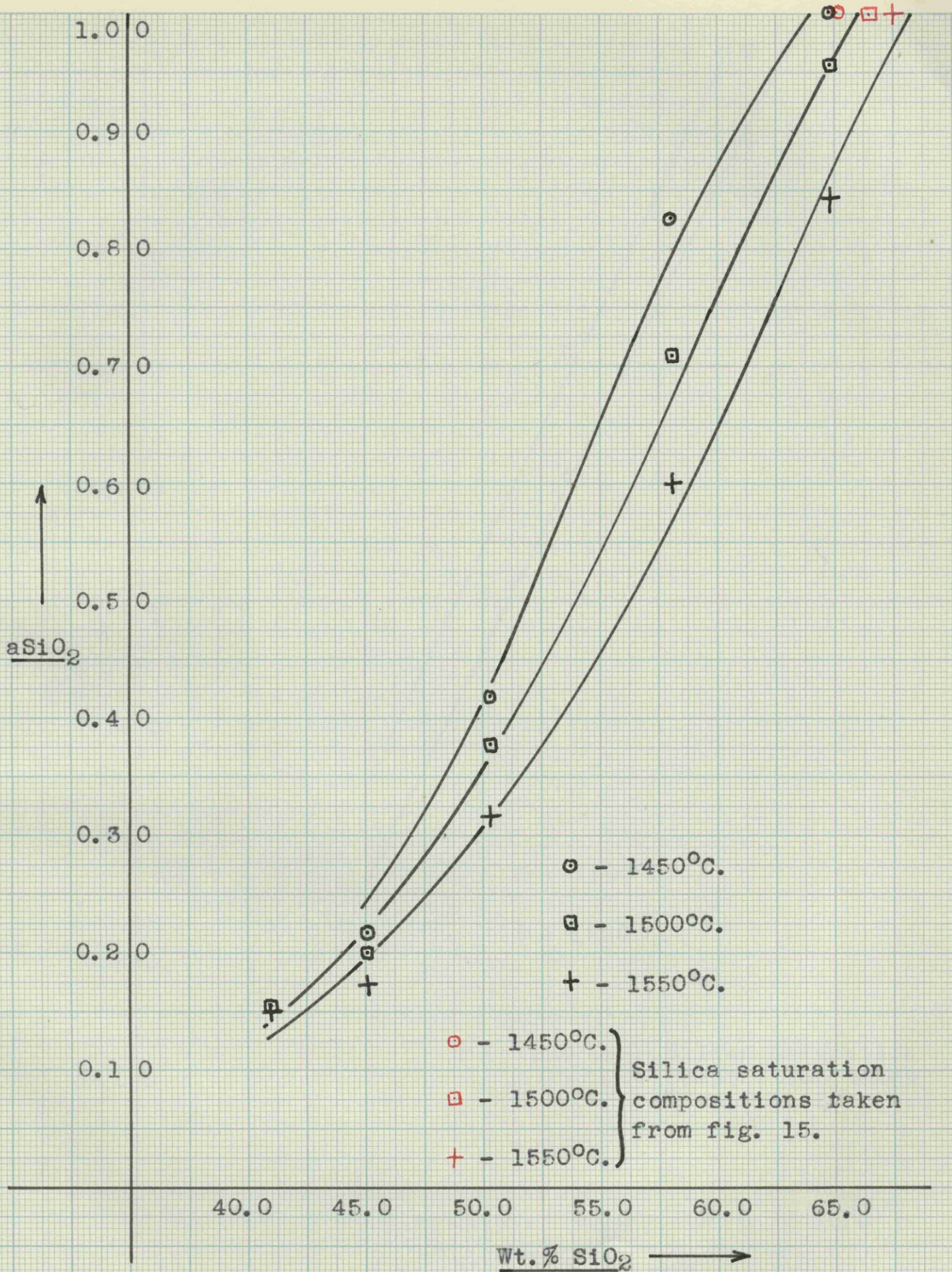


Fig. 17. - Silica activities of CaO-MgO-SiO₂ slags.
(20% MgO)

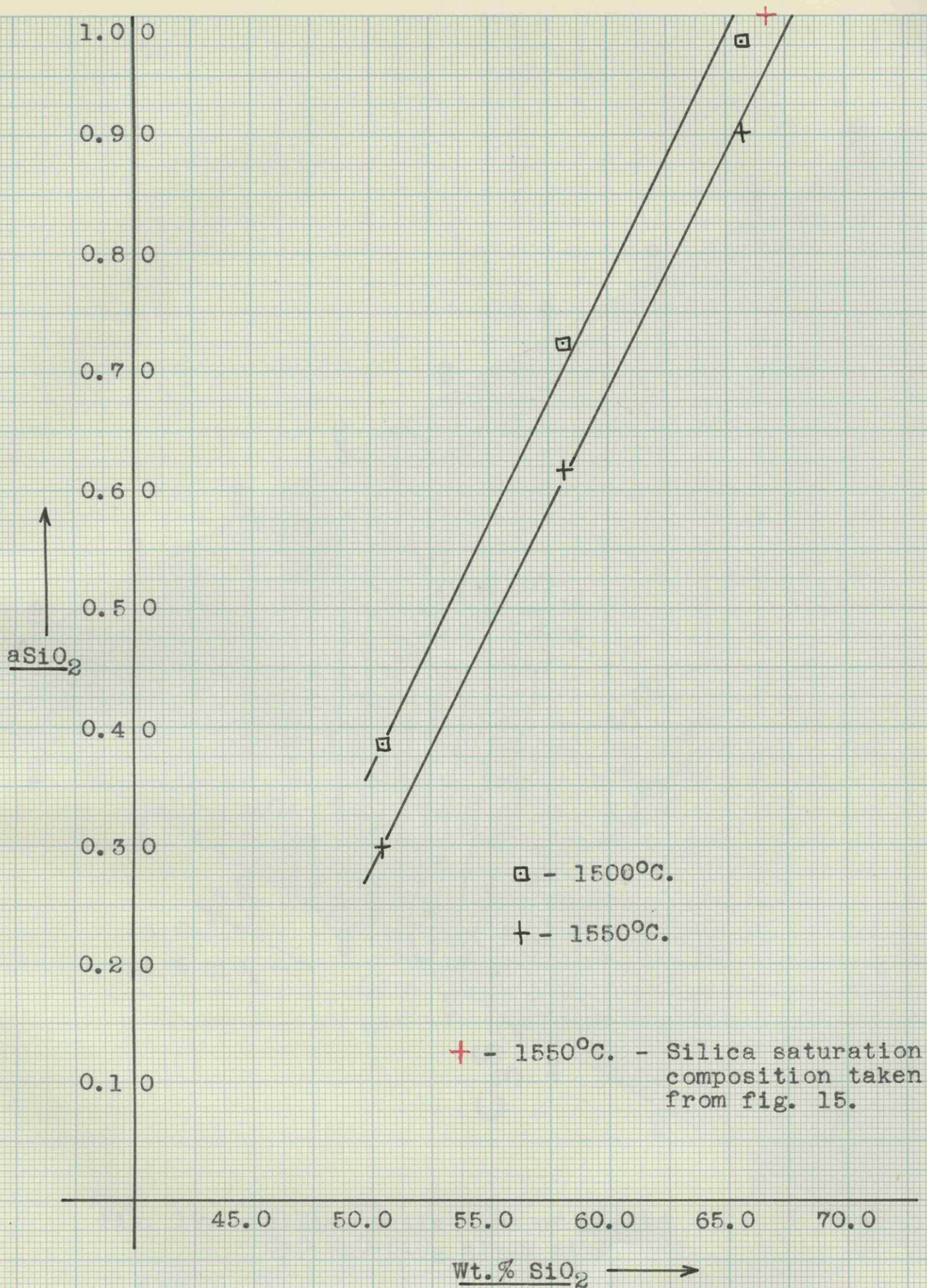


Fig. 18 - Silica activities of $CaO-MgO-SiO_2$ slags.

(30% MgO)

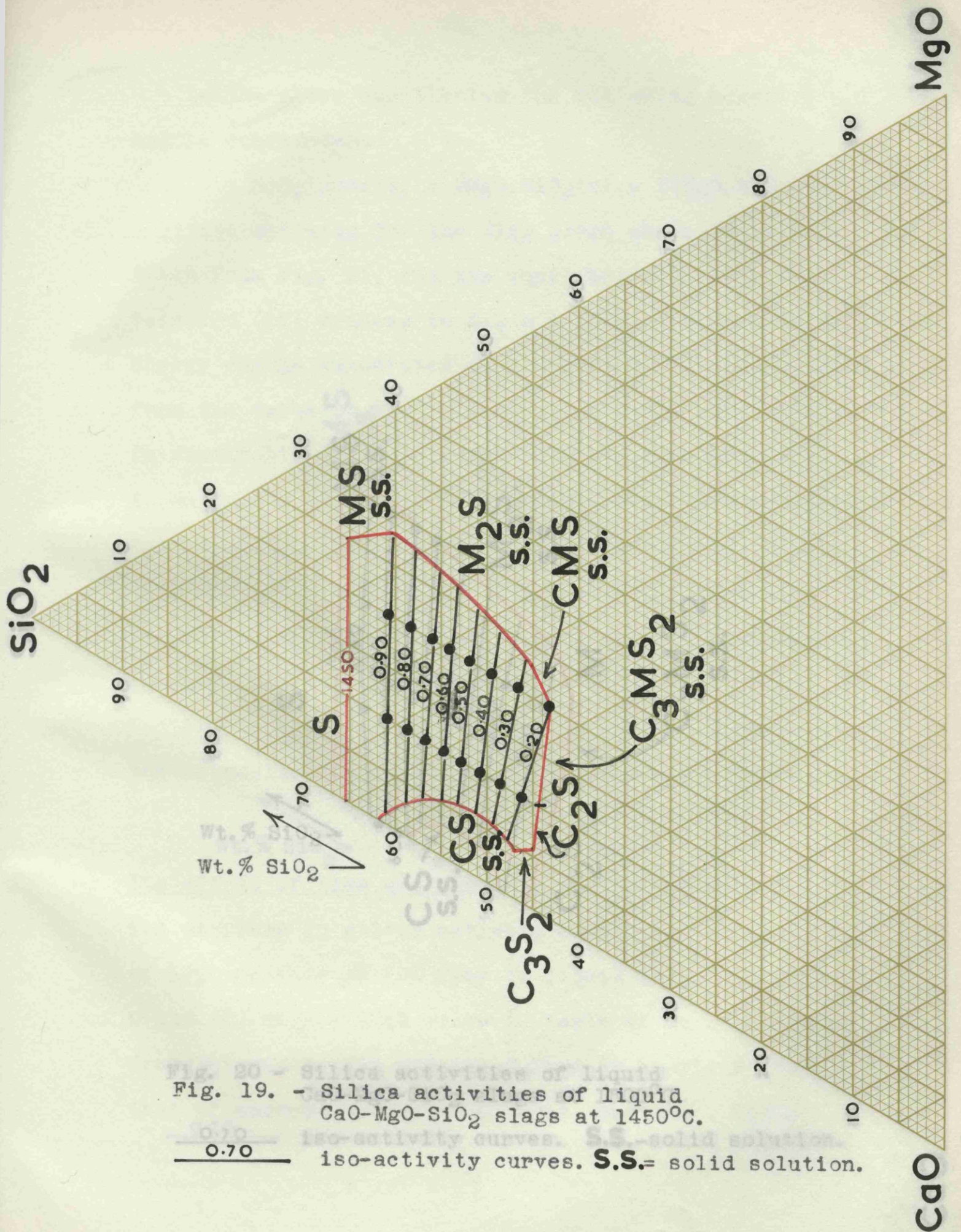
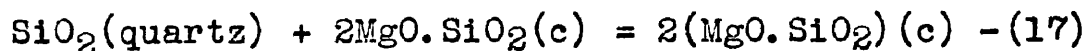


Fig. 20 - Silica activities of liquid
 Fig. 19. - Silica activities of liquid
 CaO-MgO-SiO₂ slags at 1450°C.
 iso-activity curves. S.S. = solid solution.
 0.70
 iso-activity curves. S.S. = solid solution.

In the above equilibrium the following reaction may be considered,



A silica activity for the slag given above, of 0.8 is taken from fig. 21, and the equilibrium constant for reaction (17) reduces to $K_{17} = 1/a_{\text{SiO}_2} = 1.25$. The free energy change associated with reaction (17), calculated from the value of K_{17} is $\Delta_{17}G_{1830}^0 = -810 \text{ cal./mol.}$ On combination of this value with the free energy of formation of magnesium metasilicate from the constituent oxides, given by Richardson et al¹⁴ and quoted in the appendix, the free energy of formation of magnesium orthosilicate from the constituent oxides is calculated as $-13,000 \text{ cal./mol. at } 1550^\circ\text{C.}$

In the above calculation it is assumed that both the orthosilicate and metasilicate are stoichiometric.

The effect of lime and magnesia on the activity of silica.

The decrease in silica activity caused by the addition of 10% magnesia or 10% lime to liquid slags containing 0 and 20% magnesia is shown in table 9. As can be seen from this table the effect of lime is nearly 2 times that of magnesia, on a wt.% Basis. On a mol. basis

Table 9 - The relative effect of lime and magnesia additions on the silica activities of CaO-MgO-SiO₂ liquid slags at 1550°C.

a_{SiO_2}	$\Delta_{MaSiO_2, C:S=k}$, after addition of 10% MgO.	$\Delta_{CaSiO_2, M:S=k}$, after addition of 10% CaO.	$\frac{\Delta_{CaSiO_2}}{\Delta_{MaSiO_2}}$
0.0% MgO.			
0.90	0.32	0.49	1.5
0.80	0.31	0.50	1.6
0.70	0.30	0.48	1.6
0.60	0.27	0.42	1.6
0.50	0.22	0.36	1.6
0.40	0.17	0.31	1.8
20.0% MgO.			
0.90	0.34	0.32	0.9
0.80	0.30	0.32	1.1
0.70	0.28	0.29	1.0
0.60	0.24	0.27	1.1
0.50	0.20	0.24	1.2
0.40	0.14	0.21	1.5
0.30	0.09	0.16	1.8

approximately 3 mols. of magnesia are equivalent to 1 mol. of lime.

As in the case of the effect of alumina and lime additions on silica activities, the above results are not applied to theories of slag constitution.

THE CaO-Al₂O₃-MgO-SiO₂ SYSTEM.

The 10% and 20% alumina sections of the quaternary system are shown in figs. 22 and 28 respectively²⁷.

The silica activities of liquid slags in these systems are given in tables 10 and 11, and shown in figs. 23 - 27 and 29 - 33 respectively.

The slags investigated actually contained approximately 11% and 21% alumina but the error in approximating the 10% and 20% Al₂O₃ phase diagram sections, to sections of 11% and 21% Al₂O₃ respectively, is considered to be very small.

Table 10 - The silica activities of CaO-Al₂O₃-MgO-SiO₂ liquid slags containing 11% Al₂O₃.

1450°C.

Run No.	Liquid slag comp.				t°C	pCO+pSiO atm.	pCO atm.	aSiO ₂
	CaO	wt.% Al ₂ O ₃	MgO	SiO ₂				
62	9.8	11.0	9.9	69.3	1449	0.428	0.416	1.040
63	18.3	10.7	9.9	61.1	1449	0.389	0.378	0.859
64	27.3	10.5	9.9	52.3	1448	0.325	0.316	0.615
65	36.1	10.2	9.9	43.8	1448	0.190	0.185	0.210
67	3.4	11.0	19.6	66.0	1451	0.421	0.409	0.983
68	11.3	10.9	19.6	58.2	1449	0.382	0.372	0.830
69	19.1	10.9	19.6	50.4	1449	0.312	0.303	0.552
70	26.9	10.8	19.7	42.6	1450	0.190	0.184	0.199

Table 10 - The silica activities of CaO-Al₂O₃-MgO-SiO₂ liquid slags containing 11% Al₂O₃.

1500°C.

Run No.	Liquid slag comp.				t°C	pCO+pSiO atm.	pCO atm.	aSiO ₂
	CaO	Al ₂ O ₃ wt. %	MgO	SiO ₂				
62	9.8	11.0	9.9	69.3	1497	0.741	0.720	0.980
63	18.3	10.7	9.9	61.1	1499	0.655	0.636	0.730
64	27.3	10.5	9.9	52.3	1499	0.548	0.532	0.510
65	36.1	10.2	9.9	43.8	1497	0.336	0.326	0.201
66	44.9	9.9	9.9	35.3	1499	0.213	0.207	0.078
67	3.4	11.0	19.6	66.0	1500	0.721	0.700	0.865
68	11.3	10.9	19.6	58.2	1500	0.635	0.616	0.673
69	19.1	10.9	19.6	50.4	1499	0.495	0.481	0.417
70	26.9	10.8	19.7	42.6	1499	0.320	0.311	0.175
71	34.8	10.7	19.7	34.8	1498	0.235	0.228	0.096

Table 10 - The silica activities of CaO-Al₂O₃-MgO-SiO₂ liquid slags containing 11% Al₂O₃.

1550°C.

Run No.	Liquid slag comp.				t°C	pCO+pSiO atm.	pCO atm.	aSiO ₂
	CaO	wt.% Al ₂ O ₃	MgO	SiO ₂				
62	9.8	11.0	9.9	69.3	1547	1.167	1.130	0.772
63	18.3	10.7	9.9	61.1	1549	1.077	1.043	0.630
64	27.3	10.5	9.9	52.3	1548	0.859	0.832	0.410
65	36.1	10.2	9.9	43.8	1548	0.564	0.546	0.176
66	44.9	9.9	9.9	35.3	1548	0.384	0.372	0.080
67	3.4	11.0	19.6	66.0	1549	1.134	1.098	0.700
68	11.3	10.9	19.6	58.2	1549	1.046	1.013	0.593
69	19.1	10.9	19.6	50.4	1548	0.813	0.788	0.359
70	26.9	10.8	19.7	42.6	1549	0.565	0.547	0.169
71	34.8	10.7	19.7	34.8	1549	0.398	0.386	0.090

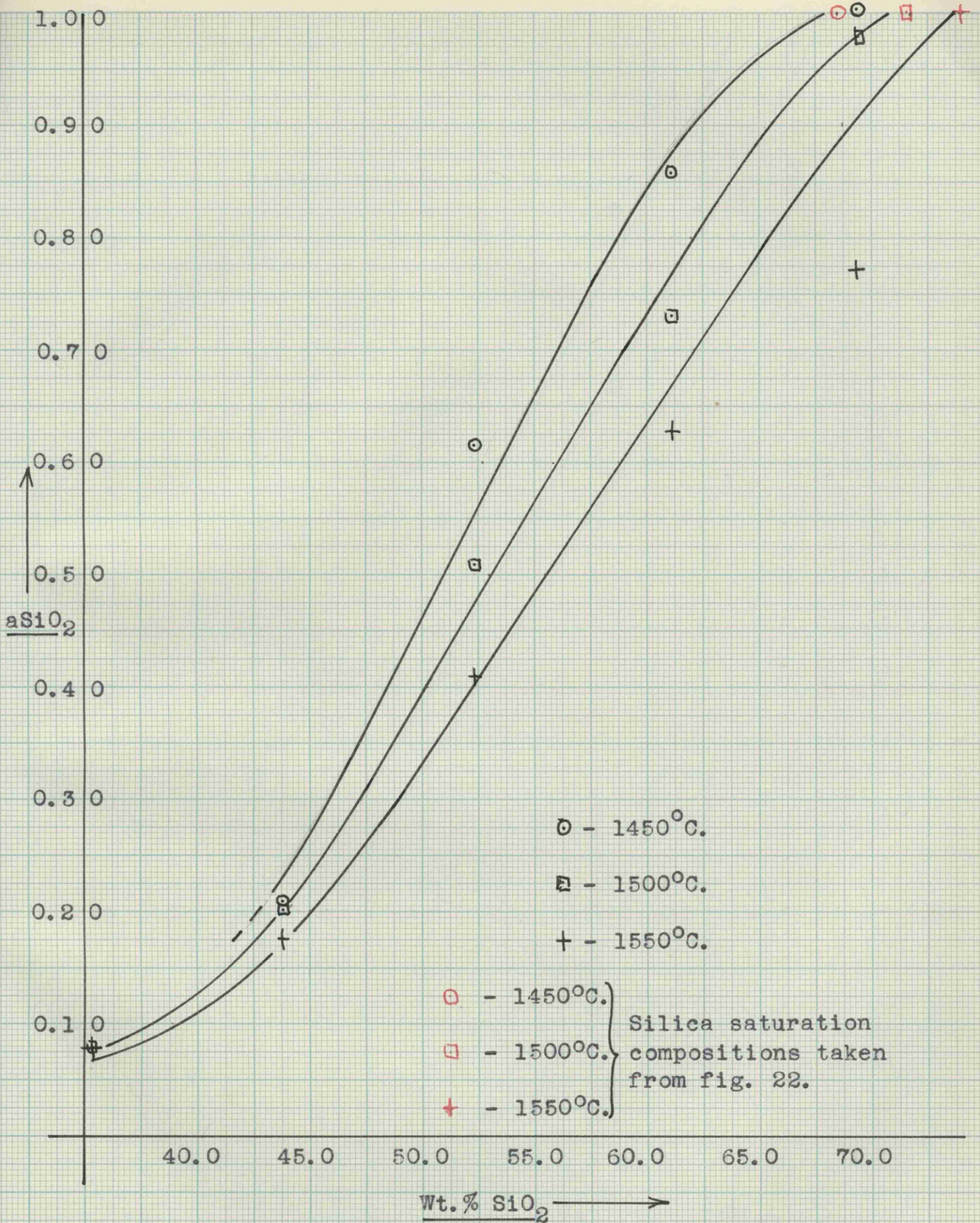


Fig. 23 - Silica activities of CaO-Al₂O₃-MgO-SiO₂ slags.
 (11% Al₂O₃, 10% MgO)

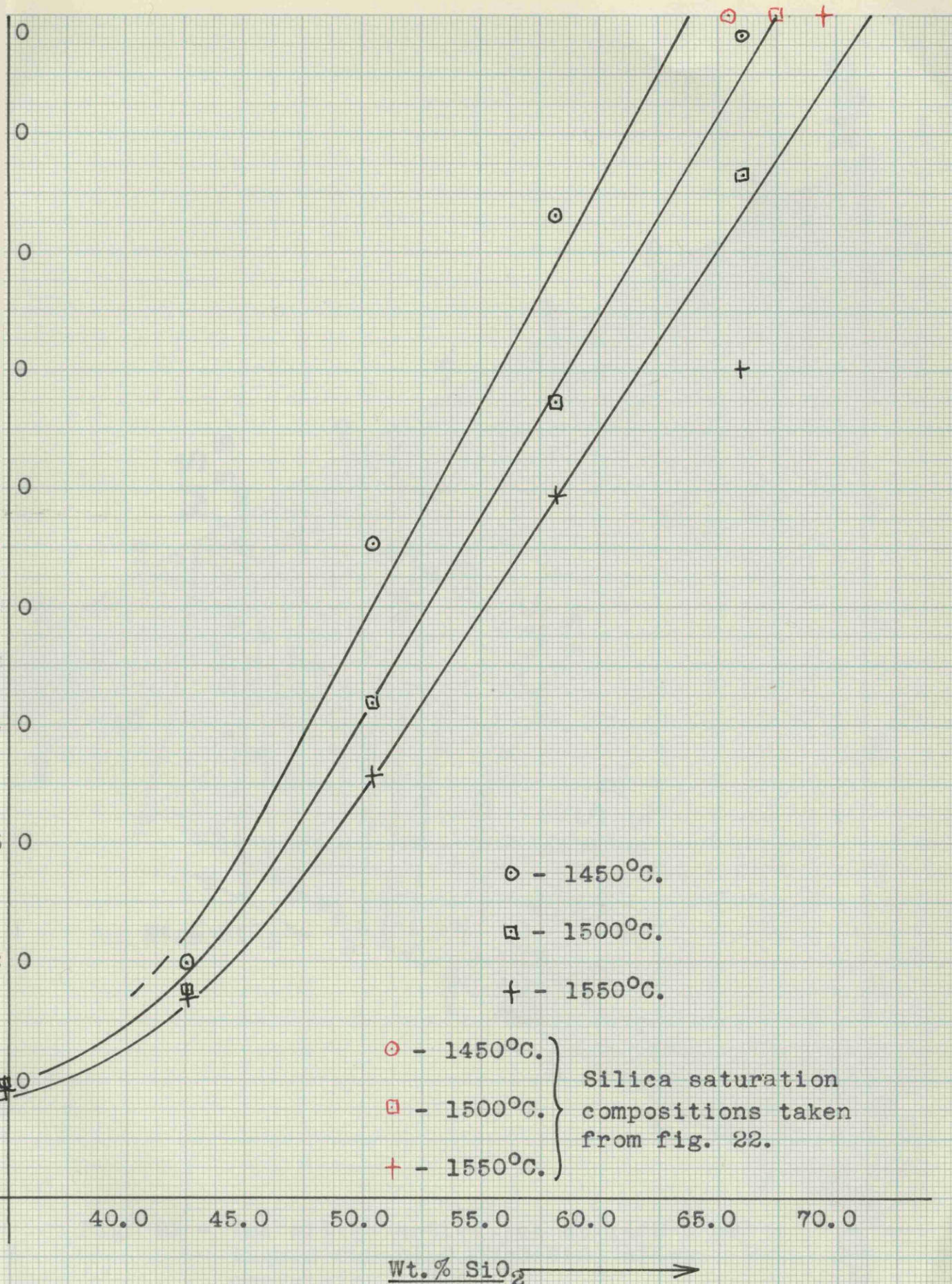


Fig. 24 - Silica activities of CaO-Al₂O₃-MgO-SiO₂ slags.
 (11% Al₂O₃, 20% MgO)

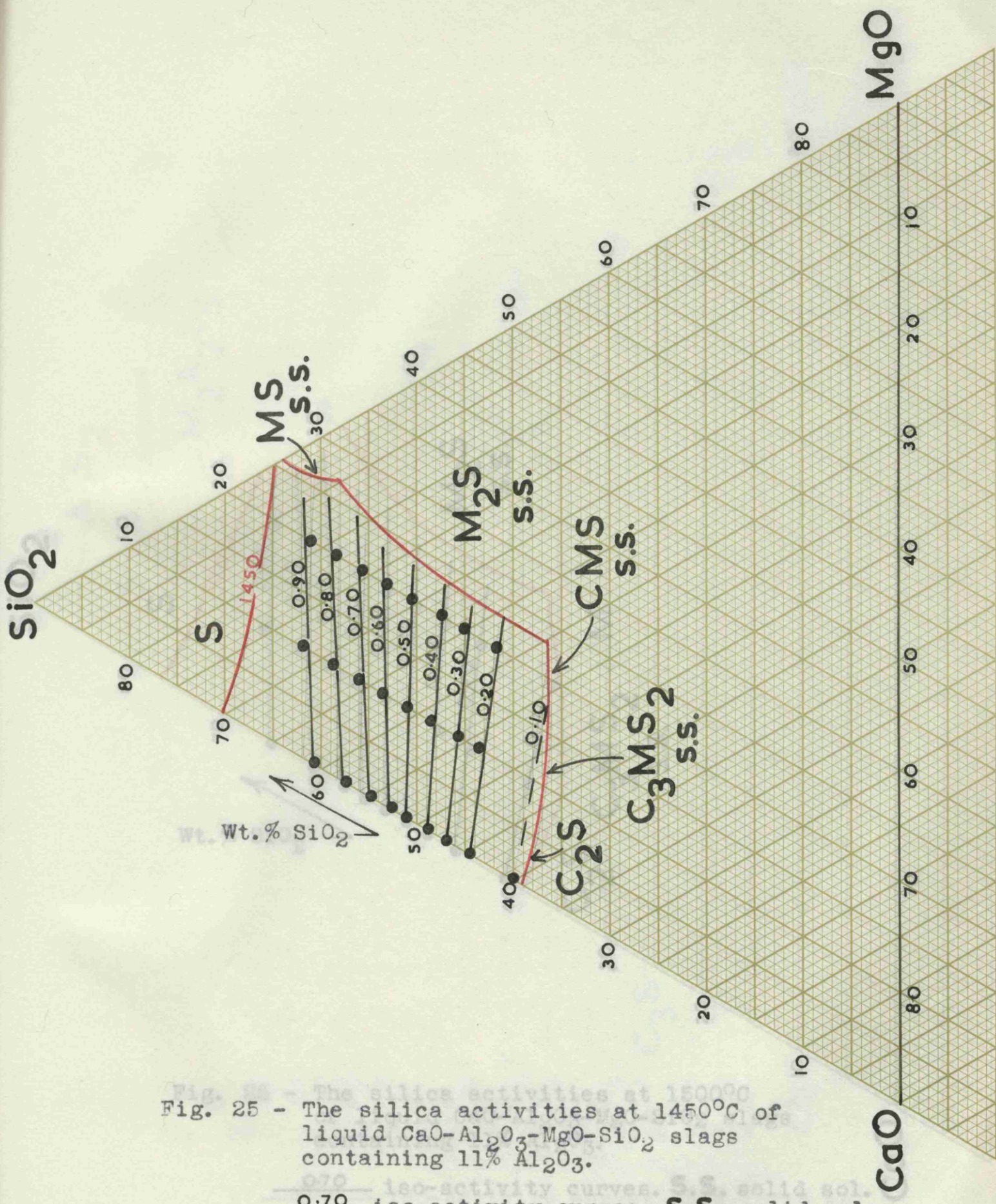


Fig. 25 - The silica activities at 1450°C of liquid CaO-Al₂O₃-MgO-SiO₂ slags containing 11% Al₂O₃.

— 0.70 iso-activity curves. S.S. solid sol.

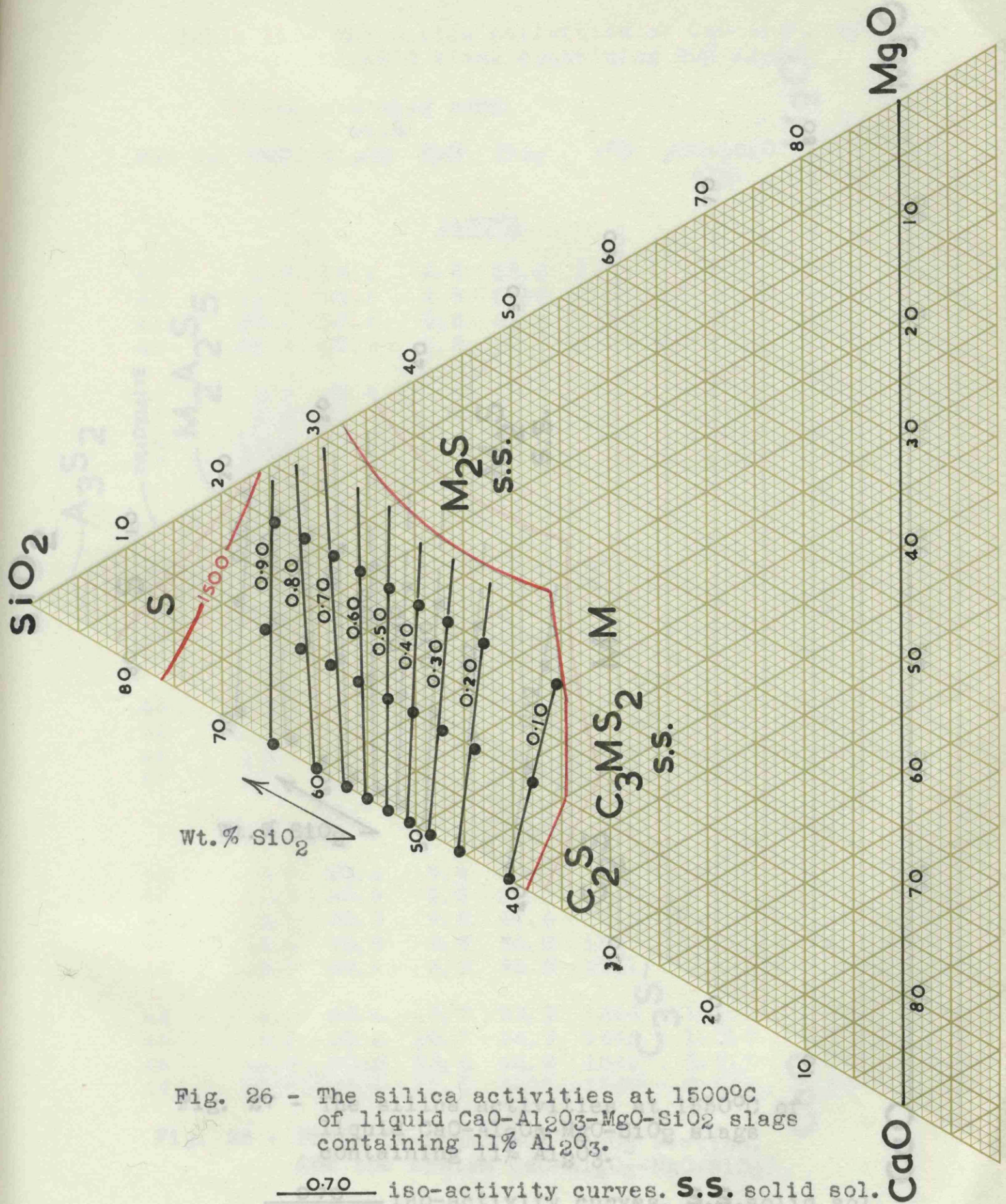


Fig. 26 - The silica activities at 1500°C of liquid CaO-Al₂O₃-MgO-SiO₂ slags containing 11% Al₂O₃.

— 0.70 — iso-activity curves. **S.S.** solid sol.

Table 11 - The silica activities of CaO-Al₂O₃-MgO-SiO₂ liquid slags containing 20% Al₂O₃

Liquid slag comp.

Run No. CaO Al₂O₃ MgO SiO₂ t°C pCO+pSiO₂ atm.

1450°C.

59	1.3	20.4	9.8	68.5	1450	0.800
40	11.3	20.3	9.8	50.6	1450	0.717
41	22.5	20.3	9.8	47.4	1450	0.717
42	33.8	20.2	9.8	36.2	1450	0.717
43	45.0	20.1	9.9	25.0	1551	0.800
44	0.0	20.4	19.7	59.9	1548	1.000
45	5.0	20.4	19.7	54.9	1548	1.013
46	14.8	20.5	19.6	44.9	1548	0.717
47	19.8	20.6	19.8	39.8	1549	0.800

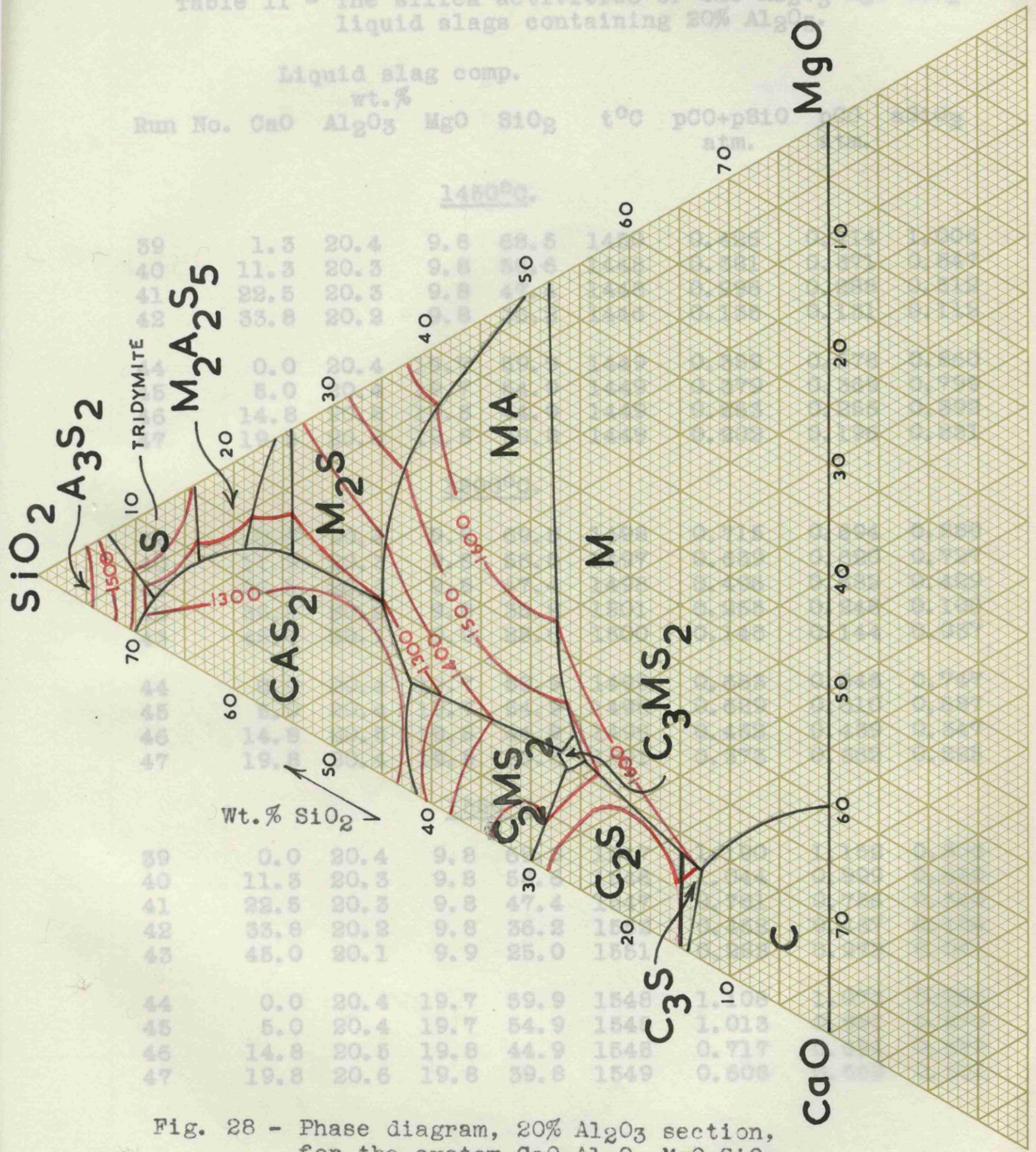


Fig. 28 - Phase diagram, 20% Al₂O₃ section, for the system CaO-Al₂O₃-MgO-SiO₂.

Table 11 - The silica activities of CaO-Al₂O₃-MgO-SiO₂ liquid slags containing 20% Al₂O₃.

Run No.	Liquid slag comp.				t°C	pCO+pSiO atm.	pCO atm.	aSiO ₂
	CaO	wt.% Al ₂ O ₃	MgO	SiO ₂				
<u>1450°C.</u>								
39	1.3	20.4	9.8	68.5	1450	0.426	0.414	1.006
40	11.3	20.3	9.8	58.6	1448	0.381	0.371	0.847
41	22.5	20.3	9.8	47.4	1448	0.296	0.288	0.512
42	33.8	20.2	9.8	36.2	1446	0.135	0.131	0.112
44	0.0	20.4	19.7	59.9	1449	0.389	0.378	0.860
45	5.0	20.4	19.7	54.9	1449	0.379	0.369	0.799
46	14.8	20.5	19.8	44.9	1449	0.263	0.255	0.392
47	19.8	20.6	19.8	39.8	1449	0.202	0.196	0.231
<u>1500°C.</u>								
39	0.0	20.4	9.8	69.8	1498	0.715	0.694	0.889
40	11.3	20.3	9.8	58.6	1497	0.639	0.620	0.727
41	22.5	20.3	9.8	47.4	1498	0.496	0.482	0.429
42	33.8	20.2	9.8	36.2	1501	0.255	0.248	0.106
43	45.0	20.1	9.9	25.0	1500	0.148	0.144	0.037
44	0.0	20.4	19.7	59.9	1499	0.663	0.643	0.747
45	5.0	20.4	19.7	54.9	1498	0.629	0.610	0.687
46	14.8	20.5	19.8	44.9	1499	0.452	0.439	0.347
47	19.8	20.4	19.8	39.8	1501	0.373	0.362	0.225
<u>1550°C.</u>								
39	0.0	20.4	9.8	69.8	1547	1.190	1.152	0.803
40	11.3	20.3	9.8	58.6	1546	1.044	0.999	0.632
41	22.5	20.3	9.8	47.4	1547	0.781	0.756	0.346
42	33.8	20.2	9.8	36.2	1552	0.452	0.437	0.104
43	45.0	20.1	9.9	25.0	1551	0.282	0.273	0.041
44	0.0	20.4	19.7	59.9	1548	1.108	1.073	0.666
45	5.0	20.4	19.7	54.9	1548	1.013	0.981	0.570
46	14.8	20.5	19.8	44.9	1548	0.717	0.694	0.298
47	19.8	20.6	19.8	39.8	1549	0.608	0.589	0.201

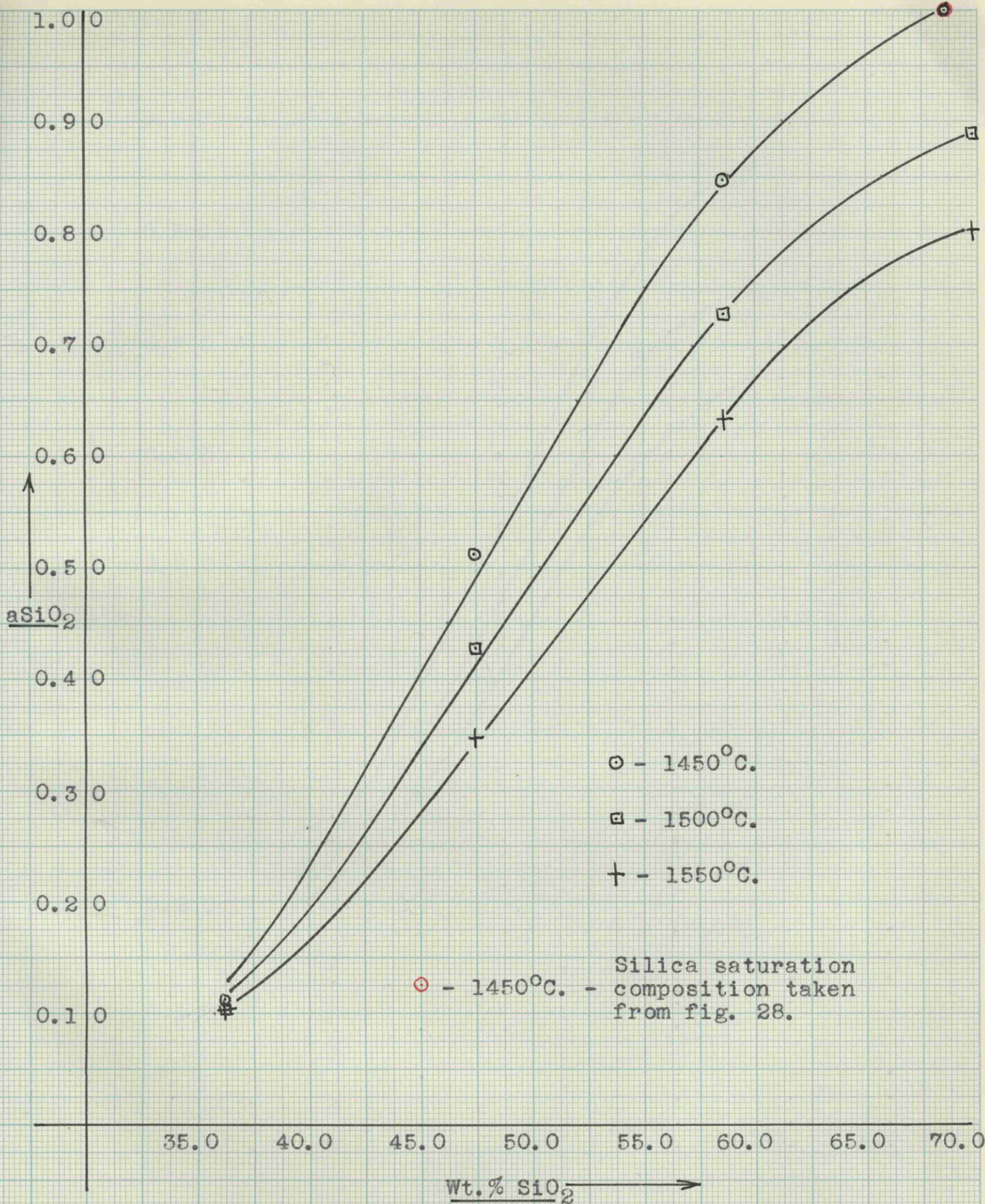


Fig. 29 - Silica activities of $CaO-Al_2O_3-MgO-SiO_2$ slags.
 (20% Al_2O_3 , 10% MgO)

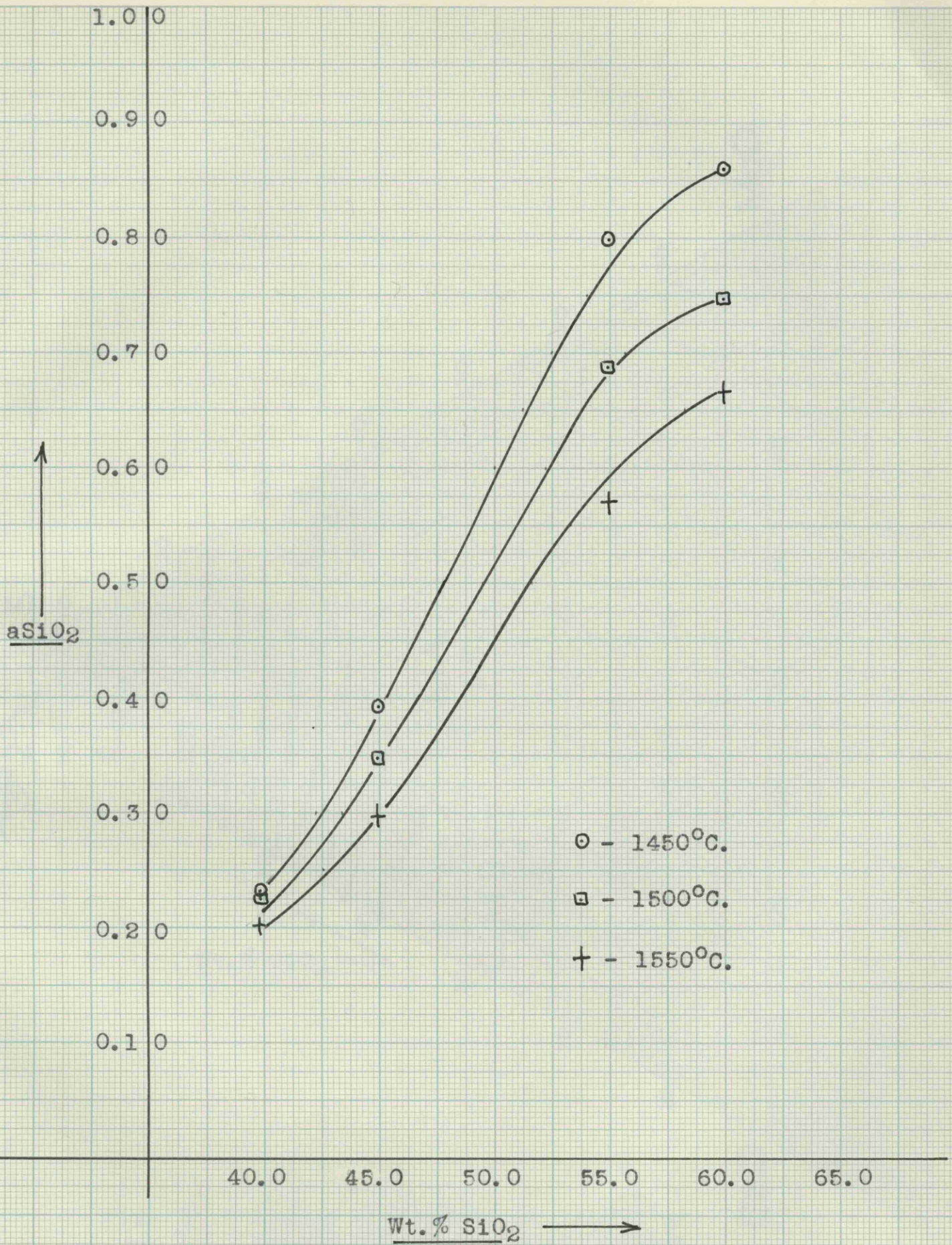


Fig. 30 - Silica activities of CaO-Al₂O₃-MgO-SiO₂ slags.
(20% Al₂O₃, 20% MgO)

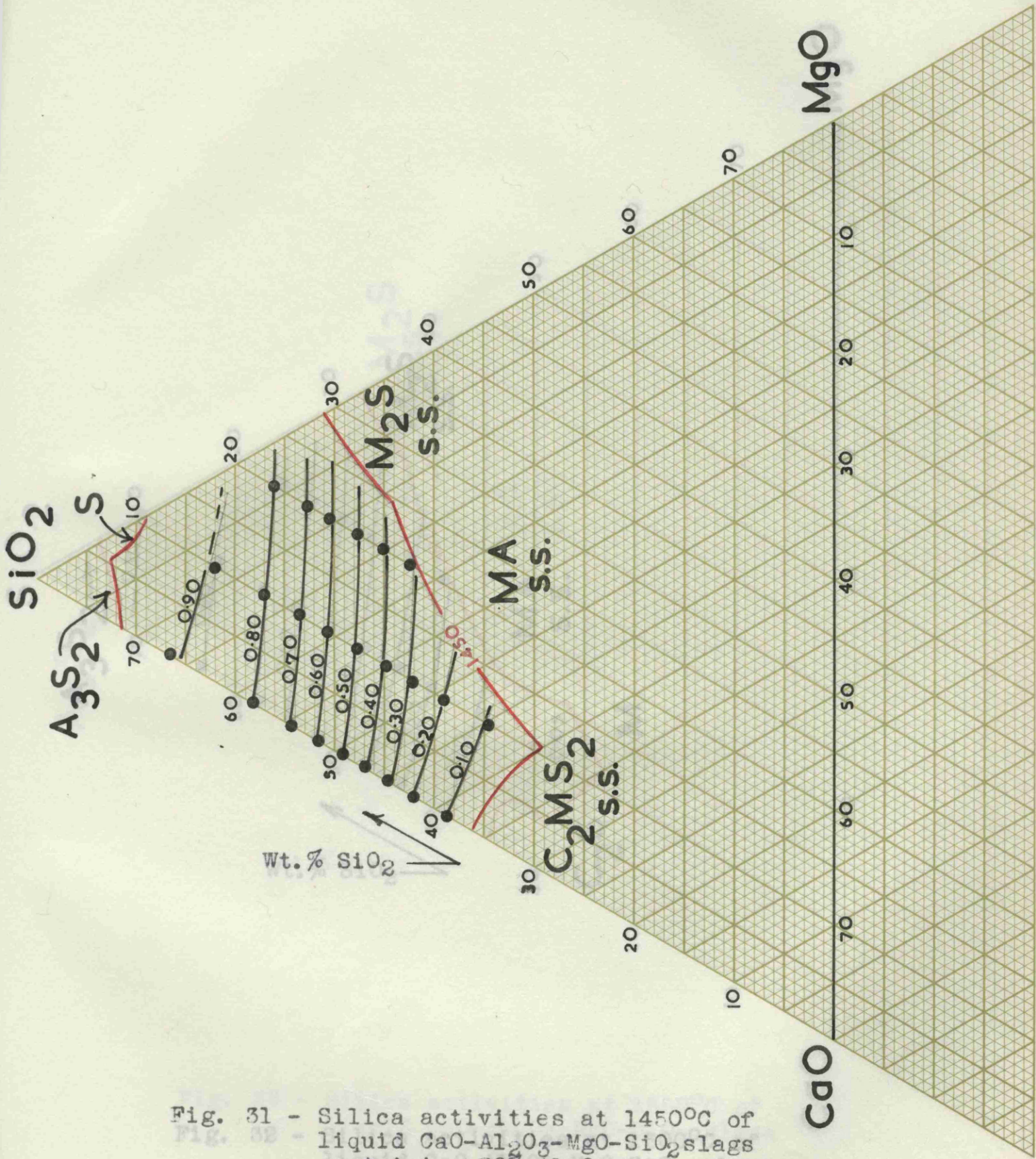


Fig. 31 - Silica activities at 1450°C of liquid CaO-Al₂O₃-MgO-SiO₂ slags containing 20% Al₂O₃

— 0.70 — iso-activity curves. S.S. solid solution.

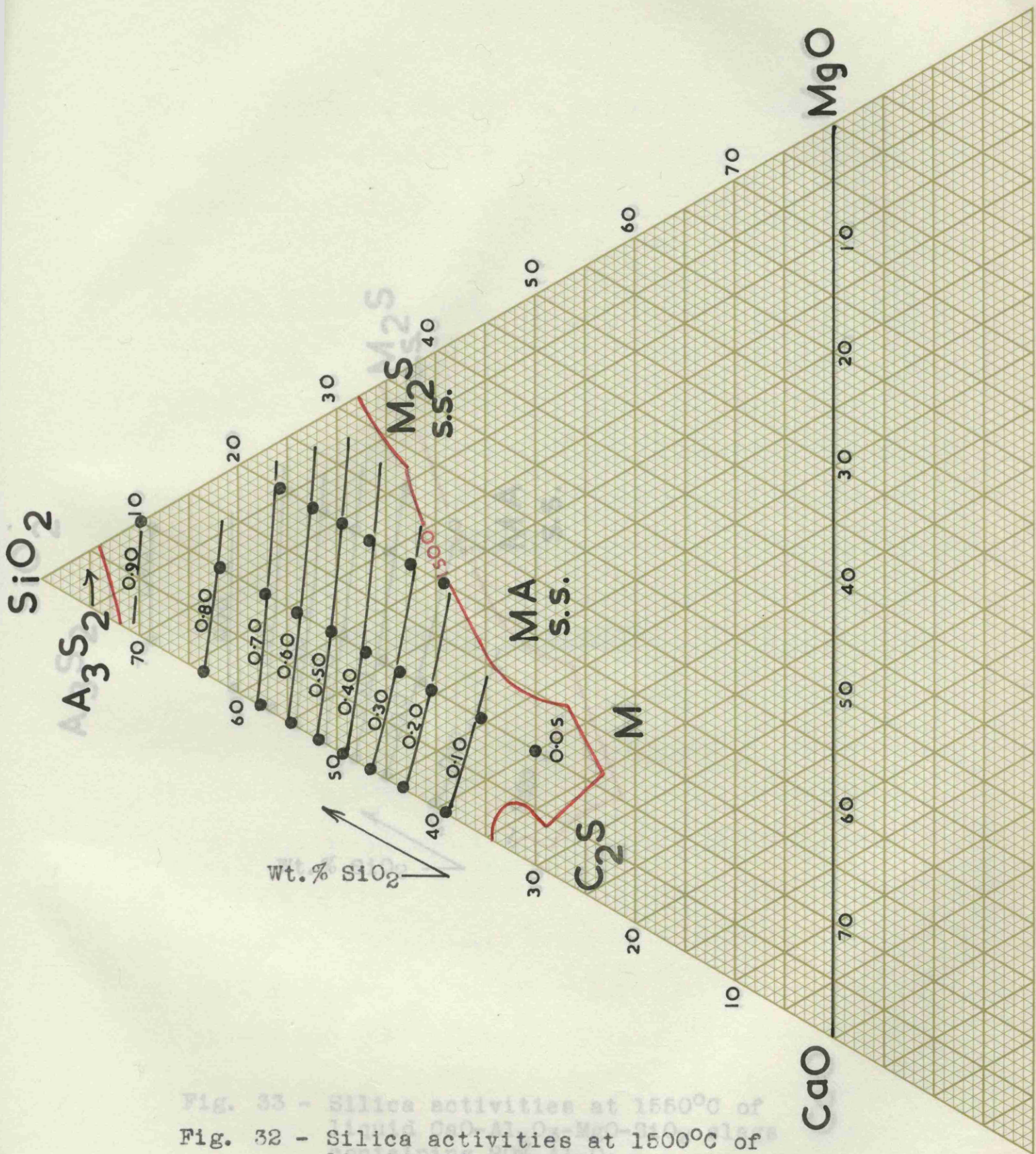


Fig. 32 - Silica activities at 1500°C of liquid CaO-Al₂O₃-MgO-SiO₂ slags containing 20% Al₂O₃.

— 0.70 — iso-activity curves. S.S. solid solution.

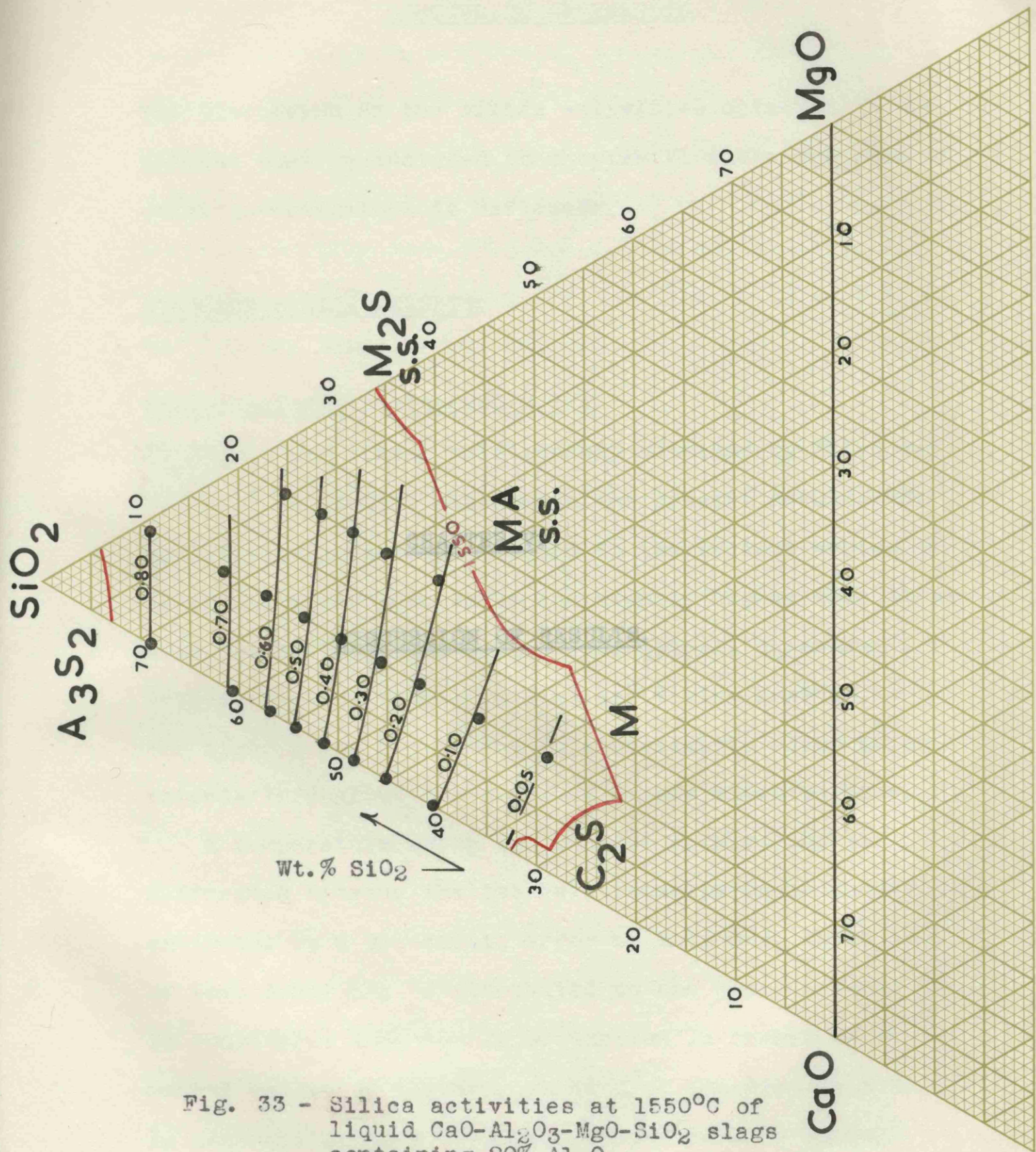


Fig. 33 - Silica activities at 1550°C of liquid CaO-Al₂O₃-MgO-SiO₂ slags containing 20% Al₂O₃.

0.70 iso-activity curves. S.S. solid solution.

CHAPTER V.

DISCUSSION OF RESULTS.

DISCUSSION OF RESULTS.

The discussion on the silica activities obtained in the present work is included in chapter VI where the work of other investigators is reviewed.

STANDARD SILICA RESULTS.

The relationship $\log_{10} p_{CO} / 1/T$.

In fig. 3 the linear relationship obtained by Baird and Taylor¹⁵ is plotted along with the present result. The equilibrium pressures obtained in the present series of experiments are seen to be consistently higher than those obtained by Baird and Taylor. The general agreement between the two sets of silica activities however, - see figs. 5 and 7 - points to a systematic error which extends throughout the whole of either investigation.

A temperature error is the most likely, and the difference between the two relationships is accounted for entirely, by a systematic error of only 6°C. While some of this error may be attributed to the present work, it is considered that the major portion is caused by the manual method of temperature control employed by Baird²⁸. In controlling to a specified temperature by manual

manipulation of the Variac transformer there is a natural tendency to control at a slightly lower temperature than that specified. The automatic control adopted in the present investigation, which did not involve controlling to a specified temperature, is considered to be more accurate. Baird and Taylor quote a temperature control of $\pm 2^{\circ}\text{C}$ but this is thought to be a slightly optimistic estimation.

The free energies of formation of quartz and cristobalite.

The free energies of formation of quartz and cristobalite are given in tables A and B respectively, in the appendix.

The negative free energy of formation of quartz is seen to be greater than that of cristobalite throughout the temperature range under consideration, although β cristobalite is the more stable phase above 1743°K .

This anomaly does in fact give a choice of values for the free energy of formation of β cristobalite - i.e. either table A or table B in the appendix. In the presentation of results the free energy change for reaction (1) has been derived from both values and equations (6a) and (6b) give almost identical free energy changes in the temperature range $1705 - 1828^{\circ}\text{K}$.

The free energy change for reaction (1), given by

equations (6a) or (6b) is thus independent of errors in the thermodynamic data used in its derivation, provided these errors are not excessive. The experimental error has already been given as ± 500 cal. - see p. 25.

Since the free energies of formation of quartz and cristobalite must be nearly identical in the experimental temperature range, the reference state for the silica activities may be taken as either quartz or cristobalite.

The silicon carbide thermodynamic data.

The mean value of the heat of formation of silicon carbide at 298°K, derived from equations (8b) and (8c) is -8,400 cal./mol. The value obtained thermochemically by Humphrey et al⁷ is 13.0 ± 1 k.cal./mol. and at first sight the difference between these values is unaccountably large. Nevertheless, it is thought that the difference of about 5 k.cals. can be attributed to errors in the thermodynamic and thermochemical data used in the derivation of the two values. A list of the data is given below.

1). The free energy change for reaction (1) - present work.

2). The free energy of formation of quartz or cristobalite in the range (1723 - 1823°K).

3). The free energy of formation of carbon monoxide in the temperature range (1723 - 1823°K).

4). Thermochemical data associated with the entropy of formation of silicon carbide at 298°K, and data associated with heat content and entropy increments of silicon carbide.

5). The heat of combustion of silicon carbide at 298°K.

6). The heat of formation of carbon dioxide at 298°K.

7). The heat of formation of α quartz at 298°K.

Each item is not completely independent but the list is formidable. The assessment of errors in each individual item is difficult but a significant estimation of the total error is impossible. An idea of the order of the magnitude of errors to be expected in thermochemical and thermodynamic data can be given however.

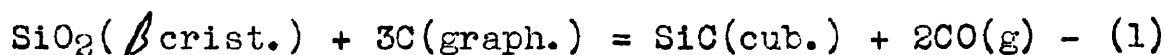
Richardson, Jeffes and Withers¹⁴, assign values of ± 1 k.cal., ± 3 k.cal., ± 10 k. cal. and 'greater than 10 k.cals.' to free energies of formation. These limits have no precise statistical significance and take into account " the opinion of the authors concerning the likely accuracies of the techniques employed and the reliability

of the various investigators".

The same approach is taken by Kubaschewski and Evans⁸ who make the limits of accuracy of a given value wide enough for a further determination of that value to fall inside those limits. In the majority of cases the limits of Kubaschewski and Evans are not those quoted by the original authors, two examples being the errors of ± 3 k.cals. and ± 750 cal. ascribed to items 5) and 7) respectively.

The estimation of errors is seen to be almost intangible and no attempt is made to estimate the errors of the thermodynamic functions given in the appendix.

An error of 5,000 cal. in items 1 - 7 is now seen to be quite possible and the magnitude of the error in no way invalidates the free energy change for reaction (1) which has been obtained in the present work.



$$\Delta_1 G_1^0 = + 146,000 - 81.22T \text{ cal./mol.}, (1705-1828^\circ\text{K}) - - - (6a)$$

An error of ± 500 cal./mol. has been ascribed to the value given by equation (6a) and if this appears unreasonably small in view of what has been stated above, it is pointed out that the method of determination is relatively simple and is also practically independent of any thermochemical data.

The errors in the thermochemical and thermodynamic data prevent, however, any rigid calculation of the free energy of formation of silicon carbide or the heat of formation of silicon carbide from the results of the present work and in the circumstances the values obtained cannot be regarded as reliable.

THE CaO-SiO₂ SYSTEM.

The free energy of formation of calcium metasilicate (α)
The free energy of formation from the constituent oxides obtained from the present results is - 20,500 cal./mol. in the temperature range (1723 - 1823°K). This value is to be compared with - 21,300 cal./mol. at 1723°K given by the equation (F) of Richardson et al¹⁴, quoted in the appendix. The present results at 1450°C and 1500°C indicate that temperature coefficient is small as in fact is the case in the equation of Richardson et al. The error of \pm 3 k.cals. in that equation, however, precludes any rigid confirmation of the present experimental silica activities.

The value obtained in the present work is ofcourse dependent on the free energy of formation from the constituent oxides of the orthosilicate.

The activity of lime.

The lime activities of fig.13, plotted against wt.% CaO, are seen to lie in a narrow band. While this is generally satisfactory, no temperature effect is apparent and it is as well to emphasise the following points.

1). The free energy of calcium metasilicate is assumed to be temperature independent and there is a possible error in the free energy of the orthosilicate.

2). The error involved in the silica, metasilicate, and orthosilicate saturation compositions taken from the CaO-SiO₂ phase diagram is appreciable.

3). The lime activities derived for slags saturated with the metasilicate and/or the orthosilicate depend on spot silica activities.

In general, the data used for the calculation of lime activities is of insufficient accuracy for the determination of any temperature effect.

The lime activities are in excellent agreement with those of Carter and Macfarlane²², which are also given in fig. 13, and the significance of this is discussed in the next chapter.

THE CaO-Al₂O₃-SiO₂ SYSTEM.The silica activity of 'mullite'.

This has been very thoroughly dealt with in the presentation of results. There appears to be no previous data on the free energy of formation from the constituent oxides of 'mullite' in equilibrium with alumina and the derived equation is given below again.

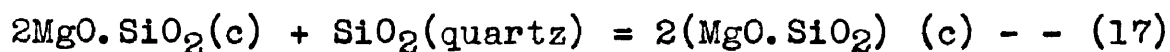
$$\Delta G_T^0 = + 29,600 - 19.52T \text{ cal. / mol. (1673 - 1873}^\circ\text{K) } \text{--- (15)}$$

This equation indicates that the minimum temperature for the formation of mullite is approximately 1250°C. This is consistent with the observed action of heat on kaolinite (Al₂O₃.2SiO₂). Colgrave and Rigby²⁹, for example, carried out differential thermal analyses on samples of pure kaolinite and found that 'mullite', which was detected by X-ray analysis, was not formed below 1100°C. They associated this fact with the formation of γalumina at about 1000°C and suggested that γalumina was essential for the formation of 'mullite'. The above free energy data may supply an additional reason.

It is again stated that the impurity of the 'mullite' used for the determinations may impair the validity of the results obtained.

THE CaO-MgO-SiO₂ SYSTEM.The free energy of formation of magnesium orthosilicate.

The free energies of formation from the constituent oxides of magnesium orthosilicate and magnesium metasilicate, given by equations G and H in the appendix, are - 6,900 cal./mol. and - 15,100 cal./mol., respectively, at 1550°C. Richardson et al¹⁴ place accuracies on these values of ± 1 k.cal. and ± 3 k.cals. respectively. Combination of these values gives a free energy change of + 1,300 cal./mol. for the equilibrium



$$\Delta_{17}^{\text{G}}_{1823} = + 1,300 \text{ cal./mol.}$$

In the presence of solid orthosilicate and metasilicate the equilibrium constant reduces to $K_{17} = 1/a_{\text{SiO}_2}$. The value of this constant obtained from the above free energy change is 0.69 i.e. $a_{\text{SiO}_2} = 1.45$.

The binary MgO-SiO₂ phase diagram shows that a liquid slag containing 62% SiO₂ and 38% MgO is in equilibrium with magnesium orthosilicate and metasilicate at 1557°C - taken as 1550°C. The equilibrium of equation (17) does then exist. The silica activity of 1.45 is of course impossible as the standard state is solid silica.

According to the phase diagram the silica activity

of the slag in equilibrium with the orthosilicate and the metasilicate is less than unity and the present results indicate a silica activity of 0.8 at 1550°C. Using this silica activity, a free energy change of - 810 cal./mol. at 1823°K is obtained for reaction (17).

Since the error in the free energy of formation of the metasilicate is only ± 1 k.cal. the value of - 6,900 cal./mol. at 1550°C is used as the basis for the calculation of the free energy of formation from the constituent oxides at 1550°C of the orthosilicate. A free energy of - 13,000 cal./mol. is calculated by combining the free energy change of - 810 cal./mol. for reaction (17) with the free energy of formation of the metasilicate. This value is consistent with the accurate metasilicate free energy of formation and with the MgO-SiO₂ phase diagram. The value also falls inside the accuracy limits of the value given by Richardson et al.

The free energy of formation of the orthosilicate might also have been obtained from the silica activity of a slag of composition X, given in the CaO-MgO-SiO₂ phase diagram of fig. 15. This slag which is apparently in equilibrium with magnesium orthosilicate and magnesia at 1550°C, has a silica activity of 0.18. These data lead to a free energy of formation of the orthosilicate

of - 6,200 cal./mol. The solubility of lime in magnesium orthosilicate is considerable however, - about 25 wt.% - and the above calculation emphasises the importance of determining whether the compound under consideration is stoichiometric.

The effect of the presence of magnesium vapour, as discussed on page 25, may account partially for the low negative free energy obtained.

CHAPTER VI.

COMPARATIVE REVIEW.

COMPARATIVE REVIEW.

In this chapter the silica and/or lime activities obtained in the present investigation are compared with the results of other workers. The comparison also includes a summary of the methods employed by the various investigators.

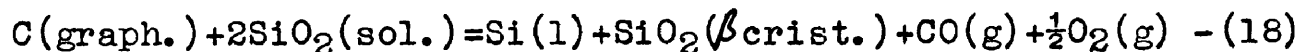
Sakagami and Matsushita.²⁰The CaO-SiO₂ system.

The silica activities obtained by Sakagami and Matsushita are shown in fig. 12.

The calculation of silica activities was based on e.m.f. (E) and decomposition voltage (E_D) measurements. The cell adopted for the e.m.f. measurements was similar to that used by Chang and Derge²¹. In the binary CaO-SiO₂ system the e.m.f./composition curve at a given temperature showed a very sharp minimum at 50 wt.% SiO₂ (NSiO₂ = 0.483), and consideration of this fact along with e.m.f. relationships in other silicate systems, led to the assumption that silica alone contributes to the e.m.f. in slags containing more than 50 wt.% silica, and that lime alone contributes to the e.m.f. in slags containing less than 50 wt.% silica.

The decomposition voltage/ composition curve was

found to be the reciprocal of the e.m.f./composition curve, and the decomposition reaction



gave the best agreement between the theoretical and experimental decomposition voltages.

Reaction (18) and the reciprocity relationship were used to prove that in slags containing more than 50 wt.% silica

$$E_D^0 - E_D = E - E^0 = RT \ln a_{\text{SiO}_2} / 2F \quad (19)$$

where E_D^0 and E^0 are the standard decomposition voltage and the standard e.m.f. respectively. The standard referred to is that of cristobalite. In formulating equation (19) Sakagami and Matsushita avoided the difficult problem of finding a cell reaction to fit their results.

The thermal e.m.f. effect which tended to mask the actual cell e.m.f. in the work of Chang and Derge²¹, was eliminated by Sakagami and Matsushata and on this account their experimental results are considered to be more accurate than those of the former workers.

The only incorrect assumption is that which attributes the e.m.f. solely to silica or lime depending on whether the slag contains more or less than 50 wt.% silica respectively. As the 50 wt.% composition is

approached from the high silica side the contribution of lime to the e.m.f. must progressively increase, and in attributing that e.m.f. to silica alone, the calculated silica activities must become progressively larger than their actual value as the 50 wt.% composition is approached. The relative positions of the curve of Sakagami and Matsushita and that representing the present work at 1550°C, given in fig. 12, are thus satisfactorily explained.

The measured e.m.f. for a 50 wt.% silica slag at 1550°C is 16 mV., and the standard e.m.f. (E°) is 107 mV. If, as a rough estimation, only half of the measured e.m.f. is attributed to silica, a silica activity of 0.28 is calculated from equation (19). This value is in slightly better agreement with the results of the present work and indicates the order of the error in the silica activities of Sakagami and Matsushita, at high lime contents.

By similar reasoning to that adopted for the activity of silica it was also deduced that the calcium orthosilicate activity of a slag containing less than 50 wt.% silica is given by the equation

$$E - E^{\circ} = RT \ln a_{C_2S} / 2F - - - - - (20)$$

where E° refers to the standard e.m.f. at orthosilicate

saturation.

Sakagami and Matsushita also obtained orthosilicate activities, shown in fig. 12, from their experimental silica activities by the Gibbs-Duhem equation. These were in excellent agreement with the orthosilicate activities obtained by means of equation (20).

At first sight, this would appear to confirm the silica activities of Sakagami and Matsushita throughout the entire composition range. The Gibbs-Duhem equation, however, provides only the shape of an activity curve, and that shape has to be calibrated by a point of known activity, in this case orthosilicate saturation. The derived orthosilicate activity curve must therefore be accurate near orthosilicates saturation and as the experimentally determined activities are also accurate in this region agreement is not surprising. The agreement, however, does not confirm the silica activities of slags with a high lime content and the relative positions of the two sets of a_{SiO_2} and $a_{\text{C}_2\text{S}}$ curves, shown in fig. 12, confirm this point.

The ternary CaO-Al₂O₃-SiO₂ system.

Sakagami and Matsushita determined silica activities in this system by the application of equation (19) to the

e.m.f measurements for liquid $\text{CaO-Al}_2\text{O}_3\text{-SiO}_2$ slags. The justification for this procedure is unfounded, however, as even the e.m.f./composition curve at constant temperature and alumina content no longer showed a sharp minimum, indicating that the lime and/or alumina was making a substantial contribution to the e.m.f. over a considerable range of slag compositions.

The agreement with the present work is poor and it is considered that the silica activities of Sakagami and Matsushita for liquid slags in this system are too high.

The silica activities of liquid slags in the quaternary $\text{CaO-MgO-Al}_2\text{O}_3\text{-SiO}_2$ system were also determined. The criticisms made of the ternary silica activities are even more applicable to the quaternary activities and there is complete lack of agreement with the results of the present work, the silica activities of Sakagami and Matsushita being too high.

Chang and Derge²¹.

The silica activities of Chang and Derge for the CaO-SiO_2 system are shown in fig. 12.

These silica activities are based on e.m.f. measure-

ments obtained from a SiC/slag/C cell. The derivation of the cell reaction has caused much criticism and speculation, but despite this, the equation adopted for the calculation of silica activities is the same as that derived by Sakagami and Matsushita²⁰.

The silica activities of Chang and Derge can thus be expected to show the same trends as those of Sakagami and Matsushita. In this case, however, the total cell e.m.f. was the algebraic sum of the actual cell e.m.f. and a thermal e.m.f. caused by the electrodes themselves acting as a thermocouple. The measurement of the actual cell e.m.f. then involved a correction which accounted for 80 - 100% of the total e.m.f. observed. The results of Chang and Derge are thus not so accurate as those of Sakagami and Matsushita, who managed to eliminate the thermal e.m.f. effect. The two sets of silica activities however, show a fair measure of agreement, as is shown in fig. 12.

Richardson³⁰

The calculated silica activity curve for CaO-SiO₂ melts at 1600°C of Richardson was later corrected by Fincham and Richardson³¹ but a brief account of the method is given.

The calculation was based on the formation thermodynamics of the calcium silicates at 1600°C and the CaO-SiO₂ phase diagram. The free energy of formation/mol. fraction curve was drawn through points representing the calculated free energies of formation of certain melts. The chemical potentials of the oxide components were obtained by taking tangents of the free energy curve and reading off the intercepts on the lime and silica ordinates. Activities were then calculated from the silica chemical potentials.

A rough check on the form of the free energy curve was obtained from the phase diagram eutectics, which enabled two simultaneous equations to be solved giving the chemical potentials of the component oxides at the eutectic temperature. Assuming that the heats of formation of the liquids at the eutectic compositions could be obtained by interpolation between the heats of formation of the compounds, and that the heats and entropies of formation of the liquids were independent of temperature, the free energies of formation of the melts were calculated at 1600°C.

As can be seen from this account the calculation was only approximate, and indeed Richardson never intend-

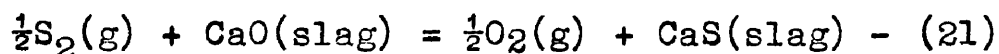
ed it to be otherwise for the calculation was made at a time when there was little experimental data on silica activities.

Fincham and Richardson³¹.

The results obtained from sulphur equilibria determinations in this work were also used to adjust the silica activities of CaO-SiO₂ melts previously calculated by Richardson³⁰, and the corrected curve is shown in fig. 34.

In part of the investigation lime-silica slags were brought into equilibrium, at temperatures between 1350 and 1650°C, with gas phases containing carbon dioxide and sulphur dioxide at room temperature.

When the partial pressure of oxygen was less than $1 \cdot 10^{-5}$ atm. the equilibrium



was found to hold.

Since it was desirable to compare results for melts of various compositions at the same temperature but at different oxygen partial pressures, the sulphide capacity of a slag was defined as

$$C_s = (\%S) \cdot (pO_2/pS_2)^{\frac{1}{2}} - - - - - (22)$$

The equilibrium constant for reaction (21) must be the same as that involving the pure metal oxides and

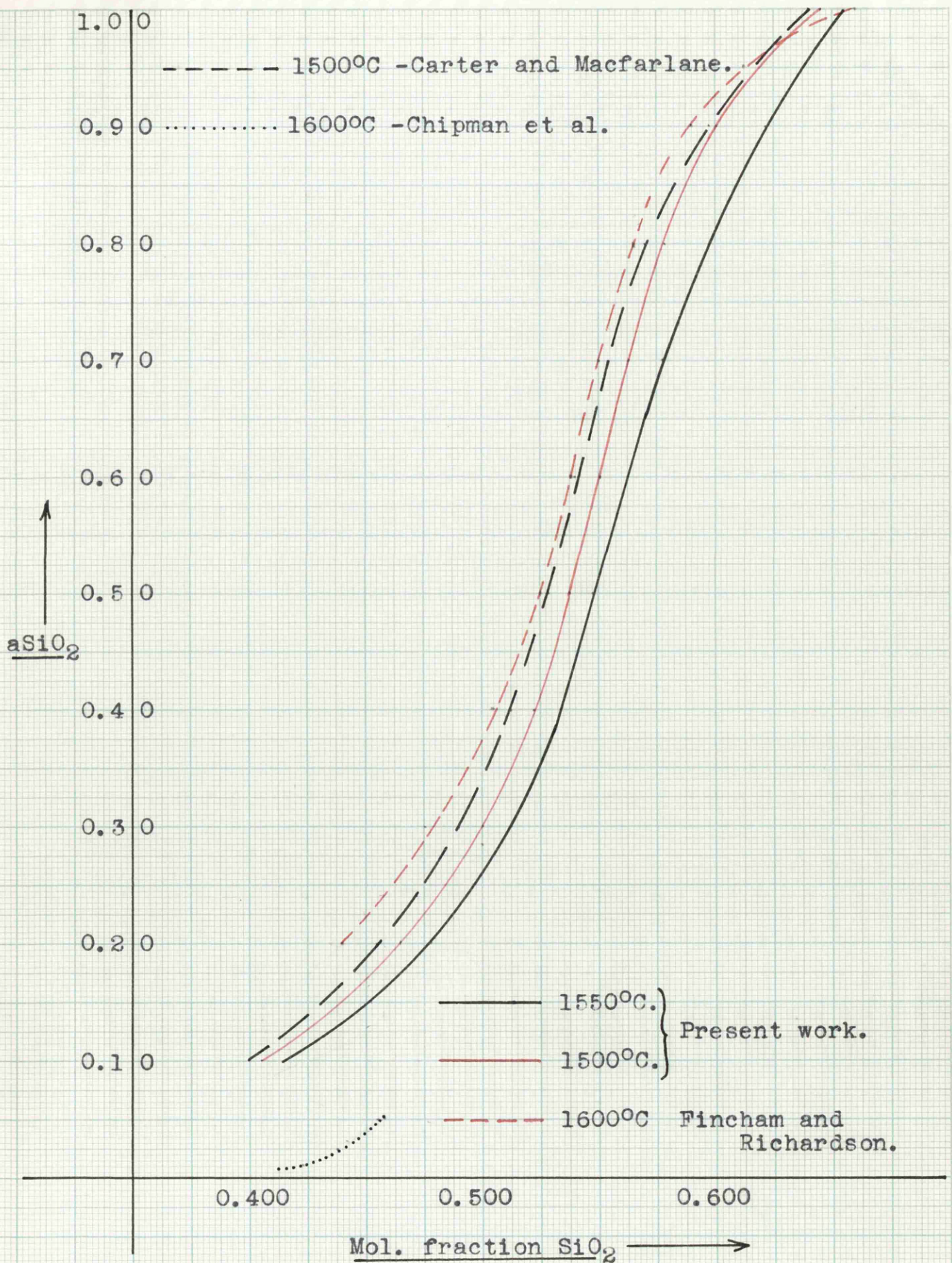


Fig. 34 - The silica activities of CaO-SiO₂ slags.

sulphides as long as the correct activities are used.



$$K_{23} = (p\text{O}_2/p\text{S}_2)^{\frac{1}{2}} \text{ - - - - - (24)}$$

Using values of K_{23} derived from thermodynamic data, and the lime activities of Richardson³⁰, values of the function $p^{\frac{1}{2}}\text{O}_2 \cdot a_{\text{CaS}}/p^{\frac{1}{2}}\text{S}_2$ were obtained for the various melt compositions. Combination of this function with the experimentally determined sulphide capacities gave values of γ_{CaS} (mol. fraction basis). One of these values of γ_{CaS} was extraordinarily high and the partial molal free energies of lime and silica of Richardson were adjusted to bring the value of γ_{CaS} more in line with those obtained for other melts.

It is seen from the above account that the calculated values of γ_{CaS} , which depend inter alia on an approximate free energy change for reaction (23), have been used rather empirically to correct the partial molal free energies of formation for lime and silica of Richardson. While the correction may indicate that the silica activity curve of Richardson was too low at high lime contents, the corrected curve of Fincham and Richardson remains at the best, an approximation.

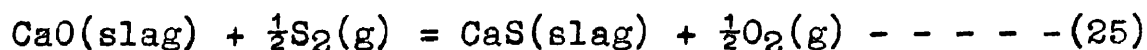
It is interesting to note that constancy of γ_{CaS}

was also assumed by Carter and Macfarlane²².

Carter and Macfarlane²²

In the investigation of Carter and Macfarlane, silica activities at 1500°C were derived from experimentally determined lime activities by means of the Gibbs-Duhem equation, and an account of the method of determination of these lime activities is first given.

The reaction



was investigated by studying the equilibrium between CO-CO₂-SO₂ gas mixtures and CaO-SiO₂ slags at 1500°C.

Defining the sulphurising potential of a gas as

$$A = (p_{\text{S}_2}/p_{\text{O}_2})^{\frac{1}{2}},$$

$$K_{25} = (a_{\text{CaS}})/(a_{\text{CaO}}) \cdot (p_{\text{O}_2}/p_{\text{S}_2})^{\frac{1}{2}} = (a_{\text{CaS}})/(a_{\text{CaO}}) \cdot A \text{ --- (26)}$$

Thus for a standard slag of unit lime activity and an activity of CaS = $a^{\circ}\text{CaS}$, in equilibrium with a gas whose sulphurising potential is A°

$$K_{25} = (a^{\circ}\text{CaS})/A^{\circ} \text{ --- (27)}$$

Combining the equation of the standard slag with that for any other slag

$$a_{\text{CaO}} = a_{\text{CaS}}/a^{\circ}\text{CaS} \cdot A^{\circ}/A = (\%S)/(\%S^{\circ}) \cdot A^{\circ}/A \cdot \gamma_{\text{CaS}}/\gamma^{\circ}\text{CaS} \text{ --- (28)}$$

where A° , $a^{\circ}\text{CaS}$, $\%S^{\circ}$ and $\gamma^{\circ}\text{CaS}$ refer to the standard slag.

On the assumption that at low sulphur concentrations

γ_{CaS} is proportional to that of the same slag at sulphur saturation, given that the solubility of sulphur in the standard slag is 2.5 - 3.0%, and 3.5 - 5.5% in CaO-SiO₂ slags, the ratio $\gamma_{\text{CaS}}/\gamma^{\circ}_{\text{CaS}}$ is calculated as 0.75. Thus,

$$a_{\text{CaO}} = \%S/\%S^{\circ} \cdot A/A^{\circ} \cdot 0.75 \text{ - - - - - (29)}$$

In the above calculations three other assumptions were made :

1). The activity coefficient of CaS does not vary significantly with slag composition or sulphur concentration.

2). a_{CaO} is not significantly lowered by the substitution of small amounts of sulphide for oxide at low sulphur concentrations.

3). No appreciable amount of sulphur is present in the slag as aluminium or silicon sulphide.

Calculation of the sulphurising potential of a gas was complicated by three different sets of data for the free energies of formation of the gaseous compounds present in the CO-CO₂-SO₂ gas mixtures. Each set gave a different value of A, and since it was impossible to equilibrate all slags with a gas mixture similar to that used for the standard slag, the calculated lime activities are dependent on the correct choice of thermo-

dynamic data. The results of Carter and Macfarlane have been confirmed, however, in the recent work of M. R. Kalyanram³².

The silica activities derived from the experimental lime activities at 1500°C, by the Gibbs-Duhem equation are shown in fig. 34. Silica activities from the present work are also shown in this figure and agreement between the two curves is good, the largest difference being only about 20%. As pointed out by Carter and Macfarlane, the choice of thermodynamic data made in the calculation of 'sulphurising potential' does not affect the a_{SiO_2} curve derived by the Gibbs-Duhem equation, as the lime activities obtained with each set of data are in almost constant proportion to one another. The a_{SiO_2} curve is also independent of the correction factor of 0.75.

The agreement between the silica activities of Carter and Macfarlane with those of the present work does not supply rigid confirmation of those activities. Carter and Macfarlane calibrated the Gibbs-Duhem calculations against the composition of a liquid slag saturated with silica i.e. $a_{\text{SiO}_2} = 1$. This standard was also used in the present investigation and the two sets of results must agree at silica saturation. The agreement

does confirm the 'slope' of the curves.

The lime activities at 1500°C, derived from the experimental silica activities of the present work by the Gibbs-Duhem equation, are given in fig. 13. Also given in this figure are the experimental lime activities of Carter and Macfarlane, which are in excellent agreement with those of the present work. In this case the derivation of each set of lime activities is completely independent. In the work of Carter and Macfarlane a slag of unit lime activity was the standard used and in the present work the Gibbs-Duhem calculations are calibrated from the composition of a liquid slag, saturated with calcium orthosilicate, and the free energy of formation of the orthosilicate. The agreement between the two sets of lime activities thus supplies independent confirmation of both the present work and that of Carter and Macfarlane.

Fulton and Chipman³³

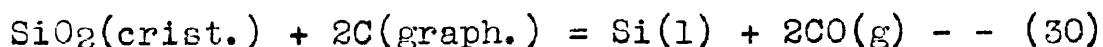
Fulton, Grant and Chipman³⁴.

Langenberg, Kaplan and Chipman³⁵

The silica activities for CaO-SiO₂ slags obtained by the above investigators are shown in fig. 34 and the activity curve is seen to be very much lower than that obtained

in the present work.

The method employed by the above investigators is based on the silicon distribution between graphite saturated Fe-Si-C alloys and CaO-Al₂O₃-SiO₂ slags.



The free energy change for reaction (30) was calculated by Fulton and Chipman from the data of Kelley^{2,3}, Coughlin³⁶, Humphrey and King¹ and Olette⁵. The linear free energy equation which was obtained is

$$\Delta_{30} G_T^0 = + 161,500 - 87.4T \text{ cal./mol.} \quad - - \quad (31)$$

The melts were graphite saturated and under one atmosphere of carbon monoxide and hence

$$K_{30} = a_{\text{Si}}/a_{\text{SiO}_2} \quad - - - - - \quad (32)$$

Silica activities were then calculated using equation (32) and the activities of silicon in carbon saturated iron.

The silicon activities in Fe-Si and Fe-Si-C alloys were determined by Chipman, Fulton, Gokcen and Caskie³⁷, who determined the distribution coefficient of silicon between iron and silver at 1420°C for both Fe-Si and Fe-Si-C alloys. The activity of silicon is the same in the iron and silver layers, and assuming that the activity coefficient of silicon in the silver layer was constant it followed that in the binary Fe-Si system,

$$\ln N_1 \text{Si}^{\text{Ag}} / N_1 \text{Si}^{\text{Fe}} - \ln N_2 \text{Si}^{\text{Ag}} / N_2 \text{Si}^{\text{Fe}} = \ln \gamma_1 \text{Si}^{\text{Fe}} - \ln \gamma_2 \text{Si}^{\text{Fe}} \quad \text{--(33)}$$

Given that carbon was insoluble in silver it also followed that

$$N' \text{Si}^{\text{Ag}} / N \text{Si}^{\text{Ag}} = \gamma' \text{Si}^{\text{Fe}} / \gamma \text{Si}^{\text{Fe}} \quad \text{-- (34)}$$

where the prime refers to the ternary Fe-Si-C alloys and where both $N' \text{Si}^{\text{Ag}}$ and $N \text{Si}^{\text{Ag}}$ refer to the same mol. fraction of silicon in the iron layer.

From equation (33) the silicon coefficients were calculated throughout the experimental range using a composition of known silicon activity. This point of known silicon activity was obtained from the Fe-Si phase diagram, where a liquid solution of $N \text{Si} = 0.73$ is in equilibrium with essentially pure solid silicon at 1207°C . The heat of fusion of silicon was taken as 11,100 cal./gm. atom at 1414°C ⁶ and the substitution of the appropriate partial molal free energy of silicon, as determined from the data of Korber and Oelson⁶, in the relationship $\partial \ln \gamma_{\text{Si}} / \partial T = - \bar{L}_{\text{Si}} / RT^2$, gave a value of $\gamma_{\text{Si}}^{\text{Fe}}$ of 0.84 at $N \text{Si} = 0.73$ and 1420°C . The interval between this composition and the highest concentration of silicon in the distribution study was bridged by the assumption that $\ln \gamma_{\text{Si}}^{\text{Fe}} / (1 - N \text{Si})^2$ is constant. This led to a value of $\log \gamma_{\text{Si}}^{\text{Fe}}$ of - 0.15 at $N \text{Si} = 0.55$ and 1420°C . The plot of

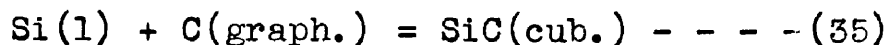
$\log \gamma_{\text{Si}}/N_{\text{Si}}$ obtained by Chipman et al is reproduced in fig. 35.

Extrapolation of the above curve to infinite dilution of silicon was undertaken with the use of rather uncertain thermodynamic data which gave the result $\log \gamma^{\circ}_{\text{Si}} = -2.40 \pm 0.27$ at 1420°C .

Activity coefficients were calculated at 1500, 1600 and 1700°C from those obtained at 1420°C by the relationship $\ln \gamma_{\text{Si}}/dT = -\bar{L}_{\text{Si}}/RT^2$.

In the ternary system values of $\gamma'_{\text{Si}^{\text{Fe}}}$ were calculated at 1420°C by equation (34) and it was found that when $\log \gamma'_{\text{Si}^{\text{Fe}}}$ was plotted against $(N_{\text{C}} + N_{\text{Si}})$, the curve obtained was identical to that of the binary system. On the assumption that such a relationship held at other temperatures, values of $\gamma'_{\text{Si}^{\text{Fe}}}$ at 1500, 1600 and 1700°C were computed from the appropriate solubility data and the binary $\gamma_{\text{Si}^{\text{Fe}}}$ values.

One point on the above curves was apparently confirmed by the free energy of formation of silicon carbide as determined by Humphrey et al⁷



$$\Delta_{35}G^{\circ}_T = -24,400 + 8.3T \text{ cal.}/\text{mol.} (1683 - 2000^{\circ}\text{K.}) \text{ --- (36)}$$

On silicon carbide and graphite saturation the equilibrium constant reduces to $K_{35} = 1/a_{\text{Si}}$ where the activity

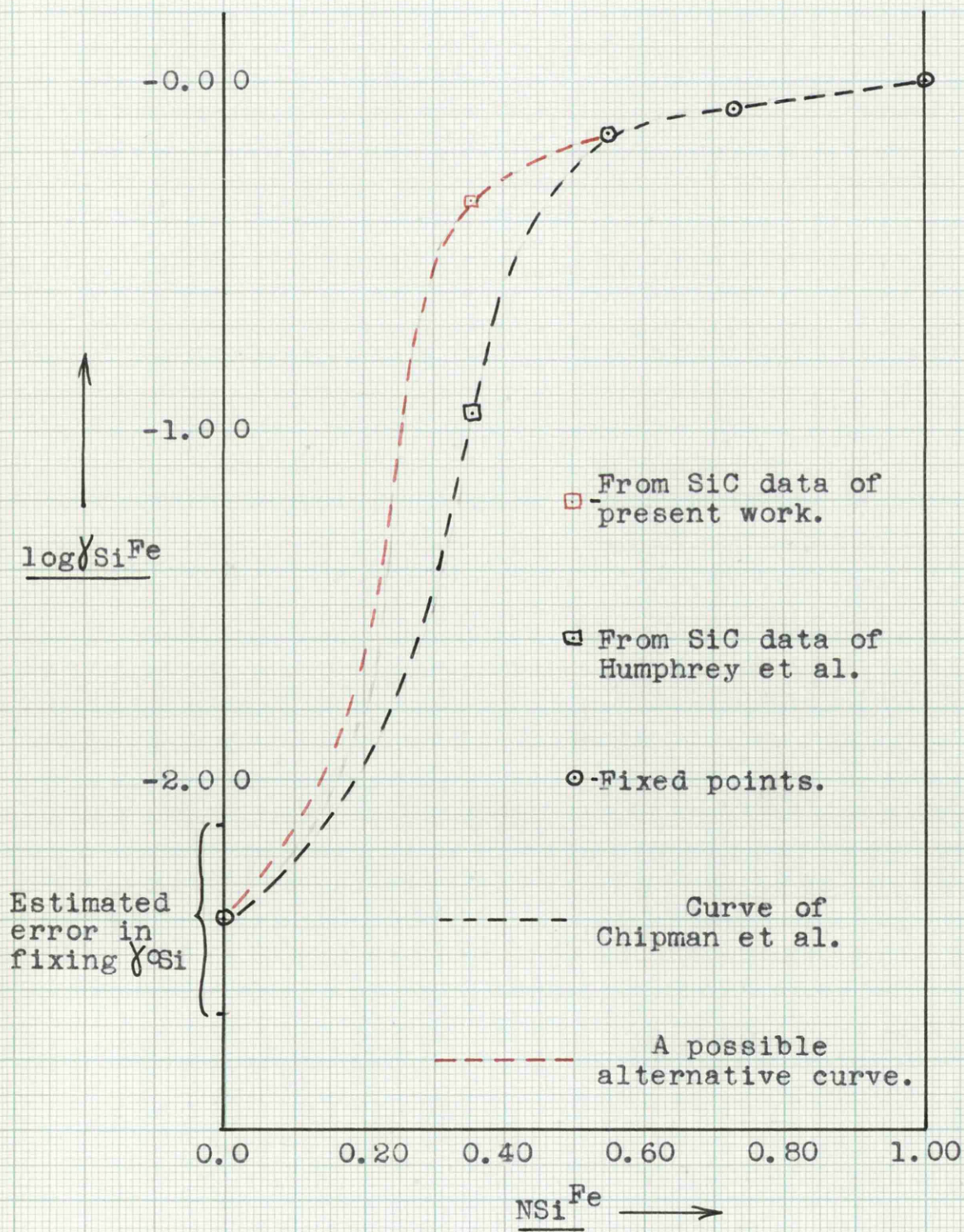
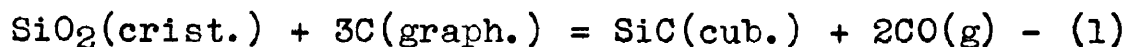


Fig. 35 - $\log \gamma_{Si}^{Fe} / N_{Si}$ in the system Fe-Si at 1420°C.

of silicon is referred to the pure liquid. Using the values of $\gamma_{\text{Si}}^{\text{Fe}}$ computed above and the silicon carbide saturation data, the calculated free energies of formation of silicon carbide at 1420, 1500, 1600 and 1700°C differed by only 0.3 k.cals./mol. from those obtained by Humphrey et al.⁷

Thus, with the use of equation (31) and the $\gamma_{\text{Si}}^{\text{Fe}}$ data of Chipman, Fulton, Gokcen and Caskie³⁷, silica activities were calculated for liquid slags in the CaO-SiO₂ and CaO-Al₂O₃-SiO₂ systems. Unfortunately, the separation of silicon carbide as a stable phase when the percentage of silicon in the metal exceeded 23 wt.%, prevented the determination of silica activities throughout the entire range of liquid slags.

Comparison of the results of Chipman et al with those of the present work is aided by the silicon carbide saturated slags at 1600°C. The compositions of these slags are given in Fig. 36 and the silica activity obtained by Chipman et al is 0.05. In the case of these slags the equilibrium



may be considered to hold. Since the system is in equilibrium with solid graphite and silicon carbide, and carbon monoxide at one atmosphere pressure, the equili-

brium constant reduces to $K_1 = 1/a\text{SiO}_2$. If the free energy change of the present work is used, equation (6a), a silica activity of 0.19 is obtained. The results of the present work have been extrapolated to 1600°C by using the statistically determined temperature coefficient, equation (16), for the sake of comparison. The extrapolated values obtained from figs. 5, 6, 7 and 8 give the iso-activity lines shown in fig. 36. The agreement with the recalculated values of Chipman et al is seen to be excellent. Similar calculations at 1700°C yield results which are more difficult to compare as the recalculated silica activity is 0.03 and the present experimental results only extend to silica activities of about 0.1. The indications are, however, that the agreement is again excellent.

This agreement indicates that the experimental work is sound in both investigations and that differences only arise in the interpretation of the results.

In chap. V the general unreliability of thermodynamic data based on thermochemical data was discussed and it is now thought that an error in the free energy change for reaction (30), given by equation (31) may account for the difference in the silica activities of Chipman et al and those of the present work. It must also

be pointed out that the silica activities of Chipman et al cannot be standardized, for example, against a

Chipman et al.

● Slags in equilibrium with SiC and C at 1600°C.

- 0.19 - Recalculated iso-activity curve.

Present work.

- 0.30 - iso-activity curves.

The results for both

are dependent on the

the binary

repro

laid

carbide data

fig. 35 the agreement

in the data of Humphrey

considering the moderate error

the agreement may prove to be large

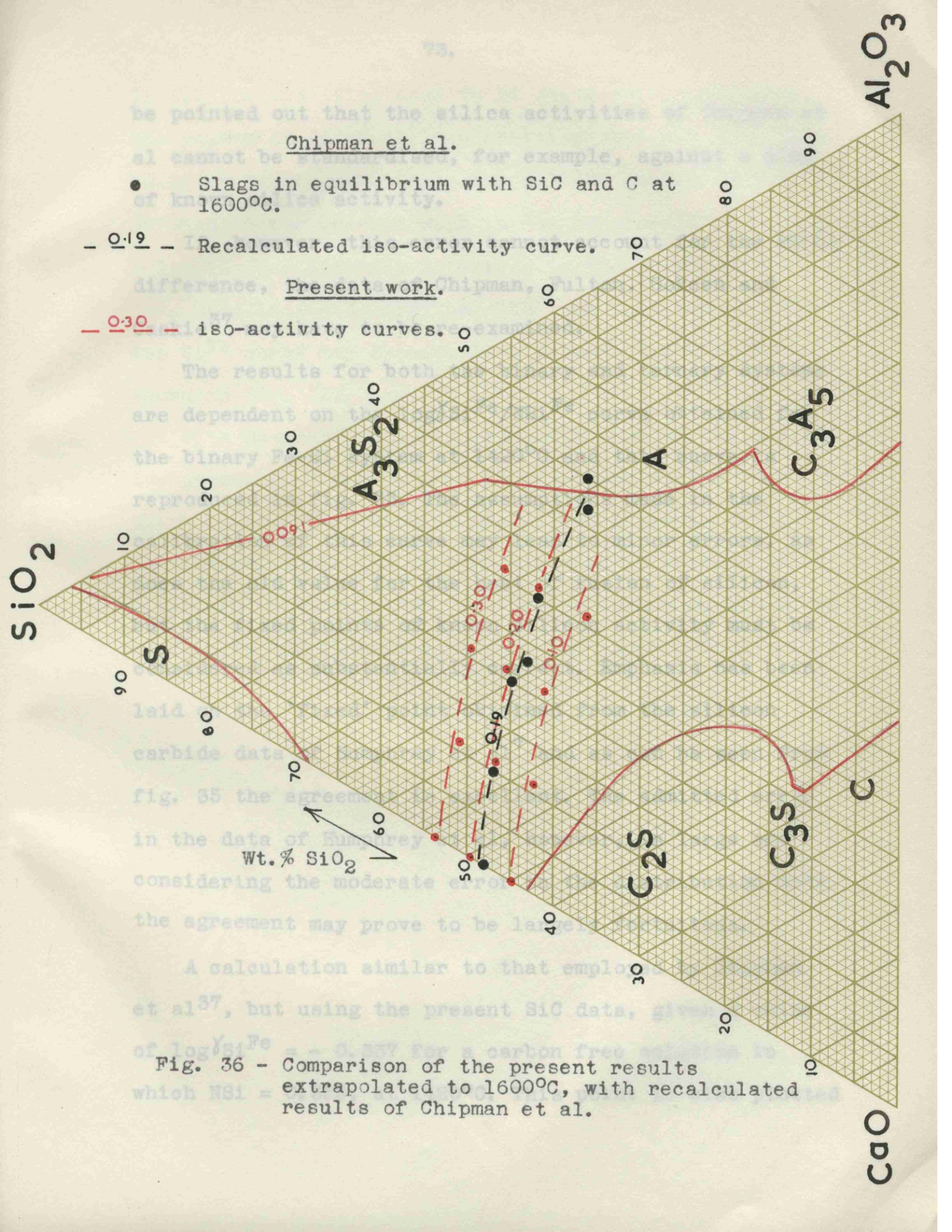
A calculation similar to that employed

et al³⁷, but using the present SiC data, gives

of $\log \gamma_{Si}^{Fe} = -3.337$ for a carbon free slag

which $NSi =$

Fig. 36 - Comparison of the present results extrapolated to 1600°C, with recalculated results of Chipman et al.



be pointed out that the silica activities of Chipman et al cannot be standardised, for example, against a slag of known silica activity.

If, however, this error cannot account for the whole difference, the data of Chipman, Fulton, Gokcen and Caskie³⁷ may have to be re-examined.

The results for both the binary and ternary systems are dependent on the $\log \gamma_{\text{Si}}^{\text{Fe}} / N_{\text{Si}}^{\text{Fe}}$ curve obtained for the binary Fe-Si system at 1420°C and this curve is reproduced in fig. 35. The assumptions made in the calibration of this curve may lead to minor errors, as does the old value for the heat of fusion of silicon, but the fixed points of known silicon activity must be considered as substantially correct. Emphasis has been laid on the 'fixed' point obtained from the silicon carbide data of Humphrey et al⁷ and as can be seen from fig. 35 the agreement is excellent. The admitted error in the data of Humphrey et al, however, is large and considering the moderate error in the distribution data the agreement may prove to be largely fortuitous.

A calculation similar to that employed by Chipman et al³⁷, but using the present SiC data, gives a value of $\log \gamma_{\text{Si}}^{\text{Fe}} = - 0.337$ for a carbon free solution in which $N_{\text{Si}} = 0.355$, at 1420°C. This point is also plotted

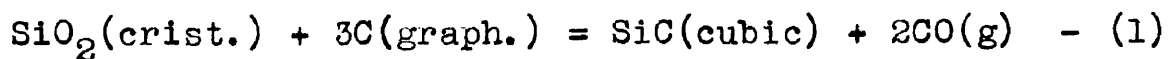
in fig. 35 and it is seen to be quite consistent with the points of fixed silicon activity obtained from the Fe-Si phase diagram. Since the silicon carbide data derived in the present work is not considered to be reliable, due entirely to errors in the thermodynamic data used in its derivation, the true position of the $\log a_{\text{Si}}^{\text{Fe}}$ curve may be somewhere between the two extremes shown in fig. 35.

With respect to the experimental part of the curve, the presence of 0.2 - 3.5 wt.% of silver in the iron phase and 0.2 wt.% iron in the silver phase is to be considered. While the effect of mutual solubility is a matter for speculation, its very presence must lead to caution in the interpretation of the experimental results.

GENERAL CONCLUSIONS.

GENERAL CONCLUSIONS

After consideration of the simple experimental technique employed and the elimination of the possibility of a dynamic equilibrium being studied, the free energy change for reaction (1) is thought to be correct.



$$\Delta_1 G_T^0 = + 146,000 - 81.22T \text{ cal./mol.}, (1705 - 1828^\circ\text{K}) - (6a)$$

The quoted possible error of ± 500 cal. for equation (6a) is thought to be a fair estimation.

The calculated free energy of formation and heat of formation of silicon carbide, however, are considered to be unreliable on account of possible errors in the thermodynamic data used in their derivation, and the disagreement with the data of Humphrey et al⁷ in no way invalidates equation (6a).

The silica activities in the present work give free energies of formation of calcium metasilicate and magnesium orthosilicate which are consistent with existing values. This gives a good indication of the reliability of those activities but the independent confirmation supplied by the work of Carter and Macfarlane²² establishes the silica activities obtained for the CaO-SiO₂ system.

The disagreement with the work of Chipman et al^{33,34,35}

is attributed largely to errors in the thermodynamic data used in their derivation.

The silica activities in the quaternary $\text{CaO-Al}_2\text{O}_3\text{-MgO-SiO}_2$ system have been given almost without comment as no reliable values have been reported previously.

In the presentation of the silica activities obtained for slags approaching magnesia saturation, however, the reservations made on page 25 concerning the vapour pressure of magnesium are emphasised.

REFERENCES.

REFERENCES.

1. G.L.Humphrey and E.G.King, J.Amer.Chem.Soc., 1952, 74, 2041.
2. K.K.Kelley, U.S.Bur.Mines Bull., 1950, 477.
3. K.K.Kelley, *ibid*, Bull., 1949, 476.
4. M.Gleiser and J.F.Elliot, Private communication.
5. M.Olette, "The Physical Chemistry of Steelmaking", Tech.Press & J.Wiley and Sons, Inc., 18, 1958.
6. F.Korber and W.Oelson, Mitt.Kaiser Wilhelm Inst. Eisenf., 1936, 18, 109.
7. G.L.Humphrey, S.S.Todd, J.P.Coughlin, and E.G.King, U.S.Bur.Mines, Rept.Inv. 4888, 1952.
8. O.Kubaschewski and E.Ll.Evans, "Metallurgical Therm-chemistry", Pergamon Press Ltd., 390, 1958.
9. "Selected Values of Thermodynamic Properties", Nat.Bur.Stand., circular 500, 1952.
10. "Tables of Thermal Properties of Gases" Nat.Bur.Stand., circular 564, 1955.
11. E.G.King, J.Amer.Chem.Soc., 1951, 73, 656.
12. S.S.Todd, *ibid*, 1951, 73, 3277.
13. J.P.Coughlin and C.J.O'Brien, J.Phys.Chem., 1959, 61, 767
14. F.D.Richardson, J.H.E.Jeffes and G.Withers, J.I.S.I., 1950, 166, 213.
15. J.D.Baird and J.Taylor, Trans.Far.Soc., 1958, 54, 527
16. H.Bennet, W.G.Hawley and R.P.Eardly, Trans.Brit.Ceram. 1958, 57, 1.
17. "Reference Tables for Pt/Pt-13%Rh Thermocouples" B.S. 1826 : 1952.

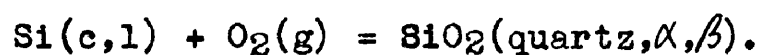
18. J. Chipman, "Thermodynamic Properties of Blast Furnace Slags", Presented at the Symposium on the Physical Chemistry of Process Metallurgy, Pittsburgh, 1959.
19. G. A. Rankin and F. E. Wright, Am. J. Sci., 1915, ser. 4, 39, 1.
J. W. Greig, ibid, 1927, ser. 5, 13, 1 and 133.
20. R. Sakagami and Y. Matsushita, Rept. Inst. Ind. Sci., Tokyo Univ., 1958, 7.
21. L. C. Chang and G. Derge, Trans. A. I. M. E., 1946, 172, 90.
22. P. T. Carter and T. G. Macfarlane, J. I. S. I., 1957, 185, 54.
23. N. A. Toropow and F. J. Galakhov, Ber. Akad. d. Wiss. U. S. S. R. 1951, 78, 299.
24. S. Aramaki and R. Roy, Nature, 1959, Supp. 9, 184, 631.
25. G. Tromel, "The Physical Chemistry of Steel Making", Tech. Press & J. Wiley and Sons. Inc., 1958, 77.
26. R. W. Ricker and E. F. Osborn, J. Amer. Chem. Soc., 1954, 37, 133.
27. E. F. Osborn, R. C. De Vries, K. H. Gee and H. M. Kraner,
J. Metals, 1954, 6, 33.
28. J. D. Baird, Ph. D. Thesis, Glasgow, 1956.
29. Colgrave and Rigby, Trans. Brit. Ceram. Soc., 1952, 51, 355
30. F. D. Richardson, "Physical Chemistry of Melts", Inst. of Min. Met., London, 1953, 75.
31. C. J. B. Fincham and F. D. Richardson, Proc. Roy. Soc., A, 1954, 223, 40.
32. M. R. Kalyanram, Ph. D. Thesis, Glasgow, 1959.
33. J. C. Fulton and J. Chipman, Trans. A. I. M. E., 1954, 200
1136.
34. J. C. Fulton, N. J. Grant, and J. Chipman, Trans. A. I. M. E., 1953, 197, 135.

35. F.C. Langenberg, H. Kaplan and J. Chipman, "The Physical Chemistry of Steel Making", Tech. Press & J. Wiley and Sons, Inc., 65, 1958.
36. J.P. Coughlin, U.S. Bur. Mines Bull., 1954, 542.
37. J. Chipman, J.C. Fulton, N. Gokcen and C.R. Caskie,
Acta Met., 1954, 2, 439.

APPENDIX

THERMODYNAMIC DATA.

Table A. - Thermodynamic data for the reaction



T°K.	ΔH_T^0 k.cals.	$T\Delta S_T^0$ k.cals.	ΔG_T^0 k.cals.
400	-210.30	-17.45	-192.85
500	-210.14	-21.72	-188.42
600	-210.06	-25.90	-184.16
700	-209.85	-29.99	-179.86
800	-209.57	-33.97	-175.60
848(α_q)	-209.43	-35.84	-173.59
848(β_q)	-209.14	-35.55	-173.59
900	-209.02	-37.63	-171.39
1000	-208.87	-41.64	-167.23
1100	-208.67	-45.63	-163.04
1200	-208.53	-49.58	-158.95
1300	-208.29	-53.53	-154.76
1400	-208.16	-57.46	-150.70
1500	-207.91	-61.35	-146.56
1600	-207.74	-65.22	-142.52
1686(c. Si)	-207.60	-68.52	-139.08
1686(l. Si)	-219.70	-80.62	-139.08
1700	-219.67	-81.26	-138.41
1800	-219.38	-85.77	-133.61
1883	-219.16	-89.39	-129.77

Table B. - Thermodynamic data for the reaction



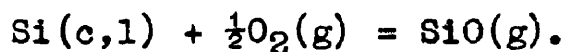
T°K.	ΔH_T^0 k.cals.	$T\Delta S_T^0$ k.cals.	ΔG_T^0 k.cals.
400	-209.36	-17.40	-191.96
500	-209.28	-21.67	-187.61
523(α cr.)	-209.24	-22.60	-186.64
523(β cr.)	-209.04	-22.40	-186.64
600	-208.86	-25.53	-183.33
700	-208.70	-29.60	-179.10
800	-208.50	-33.62	-174.88
900	-208.30	-37.61	-170.69
1000	-208.13	-41.60	-166.53
1100	-207.91	-45.57	-162.34
1200	-207.77	-49.51	-158.26
1300	-207.51	-53.43	-154.08
1400	-207.36	-57.33	-150.03
1500	-207.10	-61.20	-145.90
1600	-206.92	-65.06	-141.86
1686(c. Si)	-206.77	-68.35	-138.42
1686(l. Si)	-218.87	-80.46	-138.42
1700	-218.85	-81.09	-137.76
1800	-218.55	-85.59	-132.96
1900	-218.26	-90.04	-128.22
2000	-217.95	-94.50	-123.45

Table C. - Thermodynamic data for the reaction



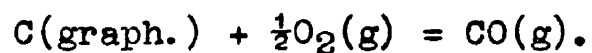
T°K.	ΔH_T° k.cals.	$T\Delta S_T^{\circ}$ k.cals.	ΔG_T° k.cals.
400	+83.22	+17.19	+66.03
500	83.03	21.27	61.76
600	82.79	25.27	57.52
700	82.50	29.17	53.33
800	82.17	32.98	49.19
848(α_q)	81.99	34.77	47.22
848(β_q)	81.85	34.63	47.22
900	81.71	36.61	45.10
1000	81.42	40.38	41.04
1100	81.15	44.12	37.03
1200	80.82	47.81	33.01
1300	80.54	51.47	29.07
1400	80.21	55.11	25.10
1500	79.92	58.72	21.20
1600	79.57	62.30	17.27
1686(c. Si)	79.27	65.37	13.90
1686(l. Si)	73.22	59.32	13.90
1700	73.17	59.76	13.41
1800	72.86	62.94	9.92
1883	72.60	65.52	7.08

Table D. - Thermodynamic data for the reaction



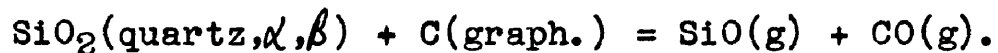
T°K.	ΔH_T° k.cals.	$T\Delta S_T^\circ$ k.cals.	ΔG_T° k.cals.
400	-21.93	+ 8.47	-30.40
500	-22.04	10.41	-32.45
600	-22.24	12.32	-34.56
700	-22.43	14.18	-36.60
800	-22.62	16.00	-38.61
900	-22.80	17.80	-40.60
1000	-23.02	19.56	-42.58
1100	-23.19	21.31	-44.49
1200	-23.45	23.02	-46.47
1300	-23.61	24.71	-48.31
1400	-23.87	26.38	-50.25
1500	-24.04	28.05	-52.08
1600	-24.30	29.69	-53.99
1686(c. Si)	-24.53	31.11	-55.64
1686(l. Si)	-36.63	19.01	-55.64
1700	-36.67	19.13	-55.80
1800	-36.83	20.06	-56.89
1900	-37.00	20.98	-57.98
2000	-37.17	21.91	-59.08

Table E. - Thermodynamic data for the reaction



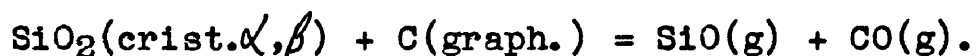
T°K.	ΔH_T^0 k.cals.	$T\Delta S_T^0$ k.cals.	ΔG_T^0 k.cals.
400	-26.32	+ 8.69	-35.00
500	-26.30	10.89	-37.19
600	-26.33	13.02	-39.35
700	-26.41	15.11	-41.52
800	-26.51	16.16	-43.67
900	-26.53	19.18	-45.81
1000	-26.76	21.19	-47.95
1100	-26.89	23.16	-50.05
1200	-27.03	25.12	-52.15
1300	-27.17	27.06	-54.23
1400	-27.32	29.00	-56.32
1500	-27.46	30.98	-58.44
1600	-27.62	32.81	-60.43
1700	-27.78	34.72	-62.50
1800	-27.94	36.58	-64.52
1900	-28.12	38.43	-66.55
2000	-28.30	40.26	-68.56

Table F. - Thermodynamic data for the reaction



T°K.	ΔH_T° k. cal.	$T\Delta S_T^{\circ}$ k. cal.	ΔG_T° k. cal.
400	+162.05	+34.60	+127.45
500	161.81	43.02	118.79
600	161.49	51.24	110.25
700	161.02	59.28	101.75
800	160.45	67.13	93.32
848 (α_q)	160.13	70.82	89.31
848 (β_q)	159.84	70.53	89.31
900	159.59	74.61	85.00
1000	159.10	82.39	76.71
1100	158.60	90.10	68.50
1200	158.06	97.72	60.34
1300	157.51	105.30	52.22
1400	156.97	112.84	44.13
1500	156.41	120.38	36.04
1600	155.82	127.72	28.10
1700	155.23	135.11	20.12
1800	154.61	142.41	12.20
1883	154.09	148.33	5.76

Table G. - Thermodynamic data for the reaction



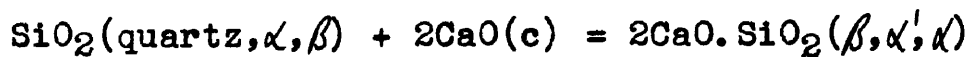
T°K.	ΔH_T° k. cal.	$T\Delta S_T^\circ$ k. cal.	ΔG_T° k. cal.
400	+161.11	+34.56	+126.55
500	160.94	42.97	117.97
523(α cr.)	160.85	44.82	116.03
523(β cr.)	160.65	44.62	116.03
600	160.29	50.87	109.42
700	159.86	58.89	100.97
800	159.37	66.78	92.59
900	158.87	74.59	84.28
1000	158.35	82.35	76.00
1100	157.83	90.04	67.79
1200	157.29	97.65	59.64
1300	156.73	105.20	51.53
1400	156.17	112.71	43.46
1500	155.60	120.23	35.37
1600	155.00	127.56	27.44
1700	154.40	134.94	19.46
1800	153.78	142.23	11.55
1900	153.14	149.45	+3.69
2000	152.48	156.67	-4.19

Table H. - Thermodynamic data for the reaction



T°K.	ΔH_T° k.cals.	$T\Delta S_T^{\circ}$ k.cals.	ΔG_T° k.cals.
400	-13.42	- 0.78	-12.64
500	-13.39	- 0.94	-12.45
600	-13.36	- 1.10	-12.26
700	-13.34	- 1.25	-12.09
800	-13.33	- 1.42	-11.91
900	-13.31	- 1.58	-11.73
1000	-13.31	- 1.73	-11.58
1100	-13.26	- 1.90	-11.36
1200	-13.32	- 2.09	-11.23
1300	-13.26	- 2.25	-11.01
1400	-13.28	- 2.38	-10.90
1500	-13.19	- 2.52	-10.67
1600	-13.20	- 2.64	-10.56
1686(c. Si)	-13.19	- 2.73	-10.46
1686(1. Si)	-25.29	-14.84	-10.46
1700	-25.29	-14.94	-10.35
1800	-25.17	-15.73	- 9.44
1900	-25.04	-16.47	- 8.57
2000	-24.90	-17.22	- 7.68

Table I. - Thermodynamic data for the reaction



T°K.	ΔH_T^0 k.cals.	$T\Delta S_T^0$ k.cals.	ΔG_T^0 k.cals.
400	-30.26	+ 0.52	-30.78
500	-30.27	0.64	-30.91
600	-30.24	0.80	-31.04
700	-30.21	0.97	-31.18
800	-30.21	1.10	-31.31
848(α_q)	-30.21	1.14	-31.35
848(β_q)	-30.50	0.85	-31.35
900	-30.43	1.01	-31.44
970(β_{C_2S})	-30.30	1.25	-31.55
970(α'_{C_2S})	-29.86	1.70	-31.56
1000	-29.79	1.78	-31.57
1100	-29.55	2.21	-31.76
1200	-29.32	2.64	-31.96
1300	-29.06	3.16	-32.22
1400	-28.72	3.74	-32.46
1500	-28.29	4.44	-32.73
1600	-27.78	5.26	-33.04
1700	-27.15	6.24	-33.39
1710(α'_{C_2S})	-27.09	6.36	-33.35
1710(α_{C_2S})	-23.70	9.75	-33.45
1800	-23.29	10.66	-33.95

THE METHOD OF COMPILATION OF TABLES 'A' TO 'I'
AND THE REPRESENTATION OF THE TABULATED DATA
BY LINEAR EQUATIONS.

The thermodynamic data given in tables 'A' to 'I' have been compiled from the thermochemical data given below under the appropriate reaction heading. The method of compilation is similar to that adopted by Humphrey, Todd, Coughlin and King⁷.

In most cases the tabulated free energy data have been represented by a linear equation. These equations have been determined mathematically, and the sum of the squares of the individual differences between the tabulated values, and the values given by the appropriate equation, is at a minimum. This method has the advantage that the derived equation is at least reproducible.

Although the tabulated thermodynamic data is given to the nearest 10 cal., this in no way indicates the order of the accuracy of such data. The error may often be in the order of k.cals. and this error must also apply to the linear free energy equations.

The limits of accuracy of the thermochemical data given by the original authors is not quoted and no estimation has been made of the accuracy of the linear free energy equations derived in the present work. The

reasons for this procedure have been fully discussed in chapter V.

The errors in the quoted linear equations of Richardson, Jeffes and Withers¹⁴, were estimated by those authors.

The reaction $\text{Si}(c,l) + \text{O}_2(g) = \text{SiO}_2(\text{quartz}, \alpha, \beta)$.

The heat of formation of α quartz given by Humphrey and King¹ is

$$\Delta H_{298}^{\circ} = - 210,260 \text{ cal./mol.}$$

and the entropy of formation obtained from the data of Kelley² is

$$\Delta S_{298}^{\circ} = - 43.51 \text{ cal./deg.mol.}$$

The above data are combined with the high temperature heat content and entropy increments for quartz and oxygen of Kelley³, and the increments for silicon given by Gleiser and Elliot⁴, to give the thermodynamic functions tabulated in table 'A'.

Gleiser and Elliot accept the heat of fusion of silicon given by Olette⁵, + 12,100 cal./gm.atom at 1686°K, in preference to the previous value of + 11,000 cal./gm.atom at 1683°K given by Korber and Oelson⁶.

In the temperature range 1686 - 1883°K the data may be represented by the linear equation

$$\Delta G_T^{\circ} = - 218,900 + 47.34T \text{ cal.}/\text{mol.} \quad (1686-1883^{\circ}\text{K}) \quad - - (A)$$

The reaction $\text{Si}(c,l) + \text{O}_2(g) = \text{SiO}_2(\text{cristobalite}, \alpha, \beta)$.

The heat of formation of α cristobalite given by Humphrey and King¹ is

$$\Delta H_{298}^{\circ} = - 209,330 \text{ cal.}/\text{mol.}$$

and the entropy of formation obtained from the data of Kelley² is

$$\Delta S_{298}^{\circ} = - 43.40 \text{ cal.}/\text{deg. mol.}$$

The above data are combined with the high temperature heat content and entropy increments for cristobalite and oxygen of Kelley³, and the increments for silicon given by Gleiser and Elliot⁴, to give the thermodynamic functions tabulated in table 'B'.

In the temperature range 1686 - 2000^oK the data may be represented by the linear equation

$$\Delta G_T^{\circ} = - 218,800 + 47.67T \text{ cal.}/\text{mol.} \quad (1686 - 2000^{\circ}\text{K}) \quad - (B)$$

The reaction $\frac{1}{2}\text{SiO}_2(\text{quartz}, \alpha, \beta) + \frac{1}{2}\text{Si}(c,l) = \text{SiO}(g)$.

The heat of formation of silicon monoxide, in the above reaction, given by Humphrey et al⁷ is

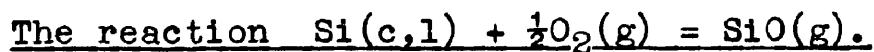
$$\Delta H_{298}^{\circ} = + 83,300 \text{ cal.}/\text{mol.}$$

and the entropy of formation given by Kelley² is

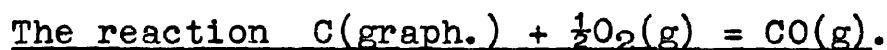
$$\Delta S_{298}^{\circ} = + 43.30 \text{ cal./deg.mol.}$$

The silicon monoxide data has been reviewed by Kubaschewski and Evans⁸ and there appears to be no reason for a revision of the above values.

The above data are combined with the high temperature heat content and entropy increments of quartz and silicon monoxide of Kelley³, and the increments for silicon given by Gleiser and Elliot⁴, to give the thermodynamic functions tabulated in table 'C'.



The thermodynamic functions for the above reaction are obtained from the data given in tables 'A' and 'C', and are tabulated in table 'D'.



The N.B.S. "Selected Values of Thermodynamic Properties"⁹, gives the heat of formation of carbon monoxide

$$\Delta H_{298}^{\circ} = - 26,400 \text{ cal./mol.}$$

and the entropy of formation

$$\Delta S_{298}^{\circ} = + 21.44 \text{ cal./deg.mol.}$$

These data are combined with the high temperature heat content and entropy increments for carbon monoxide

obtained from the N.B.S. "Tables of Thermal Properties of Gases"¹⁰, and the increments for graphite and oxygen of Kelley³, to give the thermodynamic data tabulated in table 'E'.

In the temperature range 1600 - 1900°K the data may be represented by the linear equation

$$\Delta G_T^0 = - 27,800 - 20.40T \text{ cal./mol. (1600-1900°K) - - (C)}$$

The reaction $\text{SiO}_2(\text{quartz}, \alpha, \beta) + \text{C}(\text{graph.}) = \text{CO}(\text{g}) + \text{SiO}(\text{g})$

The thermodynamic functions for this reaction, tabulated in table 'F', are obtained from the data given in tables 'A', 'D' and 'E'.

The data may be represented in the range 1600-1883°K by the linear equation

$$\Delta G_T^0 = + 154,400 - 78.99T \text{ cal./mol. (1600-1883°K) - (D)}$$

In the presence of solid quartz and graphite, the equilibrium constant for this reaction reduces to $p_{\text{CO}} \cdot p_{\text{SiO}} \text{ atm}^2$. Values of this constant derived from equation 'D' are $4.79 \cdot 10^{-3}$, $1.70 \cdot 10^{-2}$ and $5.62 \cdot 10^{-2}$ at 1450, 1500 and 1550°C respectively.

The reaction $\text{SiO}_2(\text{crist.}, \alpha, \beta) + \text{C}(\text{graph.}) = \text{CO}(\text{g}) + \text{SiO}(\text{g})$

The thermodynamic functions for this reaction, tabulated

in table 'G' are obtained from the data given in tables 'B', 'D' and 'E'.

The data may be represented in the range 1600-1900°K by the linear equation

$$\Delta G_T^0 = + 154,100 - 79.16T \text{ cal.}/\text{mol. (1600-1900°K)} \quad - - \quad (E)$$

In the presence of solid cristobalite and graphite, the equilibrium constant for this reaction reduces to $p_{CO} \cdot p_{SiO} \text{ atm.}^2$. Values of this constant derived from equation 'E' are $5.62 \cdot 10^{-3}$, $2.05 \cdot 10^{-2}$ and $6.76 \cdot 10^{-2}$ at 1450, 1500 and 1550°C respectively.

The reaction $Si(c,l) + C(\text{graph.}) = SiC(\text{cubic})$.

The heat of formation of cubic silicon carbide given by Humphrey et al⁷ is

$$\Delta H_{298}^0 = - 13,400 \text{ cal.}/\text{mol.}$$

and the entropy of formation obtained from the data of Kelley² is

$$\Delta S_{298}^0 = - 1.89 \text{ cal.}/\text{deg. mol.}$$

The above heat and entropy of formation are combined with the high temperature heat content and entropy increments of graphite, silicon and silicon carbide given respectively by Kelley³, Gleiser and Elliot⁴ and Humphrey et al⁷, to give the thermodynamic functions tabulated in table 'H'.

The reaction $\text{SiO}_2(\text{quartz}, \alpha, \beta) + 2\text{CaO}(c) = 2\text{CaO} \cdot \text{SiO}_2(\beta, \alpha', \alpha)$

The heat of formation of calcium orthosilicate given by King¹¹ is

$$\Delta H_{298}^{\circ} = - 30,200 \text{ cal./mol.}$$

and the entropy of formation obtained from the data of Kelley² and Todd¹² is

$$\Delta S_{298}^{\circ} = + 1.50 \text{ cal./deg.mol.}$$

The above data are combined with the high temperature heat content and entropy increments for lime and quartz given by Kelley³, and the increments for calcium orthosilicate given by Coughlin and O'Brien¹³, to give the thermodynamic functions tabulated in table 'I'.

Rather than derive an equation over a short temperature range, free energy changes of -33,500, -33,800 and 34,100 cal./mol., corresponding to temperatures of 1723, 1773 and 1823°K respectively, are adopted for the reaction.

The equilibrium constants derived from the above free energy values are $1.78 \cdot 10^4$, $1.46 \cdot 10^4$ and $1.22 \cdot 10^4$ at 1450, 1500 and 1550°C respectively.

The reaction $\text{SiO}_2(\text{quartz}) + \text{CaO}(c) = \text{CaO} \cdot \text{SiO}_2(c)$.

The free energy of formation of calcium metasilicate from the constituent oxides, given by Richardson, Jeffes and Withers¹⁴ is

$$\Delta G_T^0 = - 19,900 - 0.82T \text{ cal.}/\text{mol. (1483-1813}^\circ\text{K)} - - \text{ (F)}$$

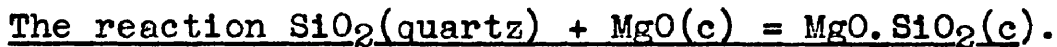
The estimated accuracy of this equation is ± 3 k.cals.



Richardson, Jeffes and Withers¹⁴ give the free energy of formation of magnesium orthosilicate from the constituent oxides as

$$\Delta G_T^0 = - 15,120 - 0.0T \text{ cal.}/\text{mol. (298 - 1700}^\circ\text{K)} - - \text{ (G)}$$

The estimated accuracy of this equation is also ± 3 k.cals.



The free energy of formation of magnesium metasilicate from the constituent oxides given by Richardson, Jeffes and Withers¹⁴ is

$$\Delta G_T^0 = - 8,900 + 1.1T \text{ cal.}/\text{mol. (298-1600}^\circ\text{K)} - - - \text{ (H)}$$

The estimated accuracy of this equation is ± 1 k.cal.

ACKNOWLEDGEMENTS.

This work was carried out in the Metallurgy Department of the Royal College of Science and Technology, Glasgow.

The author wishes to thank Professor R. Hay, the former Professor of Metallurgy, for his help during the course of this work. The author also wishes to thank Dr. J. Taylor for his understanding and patient guidance.